7-9-2020 3:00 PM

Exploring the Effects of Hemodialysis on Renal and Hepatic Blood Flow and Function using CT Perfusion Imaging

Raanan Marants, *The University of Western Ontario*

Supervisor: Lee, Ting-Yim, *The University of Western Ontario*
Joint Supervisor: McIntyre, Christopher W., *The University of Western Ontario*
A thesis submitted in partial fulfillment of the requirements for the Doctor of Philosophy degree in Medical Biophysics

Abstract

Hemodialysis (HD) is the most common form of renal replacement therapy for end-stage renal disease. However, patients develop complications that are driven by HD-induced circulatory stress from rapidly removing large fluid volumes during HD, making various vascular beds vulnerable to ischemia. By assessing how HD-induced circulatory stress affects different organs, it may be possible to characterize the mechanisms behind these complications and evaluate therapeutic interventions. This thesis aims to explore how HD affects renal and hepatic blood flow and function using CT perfusion imaging. For this work, patients received either standard or cooled HD first in a two-visit, crossover study design, where imaging was performed before, during and after each HD session.

Residual renal function is linked to improved clinical outcomes, yet characteristically declines upon HD initiation. In the first thesis project, we determined that renal perfusion decreases during HD, which could be an early manifestation of HD-mediated residual renal function loss.

Although the liver normally clears endotoxin, increased circulating endotoxin levels have been found in HD patients. In the second thesis project, we showed that concurrent hepatic perfusion redistribution and decreased liver function during HD are likely responsible for increased circulating toxin levels.

Dialysate cooling is a low-cost, feasible intervention that ameliorates HD-induced circulatory stress. In the first and second thesis projects, we found that cooling trended towards mitigating the drop in renal perfusion during HD and ameliorating the changes in liver perfusion and function during HD.

If it were possible to accurately assess glomerular filtration rate (GFR) in HD patients, HD prescriptions could be adjusted in accordance with residual renal function to preserve remaining function. In the third thesis project, we extended the CT perfusion technique to measure GFR in HD patients, yielding physiologically realistic GFR values, thus demonstrating the feasibility of this approach in terms of reliability and accuracy.

These findings help explain residual renal function loss and endotoxemia in HD patients, and showcases the protective potential of dialysate cooling. In addition, this work demonstrates the benefit of using CT perfusion as a functional imaging technique to further characterize and evaluate therapies for end-stage renal disease pathologies.

Keywords: end-stage renal disease, hemodialysis, circulatory stress, computed tomography perfusion, functional imaging, residual renal function, renal perfusion, endotoxemia, hepatic perfusion, dialysate cooling, measured glomerular filtration rate

Lay Summary

Patients with end-stage kidney failure require kidney replacement therapy, with the most common type being hemodialysis (HD). This treatment removes several litres of fluid in a 3- to 4-hour session, which stresses the ability of a patient's heart to pump blood throughout the body ("circulatory stress"). The goals of this thesis are to explore how circulatory stress:

- affects blood flow to, and function of, different organs
- leads to other health problems besides kidney failure
- can be prevented to minimize adverse effects on HD patients

These goals were achieved using computed tomography perfusion (CTP), a scanning technique that measures organ blood flow. We performed CTP on patients before, during and after HD treatment.

The small remaining kidney function is linked to improved quality of life of HD patients but declines with HD. In the first thesis project, we found that kidney blood flow deceases during HD, which could damage the kidney and cause further loss of what little remaining function there is.

The liver normally clears toxins that it receives from the gut, but HD patients have abnormally high blood toxin levels. In the second thesis project, we showed that liver blood flow redistributes to receive more toxin-filled blood from the gut and that the liver's detoxification ability was also compromised during HD, leading to increased toxin levels in HD patients.

Previous research has shown that by slightly lowering the temperature of the HD fluid, circulatory stress can be lessened. In the first and second thesis projects, we found that cooling helped to maintain kidney and liver blood flow during HD.

There is currently no rapid, reliable and accurate method to measure remaining kidney function in HD patients. In the third thesis project, we extended the CTP technique to also measure kidney function in our HD patients. This approach yielded realistic values, thus demonstrating the practicality and utility of our unique method.

These results help explain important health concerns of HD and showcase the protective potential of cooling. This work demonstrates the benefit of using CTP as a powerful imaging technique to explore and evaluate therapies for end-stage kidney failure.

Co-Authorship Statement

Chapters 2, 3 and 4 of this thesis were adapted from original research studies performed in collaboration with multiple authors. The contributions of myself and other co-authors to these works are described below.

Chapter 2 was adapted from an original research manuscript entitled “Renal Perfusion during Hemodialysis: Intradialytic Blood Flow Decline and Effects of Dialysate Cooling”, which was published in the *Journal of the American Society of Nephrology* in 2019. This manuscript was co-authored by myself, Dr. Elena Qirjazi, Dr. Claire Grant, Dr. Ting-Yim Lee and Dr. Christopher McIntyre. The study was primarily designed by Dr. Grant and Dr. Qirjazi, who were both, along with myself, involved in carrying out experiments and collecting data. I was responsible for data analysis, figure creation, and manuscript preparation, all of which was done under the supervision of Dr. Lee and Dr. McIntyre, and the latter of which also included contributions from all co-authors. The final version of the manuscript was seen and approved by all co-authors.

Chapter 3 was adapted from an original research manuscript entitled “Exploring the Link between Hepatic Perfusion and Systemic Endotoxemia in Hemodialysis Patients: A Randomized Crossover Study”, which is in preparation for submission for publication to *Kidney International Reports* in 2020. This manuscript was co-authored by myself, Dr. Elena Qirjazi, Dr. Fiona Li, Dr. Ka-Bik Lai, Dr. Cheuk-Chun Szeto, Dr. Philip Li, Dr. Ting-Yim Lee and Dr. Christopher McIntyre. The study was primarily designed by Dr. Qirjazi, who was, along with myself, Dr. Lai, Dr. Szeto and Dr. Li, involved in carrying out experiments and collecting data. I was responsible for data analysis, figure creation, and manuscript preparation, all of which was done under the supervision of Dr. Lee and Dr.

McIntyre, and the latter of which also included contributions from all co-authors. The final version of the manuscript was seen and approved by all co-authors.

Chapter 4 was adapted from an original technical development manuscript entitled “Measuring Glomerular Filtration Rate in End-Stage Renal Disease Patients on Hemodialysis using CT Perfusion Imaging”, which is in preparation for submission for publication to *Radiology* in 2020. This manuscript was co-authored by myself, Dr. Christopher McIntyre and Dr. Ting-Yim Lee. The study was primarily designed by myself and was based on the re-analysis of data from the Chapter 2 study. I was responsible for data analysis, figure creation, and manuscript preparation, all of which was done under the supervision of, and included contributions from, Dr. Lee and Dr. McIntyre. The final version of the manuscript will be seen and approved by all co-authors.

Acknowledgements

It is difficult to comprehend that five years have passes since I began my PhD studies, and that it is finally coming to an end. This has been a very positive and fulfilling experience, both on a personal and professional level, because of the wonderful people I have shared it with.

First, I would like to thank my supervisors, Dr. Ting-Yim Lee and Dr. Chris McIntyre. They have taught me how to be a more effective communicator, a stronger team member, and a better researcher. They challenged me to have a more adaptable and optimistic perspective with regards to my research work and results. Ting and Chris have occasionally described some of their awe-inspiring research ideas which in turn helped to fuel the conception and development of my own. So, Ting and Chris, thank you for your guidance, support, and encouragement. As I move forward in my academic career, I hope that I make you proud. I would also like to thank my advisory committee members, Dr. Robert Lindsay and Dr. Eugene Wong, who have provided me with their invaluable insights, helpful suggestions, and fresh perspectives throughout the course of my PhD studies.

Next, I would like to thank the two lab groups that I was lucky enough to be a part of: the Lee lab and the KCRU (a.k.a., McVader lab). Both of these groups are of high quality and quantity, and I am grateful for the (past and present) individuals in both who helped to positively shape my PhD experience. In the Lee lab, thank you to Anne Leaist, Aaron So, Errol Stewart, Kyle Burgers, Feng Su, Xiaogeng Chen, Esmaeil Enjilela, Mohammad Fazel, Elham Karami, Adam Blais, Eric Wright, Danny Yang, Fiona Li, Chidera Opara, Kevin Chung, Jennifer Hadway, Laura Morrison, Lise Dejardins, and Tony

Wales. In the McVader lab, thank you to Virginia Schuman, Laura Chambers, Alireza Akbari, Fabio Salerno, Lisa Hur, Jarrin Penny, Tanya Tomasi, Justin Dorie, Claire Grant, Elena Qirjazi, Sanjay Kharche, Marat Slessarev, and Janice Gomes.

Outside of my lab groups, I have formed strong relationships with many other students at Robarts. Thank you to Tomi Nano, Derek Gillies, Danny Gelman, Spencer Christiansen, and Greg Hong.

Last but not least, I would like to thank my family for their unending love and support. My parents, brothers, sisters-in-law, nieces, nephews, and parents-in-law have all played major roles in helping me to achieve my goals and reach this incredible milestone in my life, and I am incredibly grateful and appreciative of them. And of course, I have to especially thank my wife Clara, who has been the wind beneath my wings for this entire journey. Her faith, belief, and trust in me has been unwavering, and I hope that I have made her proud. I look forward to the next great challenge that we will face together: parenthood.

I am grateful for the amazing experience of my PhD, and I look forward to applying all that I have learned in my future academic pursuits.

Table of Contents

List of Tables

List of Figures

List of Appendices

List of Abbreviations

AIF	Arterial input function
AKI	Acute kidney injury
BP	Blood pressure
CKD	Chronic kidney disease
CT	Computed tomography
CTP	Computed tomography perfusion
DBP	Diastolic blood pressure
DC	Dialysate cooling
DRP	Decreased renal perfusion
eGFR	Estimated glomerular filtration rate
ESRD	End-stage renal disease
GFR	Glomerular filtration rate
HD	Hemodialysis
HU	Hounsfield unit
ICG	Indocyanine green
IDH	Intradialytic hypotension
KDOQI	Kidney Disease Outcomes Quality Initiative
MAP	Mean arterial pressure
mGFR	Measured glomerular filtration rate
MRI	Magnetic resonance imaging
MS	Myocardial stunning
PD	Peritoneal dialysis

PDD	Pulsed dye densitometry
PET	Positron emission tomography
ROI	Region of interest
RRF	Residual renal function
RRT	Renal replacement therapy
RWMA	Regional wall motion abnormality
SBP	Systolic blood pressure
TDC	Time density curve
UF	Ultrafiltration

CHAPTER 1

1 Introduction

1.1 Overview

Chronic kidney disease is a worldwide health burden, with a reported global prevalence of approximately 13% in 2016.[1] In Canada, nearly 4 million people are estimated to have chronic kidney disease,[2] with over 50,000 Canadians living with end-stage renal disease and about 58% of those are on dialysis.[3] Of those, approximately 75% are receiving hemodialysis,[3] which is the most expensive treatment option (costs the health care system nearly $100,000 per patient per year[4]), contributes to the development of other clinical problems (e.g., cardiovascular disease and cognitive impairment), and results in low survival (5-year survival of 42.8%[3]).

Although hemodialysis is a life-saving renal replacement therapy which works by extracorporeally removing accumulated waste products and excess fluid volumes, it is very socioeconomically draining and physiologically disruptive to the patient. Despite the multitude of technological and methodological innovations in hemodialysis over several decades, there has been no improvement in survival for end-stage renal disease patients receiving this form of renal replacement.[5] While this unfortunate reality is in large part due to the fact that kidney disease patients already carry a high disease burden upon initiation of hemodialysis, it has become increasingly recognized that hemodialysis therapy itself plays a major role in the morbidity and mortality of end-stage renal disease patients.[6]

Therefore, it is extremely important to study the direct physiological effects of hemodialysis on systemic and multi-organ hemodynamics and function, allowing for the characterization of clinical complications and development of protective interventions.

1.2 The Kidneys

1.2.1 Normal Renal Physiology

The kidneys are important for maintaining homeostasis in the body because they are responsible for excreting waste products, regulating fluid and electrolyte balance, and other specialized endocrine functions.[7] Normal renal function ensures that fluid does not accumulate in the body and that unwanted waste products from metabolism do not buildup in the body. The kidneys receive about 25% of the body's cardiac output from the renal arteries, filtering approximately 180 litres of fluid each day in the incoming blood,[8] before the filtered blood returns via the renal veins back to the systemic circulation (Figure 1.1A).

Kidneys are composed of an outer layer (cortex) and inner layer (medulla). Each kidney consists of approximately one million nephrons,[8] which are the functional units of the kidney (Figure 1.1B). Blood enters each nephron through the afferent arteriole, passes through the glomerulus and its capillaries, and then flows out through the efferent arteriole. As blood circulates through the glomerular capillaries, excess fluid and metabolic (potentially toxic) wastes are filtered through the glomerular filtration barrier into the Bowman's capsule (Figure 1.1C).[9] The glomerulus functions as a macromolecular sieve: it prevents the filtration of plasma proteins and certain large molecular weight exogenous tracers while allowing for greater permeability of water and small solutes. The water-solute filtrate then proceeds into the renal tubule, where tubular secretion and reabsorption at different points modify the filtrate and prepare it for urinary excretion.[9]

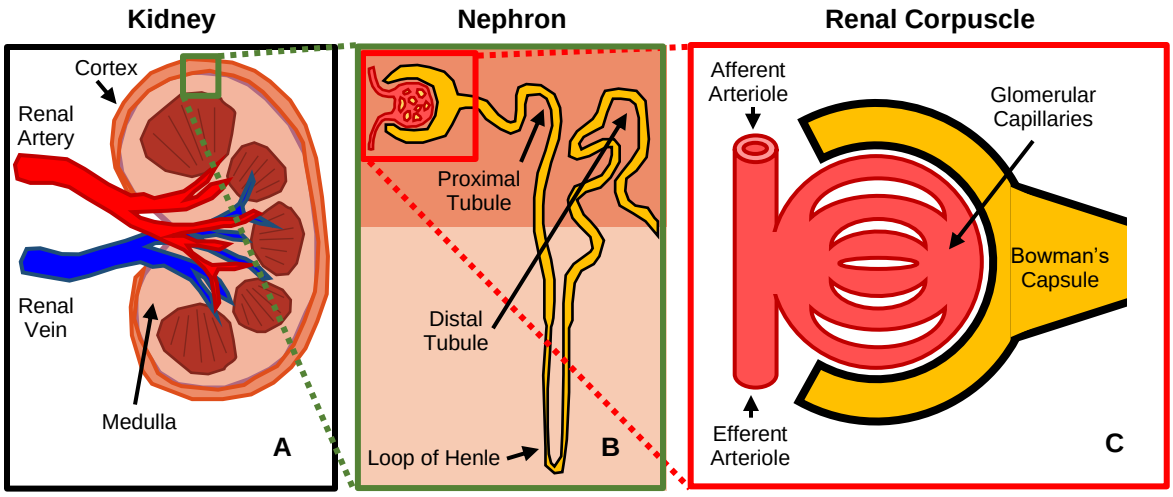

Figure 1.1: Basic structure of the kidney, nephron, and renal corpuscle. (A) Kidneys are composed of an outer layer (cortex) and inner layer (medulla). They receive about 25% of the body's cardiac output from the renal arteries, filtering approximately 180 litres of fluid each day in the incoming blood, before the filtered blood returns via the renal veins back to the systemic circulation. (B) Each kidney consists of approximately one million nephrons, which are the functional units of the kidney. (C) Blood enters each nephron through the afferent arteriole, passes through the glomerulus and its capillaries, and then flows out through the efferent arteriole. As blood circulates through the glomerular capillaries, excess fluid and metabolic wastes are filtered through the glomerular filtration barrier into the Bowman's capsule.

The glomerular filtration barrier is composed of 3 layers: endothelium, glomerular basement membrane, and podocytes.[9] The glomerular endothelium consists of flattened, highly fenestrated cells which are very permeable to water and small solutes, while at the same time demonstrate charge-selective properties due to negatively charge proteoglycans in the fenestrae.[10] The glomerular basement membrane is a thick, fibrous network that helps maintain structural integrity and is involved in barrier charge selectivity, where it accounts for most of the restriction of fluid and solute flux.[10] Podocytes are specialized epithelial cells lining the outside of glomerular capillaries that have extending

foot processes separated by filtration slit diaphragms. Podocytes help maintain glomerular permselectivity by restricting the permeation of macromolecules based on size, shape and charge.[10]

The kidney normally has several mechanisms to compensate for fluctuations in hydration and blood pressure, including the myogenic reflex (pressure receptor-mediated dilatation of afferent arteriole in response to ischemia), tubuloglomerular feedback (ATP-based afferent arteriole constriction/dilation due to increased/decreased solute delivery to tubular macula densa cells), and the renin-angiotensin system (ischemia-induced renin release which constricts the efferent arteriole).[11] Under normal physiological conditions, these mechanisms protect the kidney from ischemic challenges and allow for the autoregulation of glomerular perfusion, ultrafiltration (UF) pressure, and filtration rate.[11]

1.2.2 Glomerular Filtration Rate

The primary measure of renal function is the glomerular filtration rate (GFR), which represents the rate of fluid filtered from the glomerulus into the Bowman's capsule and is expressed in mL/min/1.73m^2. Glomerular filtration is driven by the hydrostatic and osmotic pressure gradients between the glomerular capillaries and the Bowman's capsule: $GFR \propto \left[\left(P_{glomerulus}^{hydrostatic} - P_{BowCap}^{hydrostatic}\right) + \left(P_{BowCap}^{osmotic} - P_{glomerulus}^{osmotic}\right)\right]$.[9] The GFR is used clinically to assess the health of the kidneys and as a tool for making informed treatment decisions.

The GFR can be estimated (eGFR) and measured (mGFR) using various approaches. eGFR is often assessed using population-based equations which take as inputs the individual's demographic information (age, sex, ethnicity) and an endogenous

marker level reading.[12] The most common endogenous markers considered for GFR assessment are creatinine and urea. Creatinine is a breakdown product of creatine phosphate from the metabolism of muscle and protein, while urea is waste product of protein digestion that is produced by the liver. In addition to being filtered, creatinine is subject to tubular secretion while urea is subject to tubular reabsorption, making both markers indirect reflections of GFR.[12]

mGFR can be assessed by taking sequential urine and/or plasma samples of endogenous or exogenous markers over the course of hours or days.[12] mGFR is most accurately assessed by performing 24-hour urine collection (since accuracy of plasma sampling is confounded by extra-renal clearance) following the administration of inulin, an exogenous marker which does not undergo tubular secretion or reabsorption. Other common mGFR assessments rely on radionuclide-based urine/plasma sampling of ^{51}Cr-EDTA (Europe) or ^{99m}Tc-DTPA (USA).[13]

In addition to using inulin and nuclear medicine techniques, GFR can also be assessed using dynamic CT- and MRI-based approaches by computing the filtration rate constant (determined from graphical analysis and/or tracer kinetic modelling) and measuring the kidney mass (determined from volumetric imaging).[14-17] In addition to providing useful anatomical and functional information, imaging-based techniques also enable the quantification of single-kidney GFR, which has several important clinical applications (e.g., renal artery stenosis, kidney transplant/donor, comparing left vs. right kidney function, disease characterization/progression/monitoring/diagnosis, etc.).

1.2.3 Renal Pathophysiology

1.2.3.1 Acute Kidney Injury

Previously known as acute renal failure, acute kidney injury (AKI) is defined as a rapid decline in GFR that is represented by either increased serum creatinine levels (absolute, ≥0.3 mg/dL; percentage, ≥50%; or 1.5-fold from baseline) or reduced urine production (<0.5 mL/kg/hr for >6 hours), where the injury is reversible.[18-20] AKI is grouped into three main etiologies: prerenal, postrenal, and intrinsic. Prerenal AKI results from a decrease in renal perfusion which may be caused by hypovolemia, impaired cardiac output, peripheral vasodilation or renal vasoconstriction, where renal parenchyma is undamaged following prerenal AKI and injury can be readily corrected with volume repletion. Postrenal AKI results from obstruction of the urinary tract and urinary flow, mainly due to cancerous tumors and ureteral stones, and can be treated with surgical interventions aimed at removing the obstruction. Intrinsic AKI represents the widest variety of kidney injury and can result from damage to the renal tubules (acute tubular necrosis due to ischemia or nephrotoxicity which goes though stages of injury, plateau, and recovery), glomeruli (glomerular damage due to acute glomerulonephritis), interstitium (acute interstitial nephritis due to infections or drugs/medications), and vasculature (intrarenal vessel damage due to malignant hypertension, atheroembolic disease, and vasculitides).[21,22]

Another important cause of AKI is contrast-induced nephropathy (CIN), which has traditionally defined by a ≥25% (0.5 mg/dL) increase in serum creatinine levels within 48-72 hours of the administration of contrast media.[21] Important risk factors for CIN are older age, diabetes, underlying kidney disease, and hypovolemia, with common prophylaxis

including using low contrast doses, using iso- and low-osmolarity contrast media, employing pre-hydration, and temporary halting the administration of compensatory mechanism-attenuating drugs.[21] More recently, the American College of Radiology and the National Kidney Foundation have separated kidney injury following contrast agent administration into contrast-associated AKI (any AKI occurring within 48 hours after the administration of contrast media) and contrast-induced AKI (subset of contrast-associated AKI that can be causally linked to contrast media administration) in order to emphasize that many clinical manifestations of AKI may be coincident with, but causally unrelated to, intravenous contrast media administration.[23] Although AKI resulting from CIN has historically been a clinical concern (especially in kidney disease patients who have impaired renal clearance of contrast), recent literature has disputed the nephrotoxicity of contrast media, with various clinical trials failing to demonstrate contrast-induced kidney injury.[23,24]

1.2.3.2 Chronic Kidney Disease

A long-term decrease in renal function is known as chronic kidney disease (CKD). CKD is divided into 5 stages based on GFR and markers/signs of kidney damage, most commonly being proteinuria (abnormally high levels of protein in urine). In terms of decreasing GFR, the stages of CKD are categorized as follows:

CKD Stage	1	2	3	4	5
GFR (mL/min/1.73m^2)	≥90	60-89	30-59	15-29	<15

The two primary causes of CKD in developed countries are diabetes (diabetic nephropathy) and hypertension (hypertensive nephrosclerosis), followed by other conditions such as glomerulonephritis, polycystic kidney disease and lupus nephritis.[25]

In diabetic nephropathy, proteinuria reflects glomerular damage and increased glomerular permeability to macromolecules. Hyperglycemia in these patients may cause kidney damage via advanced glycation product accumulation, increased growth factor expression, and inflammatory factor activation.[26] Increased production of angiotensin II due to hyperglycemia causes negative hemodynamic (induction of systemic vasoconstriction, increased glomerular arteriolar resistance, increased glomerular capillary pressure) and nonhemodynamic (increased glomerular capillary permeability, filtration surface area reduction, extracellular matrix protein enhancement, stimulation of renal proliferation and fibrogenic cytokines) effects.[26] In addition, the glomerular filtration barrier is harmed by increasing proteinuria resulting from the diabetic state, where decreased size- and charge-selectivity, reduction in slit-pore density, and prominent ultrastructural abnormalities lead to decreased filtration barrier effectiveness. In particular, decreased expression of nephrin and podocin, along with increased endothelin production (induced by hyperglycemia and angiotensin II), result in podocyte injury, decreased podocyte density, and increased foot process width, all of which contribute to loss of glomerular filtration barrier permselectivity.[26]

In hypertensive nephrosclerosis, chronic systemic hypertension is transmitted to the glomerular arterioles. Following initial barometric compensation by the afferent arteriole, long-term constriction of the smooth muscle cells leads to hypertrophy and barotrauma-induced release of inflammatory cytokines and extracellular matrix

components (e.g., fibrin and collagen). Hyaline arteriosclerotic lesions form around endothelial cells, resulting in narrowing of the arteriolar lumen and chronic ischemia which causes glomerular atrophy and hyalinization.[27] In addition to the degree of systemic hypertension, as well as the transmission of systemic hypertension to the glomerulus, the development of hypertensive nephrosclerosis also depends on the tissue's susceptibility to barotrauma, which is based on genetic factors, proinflammatory conditions, and the presence of comorbidities (e.g., overactivity of renin-angiotensin system in diabetic state).[28]

Complications associated with CKD include cardiovascular disease, anemia, mineral metabolism abnormalities, and malnutrition.[29] Patients with CKD have significant morbidity and mortality from cardiovascular disease, sharing similar predictors of more rapid progression (diabetes, hypertension, inflammation, anemia, hypervolemia), as well as strategies for risk factor reduction. Anemia in CKD is associated with ischemic heart disease, left ventricular hypertrophy, and impaired quality of life, and maintenance of erythropoiesis (via iron supplementation or erythropoietin stimulating agents) can effectively restore hemoglobin levels. Abnormalities in the mineral metabolism of CKD patients result in altered serum levels of calcium, phosphorous, parathyroid hormone, and vitamin D, and treatment with supplementation and dietary restriction are needed to manage hyperparathyroidism and CKD mineral-bone disorder. Malnutrition is common in late-stage CKD, and extensive guidelines for assessment of nutritional status and dietary management help mitigate the complications of kidney disease.[29]

In patients with CKD secondary to diabetic, glomerular, and hypertensive or vascular diseases, the strongest predictors of more rapid progression are hypertension

and the degree of proteinuria. Treatment of these conditions in order to control CKD progression involves lifestyle modification and drug administration (e.g., angiotensin-converting enzyme inhibitors, angiotensin receptor blockers, etc.).[29]

1.2.3.3 End-Stage Renal Disease

Patients who progress to stage 5 of CKD (i.e., GFR drops to <15 mL/min/1.73m^2) are categorized as having renal failure, or end-stage renal disease (ESRD). In developed countries, ESRD is most commonly caused by diabetic nephropathy and hypertensive nephrosclerosis (followed by glomerulonephritis), and patients with ESRD develop a number of clinical and biochemical disorders related to uremia (abnormally high levels of nitrogenous waste compounds, such as urea, in blood).[3,7] Accumulation of low- and middle-molecular weight toxins leads to a host of deleterious effects such as neurotoxicity, reduced drug protein binding, and impaired monocyte function. Loss of regulation of fluid and electrolytes necessitates dietary modification for limiting sodium, potassium and water intake. Loss of hormonal functions results in defective production of erythrocytes and calcitriol, as well as enhanced activity of the renin-angiotensin system.[7]

As survival at this stage of kidney diseases is extremely poor and preservation of homeostasis is no longer possible, patients and their healthcare providers must consider implementing some form of renal replacement therapy. The decision to initiate renal replacement therapy is usually driven by some combination of extremely low GFR (<10 mL/min/1.73m^2), high levels of urea (blood urea nitrogen >120 mg/dL) or creatinine (>10 mg/dL), and severe clinical manifestations (e.g., refractory hypertension, fluid overload, pericarditis, etc.).[7] Once the decision to initiate renal replacement therapy is made, it is

very important that the patient is prepared both physically (e.g., vascular access for dialysis) and mentally (e.g., potentially indefinite treatment).[7]

1.3 Renal Replacement Therapy

1.3.1 Kidney Transplantation

Transplantation is associated with the best survival for all patients, making it the preferred method of renal replacement therapy (RRT). It requires the patient to undergo thorough clinical workup to help ensure that the transplant surgery is successful.[30] Transplantation can be done with, and is limited by the number/availability of, kidney(s) from a cadaver (i.e., deceased donor) or living donor. The 1-year kidney graft survival for living and deceased donor transplantation are 95% and 90%, respectively.[30]

Although kidney transplant recipients have improved survival compared to patients receiving other forms RRT, they are still considered to have CKD (irrespective of GFR or presence/absence of kidney damage markers) and frequently have CKD-related complications, the prevalence of which increases with declining GFR. The manifestation of CKD-related complications in a transplant recipient depends on the duration and degree of kidney disease prior to transplantation, as well as the degree of kidney function achieved following transplantation (average of approximately 50 mL/min/1.73m^2).[31]

1.3.2 Peritoneal Dialysis

Peritoneal dialysis (PD) is an alternative RRT modality for ESRD patients that has a number of putative benefits, such as being able to be performed at home due to minimal mechanical requirements.[30] During PD, dialysate is introduced into the cavity of the

patient's own peritoneum, which is lined with a capillary-rich membrane. Solutes and fluid are exchanged between dialysate and blood across the porous walls of peritoneal capillaries, which act collectively as a dialysis membrane.[30]

At the initiation of a PD treatment, dialysate fluid, which contains solutes (e.g., sodium chloride, bicarbonate) and an osmotic agent (e.g., glucose), is infused into the peritoneal space. The resulting high osmotic pressure gradient across the peritoneal barrier (i.e., between dialysate and blood) results in UF, transporting excess water from blood to dialysate for removal.[32] Water is also transported from dialysate to blood due to the hydrostatic pressure gradient between dialysate (higher pressure) and the peritoneal tissue interstitium (lower pressure). In addition, bidirectional solute transport through the peritoneal barrier occurs during PD primarily via concentration gradient-based diffusion.[33] Following several hours of treatment, the peritoneal cavity is drained, the dialysate effluent is discarded, and fresh dialysate is introduced to initiate the next PD cycle.

As long as a patient does not have any abdominal wall defects, they can have a catheter placed and be put on PD.[30] However, most patients cannot remain on PD indefinitely, and eventually must be switched to hemodialysis (HD). Transferring from PD to HD may be due to modality-related (e.g., infections, inadequate dialysis, UF failure, catheter problems), system-related (e.g., lack of infrastructure, lack of patient modality education/training), and patient-related causes (e.g., patient burnout, loss of residual renal function, malnutrition, diabetic/abdominal/respiratory complications).[34]

1.3.3 Hemodialysis

The most common form of RRT is hemodialysis (HD), which can be done at home (conventional, short daily, or nocturnal) or, more commonly, in-center, for 4-hour sessions thrice weekly.[30] A patient who is to initiate HD requires some form of vascular access for repeated access to their circulation, the most preferable form being the arteriovenous fistula (surgical anastomosis between an artery and nearby vein which matures to allow for frequent needle cannulation). Other vascular access options include arteriovenous grafts (interposed synthetic- or bio-graft which connects an artery and vein) and central venous catheters.[35]

The goal of HD is to remove excess fluid and accumulated metabolic waste products, as well as to correct blood electrolyte composition, by the facilitated exchange between the patient's blood and a dialysate fluid across a semipermeable membrane. This process is accomplished via diffusion (transport of solutes between blood and dialysate based on concentration gradients) and UF (transport of solvent and solutes between blood and dialysate based on pressure gradients).[7] Therefore, during HD, the removal of waste products and excess fluid is accomplished via diffusion and UF, respectively. While UF effectiveness can be assessed with pre- and post-HD patient weighing (i.e., amount of intradialytic fluid removed), solute removal can be quantified by the normalized clearance per dialysis, or Kt/V (K = dialyzer urea clearance, t = dialysis duration, V = urea distribution volume). The Kt/V value, which can be computed from $C = C_0 \cdot \exp[-Kt/V] \rightarrow Kt/V = \ln[C_0/C]$ (where C_0 and C are the pre- and post-dialysis blood urea concentrations, respectively), is a marker of dialysis adequacy which has been shown to strongly correlate with clinical outcomes.[36]

A typical HD circuit (pictured in Figure 1.2) is made up of two sub-circuits: the blood circuit (patient side) and the dialysate circuit (dialysis machine side).[7] The blood circuit consists of a blood pump (controls blood flow rate), blood pressure sensors, and a detector which monitors the presence of air within the blood line. The dialysate circuit consists of a conductivity meter (monitors dialysate composition), temperature and pressure sensors, flow rate controls, a blood leak detector, dialysate and UF pumps, and a dialysate flow equalizer (maintains equal inflow and outflow rates). Following each HD session, the system is disinfected by administering chemical agents into the hydraulic circuits of the machine.[7]

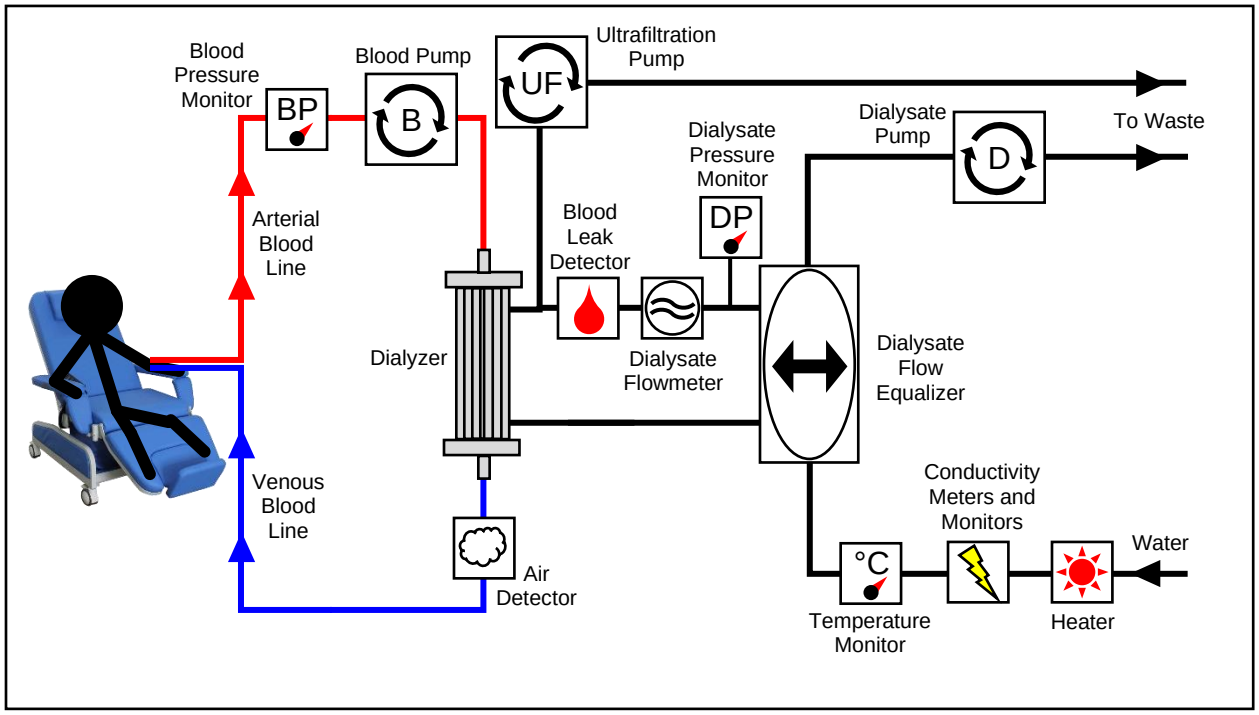

Figure 1.2: Typical HD circuit, which is made up of two sub-circuits: the blood circuit (patient side, red parts) and the dialysate circuit (dialysis machine side, black parts). Adapted from *Long-term Hemodialysis* by Man, Zingraff and Jungers, 1995.[7]

Dialysate and blood both enter and exit a dialyzer, which contains a porous, semipermeable membrane across which solutes and solvent are exchanged during HD. The hollow-fiber dialyzer is the most commonly used type in the clinic, consisting of several thousand bundled hollow fibers (diameter of 200-300 μm, wall thickness of 10-40 μm). Blood flows within the fibers while dialysate flows between and around the fibers, allowing for a high area of contact (and therefore a highly efficient exchange) between blood and dialysate.[7,36] The dialysate is composed of various electrolytes (e.g., sodium, potassium, calcium, magnesium, chloride, acetate, bicarbonate, glucose) and is designed to correct solute abnormalities which develop in ESRD patients during the interdialytic interval.[7] The two commercially available types of HD membranes are cellulose-based (chemically treated to improve bioincompatibility) and synthetic (polymer-based, biocompatible, increasable pore sizes for improved fluid and solute removal).[7,36]

1.4 Effects of HD on ESRD Patients

1.4.1 HD-Induced Circulatory Stress

Although HD is a life-saving therapy, patients are known to develop a wide range of complications. An important driving force behind the development of these complications is thought to be recurrent HD-induced circulatory stress,[6] which comes about as follows: during the interdialytic period, patients accumulate excess fluid and become hypervolemic. Then during a typical HD session, correspondingly ambitious UF targets (e.g., high UF volume and rate to achieve a desired post-HD dry weight) result in a large reduction in plasma volume,[6,37] where the rate of fluid removal exceeds the plasma-refilling rate (i.e., from extravascular to intravascular compartments), leading to

hypovolemia.[7,38] A corresponding reduction in cardiac output,[39,40] coupled with autonomic dysfunction and impaired compensatory physiological responses (e.g., no central redistribution of blood volume, no increase peripheral vascular resistance),[41] leads to intradialytic hypotension (IDH),[7,38] which makes vital organs susceptible to ischemic challenge and represents the hallmark of systemic HD-induced circulatory stress.[6]

Approximately one quarter of HD treatments are complicated by IDH (commonly defined as a symptomatic drop in systolic blood pressure >20 mmHg),[7,38] which is an independent predictor of mortality in HD patients.[42] In addition, higher rates of UF (e.g., due to higher UF volume requirements and/or shorter HD treatment times) have been shown to be independently associated with an increased HD patient risk of mortality.[37]

1.4.2 Effects of HD-Induced Circulatory Stress on Different Organs

Patients with ESRD who are on maintenance HD develop a wide range of clinical pathologies, and a great deal of research has been dedicated to characterizing the role HD-induced circulatory stress in the development of these complications. In particular, various functional imaging techniques have been used to study the hemodynamic response of multiple vascular beds to HD-induced circulatory stress. This section will focus on the effects of maintenance HD on the heart and brain.

1.4.2.1 The Heart

Cardiovascular disease is the leading cause of mortality in HD patients. Many patients have some form of cardiovascular disease at the initiation of HD (e.g., atherosclerotic heart disease, heart failure, peripheral vascular disease, previous strokes)

and are at increased risk of death due to arrythmias and sudden cardiac arrest.[43] To explore this pathophysiology, myocardial contractile function and perfusion have been assessed in multiple functional imaging studies.

The hallmark of HD-induced circulatory stress in the heart is myocardial stunning, which is the delayed recovery of regional myocardial contractile function after ischemia-reperfusion despite the absence of irreversible damage and despite restoration of normal blood flow.[44] Myocardial stunning can be quantified using speckle-tracking echocardiography, a 2D ultrasound technique which uses specialized software to track naturally occurring myocardial speckle signals over multiple temporal frames in the various segments of the left ventricle.[45] Next, the magnitude of myocardial deformation in different directions is resolved, and strain and strain rate curves are generated, from which the longitudinal strain is measured from the apical long-axis image data. Longitudinal strain can be assessed globally and segmentally (12 left ventricular segments), allowing for the determination of the presence of myocardial stunning (defined as a reduction in longitudinal strain of 20% in two or more segments of the left ventricle caused by regional wall motion abnormalities (RWMAs)).[46,47] Increased development of RWMAs has been shown to be associated with greater IDH and UF aggressiveness.[48] In addition, HD patients who develop RWMAs over the course of their maintenance HD therapy have significantly increased mortality and decreased left ventricular ejection fraction compared to those patients who do not develop RWMAs.[48]

To identify the association between myocardial stunning and perfusion, dynamic positron emission tomography (with radiolabeled water, $H_2{}^{15}0$-PET, and nitrogen-13 ammonia, ^{13}N-NH_3-PET) has been used to demonstrate that myocardial blood flow

significantly declines during HD.[46,49] Contemporaneous echocardiography was used to identify a relationship between development of RWMAs and a greater reduction in myocardial perfusion,[46] helping to more fully describe the ischemic nature of myocardial stunning. As a result, the pathological development of cardiovascular mortality in HD patients could now be summarized as follows: myocardial ischemia-reperfusion injury due to HD-induced circulatory stress results in myocardial stunning. Over time, recurrent episodes of myocardial ischemia and stunning result in RWMAs which persist post-HD. The myocardium is permanently damaged and suffers from contractile dysfunctional, which eventually leads to arrythmias and sudden cardiac arrest in this patient group.[6,44] This process is depicted in Figure 1.3.

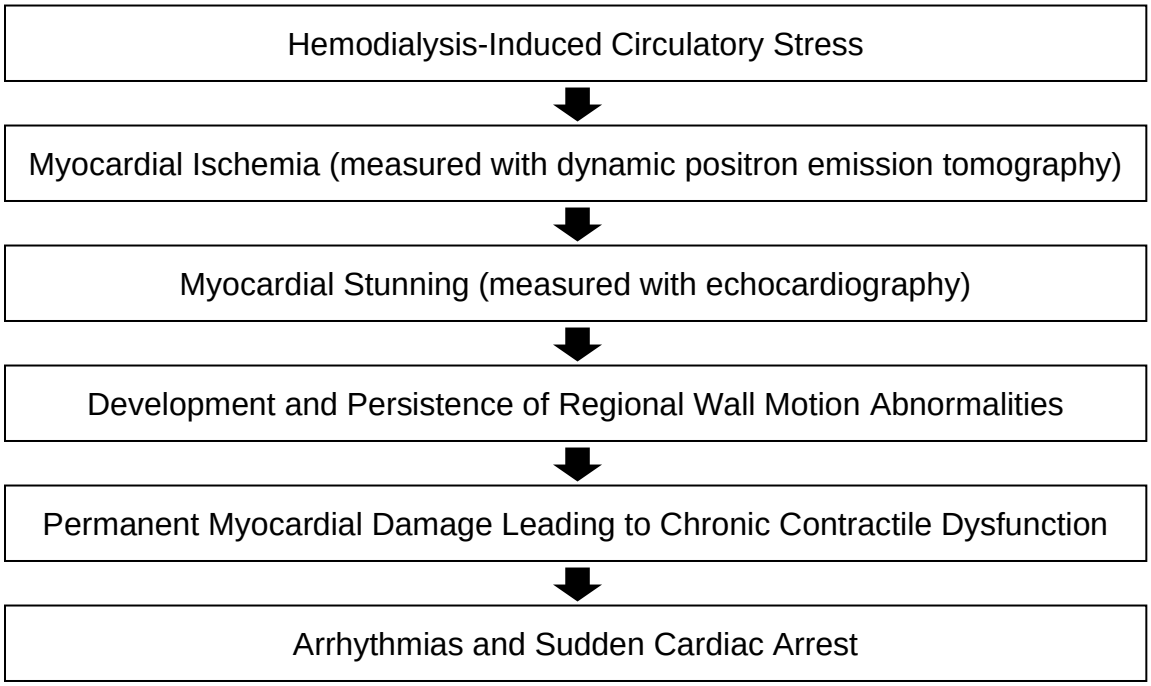

Figure 1.3: Pathophysiological progression to cardiac mortality in HD patients. Myocardial ischemia-reperfusion injury (measured with dynamic PET) due to HD-induced circulatory stress results in myocardial stunning (measured with echocardiography). Over time, recurrent episodes of myocardial ischemia and

stunning result in RWMAs which persist post-HD. The myocardium is permanently damaged and suffers from contractile dysfunctional, which eventually leads to arrythmias and sudden cardiac arrest in this patient group.

1.4.2.2 The Brain

Cognitive impairment is common in HD patients, who have been shown to suffer from important clinical complications such as dementia and depression.[50] Although cognitive decline develops as kidney disease progresses, the initiation of HD leads to even greater levels of cognitive impairment and loss of functional status, which have been linked to higher mortality rates in this population.[51] Research studies targeting this pathophysiology have assessed cerebral hemodynamics, structure and function using various imaging techniques.

Cerebral perfusion has been measured with dynamic $H_2{}^{15}0$-PET-CT, demonstrating a significant decline over the course of HD.[52] Surrogate measures of perfusion, including cerebral arterial mean flow velocity (with transcranial Doppler ultrasound) and cerebral oxygen saturation (with near-infrared spectroscopy), similarly revealed that the brain experiences ischemic challenges during HD.[53,54] In addition to hemodynamics, structural analysis with T1- and T2-weighted magnetic resonance imaging (MRI) has revealed three important cerebral pathologies in maintenance dialysis patients: silent cerebral infarction (asymptomatic ischemic insult which is a predictor for the development of symptomatic infarcts or hemorrhagic stroke),[55,56] cerebral atrophy (e.g., ventricular enlargement, brain volume reduction, focal lesions),[57,58] and leukoaraiosis (white matter changes due to ischemia-induced loss of myelin and axons, and is a risk for dementia and stroke development).[59,60] The presence of these

pathologies represents accelerated vascular aging, is a predictor for the development of strokes and dementia, and is associated with inflammation, hypertension and vascular disease.[6]

In order to spatially correlate cerebral structural abnormalities with functional measures, diffusion tensor imaging (specialized diffusion-weighted MRI technique), which can detect ultrastructural white matter abnormalities and assess white matter structural integrity, has been used for brain imaging in HD patients.[61] This imaging modality quantifies the diffusion of water molecules within tissue using anisotropy (assessment of diffusion directionality that represents the integrity of white matter tracts) and diffusivity (degree of random water motion that represents white matter structural damage) metrics.[62] Research studies utilizing diffusion tensor imaging have collectively demonstrated two main findings: First, HD patients have significantly different anisotropy and diffusivity values compared to healthy controls, indicative of white matter damage and structural integrity loss. Second, after imaging the same HD patient group over two timepoints separated by 12 months, the observed pattern of quantitative changes (i.e., increased anisotropy and decreased diffusivity) matches what is observed in acute ischemic stroke models and suggests that HD results in significant brain injury.[61-63]

1.4.3 Strategies to Ameliorate Circulatory Stress

As the role of HD-induced circulatory stress in the development and progression of complications in ESRD patients has become well-recognized, research studies have explored various intra- and inter-dialytic strategies that could help mitigate the negative effects of HD.

Aggressive UF is one of the primary driving forces of HD-induced circulatory stress, and stems from the clinical need to remove a certain amount of fluid and/or metabolic waste products during HD in order to bring the patient's body weight and plasma composition to clinically prescribed levels. Conventionally, this is achieved with thrice weekly HD at 3-5 hours per session. To lessen the strain of UF (and improve both the control of body fluid volume and clearance of middle molecules), HD treatment times could be extended, or the weekly frequency of treatments could be increased, both of which allow for lower UF rates and more sufficient time for removal of larger molecules.[64-66] In addition to schedule modifications, increased clearance of middle molecules (through the use of high flux, synthetic dialysis membranes) can help to ease intradialytic UF burden.[64,67] Also, biofeedback HD systems, which monitor intradialytic decreases in relative blood volume and dynamically lower the UF rate accordingly in order to try and avoid IDH, have been used to improve the hemodynamic tolerability of HD.[68-70] By considering these aforementioned issues, it can be understood why PD exerts less circulatory stress compared to HD: treatment times are generally longer with PD, intradialytic shifts in fluid volume are more gradual with PD, biocompatibility is inherently greater with PD, and myocardial stunning is much less frequent with PD.[71,72]

Numerous research studies have explored hemodynamic protection from HD-induced circulatory stress by applying some form of ischemic preconditioning, which involves the application of small, controlled ischemic insults prior to a larger, significant insult in order to improve the circulation's hemodynamic tolerability and reduce the magnitude of ischemia-reperfusion injury.[73] Ischemic preconditioning can also be applied remotely (usually by using a blood pressure cuff, inflated to ~200 mmHg, on a peripheral

limb to induce several cycles of transient ischemia-reperfusion), which works to confer hemodynamic protection via systemic neuronal and humoral signal transfer.[74] Because of the consistent, recurrent and predictable nature of HD-induced circulatory stress, HD represents a favorable model to study ischemic preconditioning, where HD patients stand to potentially benefit greatly from preconditioning interventions.[75] So far, while only a handful of studies have explored ischemic preconditioning in HD patients, findings have been positive (e.g., reduction in HD-induced RWMA development), demonstrating the protective potential of this technique.[76]

Another strategy to ameliorate the effects of HD-induced circulatory stress is dialysate cooling (DC), which involves lowering the temperature of the dialysate (and therefore the blood via heat exchange) during HD (typically to 35-36°C).[77,78] This is a favorable intervention to apply in HD patients because (1) it does not adversely affect dialysis adequacy or efficiency, (2) it is universally available and can be implemented at little-to-no additional cost, and (3) patients are generally tolerable of the lower temperatures.[47] Cooling helps improve systemic vascular resistance, promote peripheral vasoconstriction, and increase baroreflex sensitivity variability, allowing for increased shunting of peripheral blood flow to central organs and vascular beds (which are normally at increased risk of HD-induced ischemic insults), as well as an improved vasoactive response for the mitigation of IDH. In addition, higher dialysate temperatures have been linked to increased hemodynamic instability and higher production of nitric oxide, a vasodilatory agent.[79,80] Lastly, cooling lessens organ injury by reducing inflammation, attenuating oxidative stress, and decreasing free radical production, and has demonstrated protective potential in multiple organs in the context of therapeutic

hypothermia.[81,82] Multiple studies have explored the effectiveness of DC at ameliorating the effects of HD-induced circulatory stress, demonstrating that this intervention (1) lowers IDH incidence,[79] (2) abrogates myocardial stunning,[47] and (3) maintains cerebral integrity.[62] Some patients report being uncomfortable or having cold-related symptoms (e.g., shivering) with DC, but alternate cooling approaches such as individualized cooling (lowering dialysate temperature to 0.5°C below patient's core temperature) have shown to mitigate these negative side effects compared to standard fixed-temperature cooling.[62,83,84]

1.5 The Liver

The liver receives approximately 25% of the cardiac output.[85] In addition, various toxins and products of intestinal absorption are prevented from reaching and entering the systemic circulation by the liver, which receives these substances via the portal circulation (majority of liver blood flow) and processes them, thereby functioning as a barrier.[86] Therefore, the liver may represent another vascular bed that is vulnerable to HD-induced circulatory stress, a hypothesis which to date has been scarcely explored. In addition to its effects on hemodynamics, the effects of HD on hepatic function (e.g., liver excretory function assessment, liver injury assessment) is currently unclear and valuable to study.

The liver is the largest visceral organ, carrying out many important functions. Hepatocytes (parenchymal liver cells) are involved in uptake, transport, storage, synthesis, biotransformation and degradation of a variety of substances, including proteins, lipids, carbohydrates, hormones, drugs and bile.[87] Blood is supplied to hepatocytes through a specialized capillary system of fenestrated sinusoids, which

contain Kupffer cells. These macrophagic sinusoidal cells are responsible for maintenance of normal liver function, and are involved in processes such as phagocytosis of particulate matter, detoxification and clearance of endotoxin, secretion of mediators, etc.[87]

The liver's total blood supply is divided into two components: approximately 30% comes from the high-pressure, well-oxygenated hepatic artery (branches from abdominal aorta), while the remaining 70% comes from the low-pressure, mildly-oxygenated, nutrient-rich portal vein (outflow from splanchnic organs).[85] These blood supplies meet, mix and travel through the network of sinusoids, allowing for exchange of oxygen, substrates and metabolites with hepatocytes.[87] Due to its unique dual blood supply, the liver can effectively regulate its blood flow via the hepatic arterial buffer response, which works to increase/decrease hepatic arterial perfusion in response to a decrease/increase in portal venous perfusion.[85]

1.6 Other Important Issues in HD Patients

1.6.1 Loss of Residual Renal Function

Most ESRD patients who start on RRT are not completely anuric and still produce some small volumes of urine on a daily basis.[88] This small level of remaining GFR, known as residual renal function (RRF), provides several important physiological advantages that cannot be substituted with RRT, such as secretion of organic acids, various endocrine functions, and a more liberal fluid intake for patients.[89] The presence and preservation of RRF after HD initiation is associated with a host of beneficial effects, including: better control of serum electrolytes, hypervolemia and hypertension, improved

nutrition, reduced blood pressure, left ventricular atrophy and anemia, and higher middle molecule clearance.[90,91] This latter effect is especially valuable, as middle molecules (uremic toxins weighing 500-60000 Daltons) represent relatively large solutes that are readily cleared by the native kidneys but are difficult to remove with conventional HD (i.e., require high-flux membranes and/or increased treatment time).[36]

Preserved RRF is strongly associated with improved HD patient survival.[92] Even minimal amounts of RRF have been shown to be associated with improved survival, where every additional 0.5 mL/min/1.73m^2 increase in residual GFR is associated with a 7% increase in survival and a 250 mL increment in urine output correlates with a 36% decrease in the relative risk of death.[93] The importance of long-term RRF maintenance has been emphasized by the 2006 National Kidney Foundation KDOQI Guidelines, which recommended that “one should strive to preserve RKF in HD patients”.[94]

Despite its importance in conferring health and survival benefits, RRF characteristically declines rapidly in patients with ESRD upon initiation of RRT, with a faster rate of decline for HD compared to PD (although both decline by approximately 50% or more during the first 12 months of RRT).[89] This decline has consistently been linked to poorer outcomes and increased mortality.[95] As RRF declines, more aggressive fluid removal in subsequent HD sessions becomes necessary, increasing the burden of HD-induced circulatory stress.

Numerous factors are associated with RRF decline, such as age, CKD cause, bioincompatible dialysis membranes, hypertension, and hemodynamic instability during HD (e.g., IDH).[96] While the pathophysiological mechanism(s) behind RRF loss in HD patients remain unknown, it has been hypothesized that recurrent ischemic insults to the

kidney parenchyma (i.e., renal manifestation of HD-induced circulatory stress) may cause permanent, irreversible injury leading to declining RRF.[97,98] However, research studies to date have not focused on measuring intradialytic renal perfusion and confirming the presence of HD-induced renal ischemia. In addition, the relationship between renal perfusion with RRF loss has not been explored, preventing the evaluation of potential preservation interventions.

1.6.2 Endotoxemia

Endotoxin is a gut-derived proinflammatory agent. It is found on the cell wall of gram-negative bacteria in the gastrointestinal tract and consists primarily of lipopolysaccharide.[99] Endotoxin is a natural constituent of portal venous blood and is therefore normally received by the liver from the gut.[100,101] Under healthy conditions, hepatic Kupffer cells efficiently and selectively phagocytose and clear endotoxin,[102] limiting its presence in the systemic circulation.

However, increased endotoxin levels (i.e., endotoxemia) have been found in HD patients, with higher amounts of endotoxin compared to both the general population and to earlier stage CKD patients.[103] Endotoxemia in HD patients has been shown to be associated with drivers of HD-induced circulatory stress (UF and IDH), markers of injury and inflammation (cardiac troponin T and C-reactive protein), cardiovascular complications (myocardial stunning and left ventricular dysfunction), and a higher risk of mortality.[103,104] Upon entering the system circulation, endotoxin complexes with CD14 and lipopolysaccharide binding protein,[105] which goes on to activate monocytes and macrophages, as well as to increase the levels of proinflammatory cytokines (e.g., TNF-

α, IL-6).[106,107] This results in a systemic chronic inflammatory state, which is characteristic of ESRD patients on HD and known to be correlated with an increased risk of cardiovascular disease.[103]

Increase endotoxin translocation across the intestinal barrier during HD is understood to come about as follows: ESRD patients characteristically show signs of gut mucosal ischemia (such as gastric intramucosal acidosis),[108] which, when compounded with intradialytic hemodynamic effects (such as HD-induced circulatory stress leading to reduced splanchnic blood volume),[109,110] results in mesenteric ischemia.[103] This hypoperfusion has previously been shown to alter bowel morphology, permeability, and hemodynamics, resulting in the disruption of gut mucosal structure and function, and an increase in gut permeability.[111] Consequently, there is a loss in the selective barrier function of the bowel,[111] leading to increased translocation of enteric bacterial products (such as endotoxin) across the intestinal barrier.[112]

Understanding that the liver normally functions as an endotoxin barrier, that there is increased translocation of endotoxin during HD, and that HD patients are characteristically burdened by endotoxemia, it is reasonable to suggest that HD may somehow disrupt liver hemodynamics and function. By studying the liver's response to HD-induced circulatory stress (which may be quite different from other organs due to its unique dual blood supply), it may be possible to better understand how HD leads to the perpetuation of endotoxemia. In addition, understanding the liver's role in endotoxemia may offer the opportunity to develop effective mitigation strategies.

1.6.3 No GFR Measurement Method That Is Accurate and Feasible

As discussed in section 1.6.1, maintenance of RRF is extremely valuable in terms of yielding improved clinical outcomes and quality of life. However, despite its importance, a patient's RRF is rarely taken into account during the design of their dialysis prescription, and instead, incident HD patients are most commonly prescribed the clinical standard of thrice-weekly HD.[113-115] Various studies have demonstrated that compared to patients initiating RRT with incremental HD (i.e., starting with once- or twice-weekly HD, and increasing frequency of weekly HD sessions in accordance with decreasing RRF), those initiating with thrice-weekly HD tended to lose RRF faster in the first 12 months of HD and have a lower survival.[95,114,115] Therefore, adjusting a patients' HD prescriptions based on changes in their RRF may yield better outcomes for ESRD patients, and the importance of this philosophy has been emphasized by the 2015 KDOQI Hemodialysis Adequacy Guidelines, which state that "…in patients with significant residual native kidney function (Kru), the dose of hemodialysis may be reduced provided Kru is measured periodically to avoid inadequate dialysis".[116]

In order to fully realize this treatment philosophy, the assessment of renal function (i.e., GFR) must be accurate, reliable and feasible. Estimation of GFR (i.e., eGFR) from population-based equations is unsuitable for HD patients, as these equations are based on data collected from earlier stage CKD patients and generate erroneous results when applied to the ESRD population.[12,114] Therefore, measurement of GFR (i.e., mGFR) is necessary in this patient group, which is conventionally achieved via urinary or plasma clearance of endogenous or exogenous filtration markers. However, a number of

disadvantages associated with these mGFR techniques limit their use clinically, particularly in HD patients:[8,12,13,114,117-119]

- Endogenous marker (e.g., creatinine, urea, etc.) levels directly affected by HD and are not in a steady state during the interdialytic period
- Urine sampling is unreliable (e.g., patient-dependent) and cumbersome (e.g., 24-hour collection time, may require urinary catheterization, etc.)
- Plasma sampling takes a long time (i.e., determination of disappearance curve takes longer with lower GFR) and is inaccurate due to extrarenal elimination of filtration marker (even greater effect at lower GFR)
- Issues with availability and/or accessibility of certain exogenous markers (e.g., inulin in limited supply, ^{51}Cr-EDTA and ^{99m}Tc-DTPA not commercially available in the United States and Europe, respectively, etc.)
- No standardization of assays used to measure filtration marker levels
- Impossible to assess single-kidney GFR

These limitations may be overcome by measuring GFR using medical imaging approaches. Compared to standard mGFR methodology, imaging-based mGFR can be obtained rapidly, does not require urine and/or plasma sampling, and can be assessed contemporaneously with additional structural and functional information.[14] Over the past several decades, a multitude of research studies have explored the use of nuclear medicine-, CT-, and MRI-based approaches for measuring GFR in both animal and human subjects in various clinical contexts (e.g., renal cell carcinoma, chronic kidney disease, etc.), showing strong agreement with standard mGFR methods.[16,17,120-124] However, these techniques have never been applied in the context of ESRD and/or HD

patients. Therefore, there is currently no go-to clinical GFR quantification approach available for this population that can provide a rapid, reliable and accurate measurement of kidney function, which is a key requirement for RRF-based HD prescription adjustment.

1.7 CT Perfusion Imaging of Body Organs

In order to address these three issues in HD patients (i.e., loss of RRF, endotoxemia, no GFR measurement method for patients that is accurate and reliable), it is necessary develop methods to measure kidney and liver blood flow and associated hemodynamic parameters (particularly, for the case of kidneys, the extraction efficiency of glomerulus filtered agents like CT contrast agents). Assessment of kidney perfusion is required to confirm that HD-induced circulatory stress causes recurrent kidney ischemia, assessment of liver perfusion is required to explore whether HD leads to increased endotoxin influx from the gut, and assessment of extraction efficiency of glomerulus filtered agents[125] is required to test the feasibility of GFR measurement in HD patients. Computed tomography perfusion (CTP) imaging was used in these developments.

1.7.1 Overview of CTP

CTP is a dynamic radiological imaging technique that measures temporal changes of the x-ray attenuation characteristics in an object/region of interest (e.g., kidney and liver) from an exogenous iodinated contrast agent injected into the systemic circulation.[126] Compared to static imaging with/without contrast (which provides anatomical/structural information in a single temporal snapshot), dynamic imaging captures changes occurring over time via a series of images performed at a single anatomical location following

contrast agent administration, enabling the study of physiological processes that change over time.[127] Upon contrast injection, CTP allows investigation of two processes in kidney function (kidney is used as an illustrative example, and the following discussion applies to other organs/tissues): (1) delivery of contrast (as marker for metabolic waste) by blood flow to the afferent arterioles, and (2) permeation of the glomerular filtration barrier (the basis of glomerular filtration rate measurement, see Chapter 4).[128] These two processes would lead to a transient increase (wash-in) and decrease (wash-out) of contrast agent (concentration) in the kidney over time, which can be measured by a CT scanner as changes in x-ray attenuation (or density in Hounsfield units or CT number). Note that x-ray attenuation is a physical process involving energy much higher than the chemical reaction/interaction of contrast agent with the other molecules within the tissue microenvironment, making CTP highly linear with contrast concentration, a prerequisite for physiological (kinetic) modelling.[128]

1.7.2 Tracer Kinetic Modelling

Tracer kinetic modelling mathematically models the processes involved in the distribution of blood borne tracer (e.g., CT contrast agent) in the target tissue in as few parameters as possible. One class of tracer kinetic models is compartment models, which categorize tracer within tissue into two or three compartments – blood, free and bound tracer – where within each, tracer is assumed to be uniformly mixed and tracer concentration is only dependent on time. Except for the blood compartment, the other compartments may not exist in physically reality, but are nevertheless useful mathematical constructs to facilitate the description of tracer distribution in tissue over

time once the tracer is introduced into the systemic circulation. Treating blood vessels as a compartment assumes that fresh tracer arriving via afferent arterioles will mix instantaneously and uniformly with tracer already in the glomerulus and, more importantly, will filter through the glomerular filtration barrier at a constant rate. However, in real situation, because of the continuous loss of tracer via filtration, there is a tracer concentration gradient from afferent to efferent arterioles, so the filtration rate is not constant during the blood (vascular) transit time of the glomerulus.[128] When tissue tracer concentration was measured at time intervals shorter than the vascular transit, Larson *et al*. showed that blood flow estimated with compartment models can be erroneous.[129]

To avoid the compartment assumption for blood vessels (so as to minimize error in blood flow estimation when the time interval of contrast concentration measurement is short as in CTP studies), in this thesis we used a distributed parameter model to model the blood vessels as a tube with a concentration gradient from the arterial to the venous end.[128] This reflects the filtration of solute across the glomerular filtration barrier into the Bowman's capsule as blood travels down the length of the glomerular capillaries. The distributed parameter model used is the Johnson-Wilson model shown schematically in Figure 1.4.[128,130]

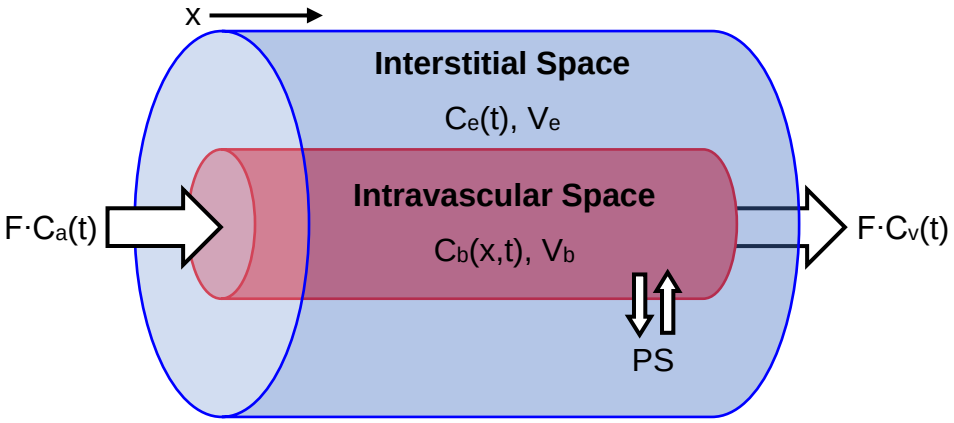

Figure 1.4: Schematic of Johnson-Wilson model. Blood vessels are modelled as a tube. There is filtration of solute (contrast) across the blood-tissue barrier (in the case of kidneys, the glomerular filtration barrier) into the interstitial space as blood travels down the length of the tube, creating a concentration gradient from arterial to venous ends. F = blood flow, $C_a(t)$ = arterial contrast concentration (i.e., arterial input function), $C_e(t)$ = venous contrast concentration, PS = permeability-surface area product, $C_b(x,t)$ = intravascular contrast concentration, V_b = intravascular volume, $C_e(t)$ = interstitial contrast concentration, V_e = interstitial volume. Adapted from *CT imaging of angiogenesis* by Lee, Purdie and Stewart (Q J Nucl Med, Vol 41, p171-187, 2003).[131]

1.7.3 Deconvolution

A central concept in tracer kinetic modelling is the flow-scaled impulse residue function, $R_F(t)$, which is the tissue tracer (contrast) concentration in response to a bolus injection of a contrast mass (numerically) equal to blood flow (F) at the afferent arterioles.[128] If the contrast distribution process(es) in the kidney is unchanging with time, then by the principle of superposition, in response to a systemic injection of contrast giving rise to contrast concentration at the afferent arterioles, $C'_a(t)$, the tissue contrast concentration, Q(t), is given by:

$$Q(t) = C'_a(t) \otimes R_F(t)$$

where $\otimes$ is the convolution operator. As is usually the case, the afferent arterioles, or even afferent artery, is too small to be visualized by CT. As a result, contrast concentration, $C_a(t)$, could be measured at a large artery such as the renal artery or aorta. In that case, $C'_a(t)$ is assumed to be a time-shifted version of $C_a(t)$, which is expressed mathematically as:

$$C'_a(t) = C_a(t - T_0)$$

Where T_0 is the delay in contrast arrival at the afferent arteriole relative to the large artery where $C_a(t)$ is measured. The flow-scaled impulse residue function, RF(t), of the Johnson-Wilson model (as depicted in Figure 1.5) can be expressed as:

$$R_F(t) = \begin{cases} F & ,0 \le t \le MTT \\ F \cdot E \cdot e^{-k(t-MTT)} & ,t > MTT \end{cases}$$

where k (= FE/V_e) is the efflux rate constant. Thus, the distribution of blood borne contrast in the kidney as described by the Johnson-Wilson model can be summarized by four parameters – blood flow (F), extraction efficiency of contrast (E), mean transit time (MTT) and contrast distribution volume (V_e).

In a CTP study, $C_a(t)$ and Q(t) are measured as changes in CT number over time (i.e., time-density curve, TDC) in a larger artery region and the kidney, respectively, and are used to calculate $R_F(t)$ by a mathematical operation called deconvolution. Whereas $R_F(t)$ is the tissue TDC in response to a $C_a(t)$ that is very brief (delta function) from a bolus injection at the afferent arteriole, Q(t) corresponds to a more drawn out $C_a(t)$ from a systemic injection. Thus, to get $R_F(t)$ from Q(t), the influence of $C_a(t)$ has to be removed via deconvolution. This is achieved by iteratively changing the four parameters of $R_F(t)$ – F, MTT, E and k – and T_0 so that the convolution of $R_F(t)$ with $C_a(t–T_0)$ will minimize the sum of squared deviations from the measured Q(t).[128] When the measured $C_a(t)$ is

systematically deconvolved from Q(t) for each small discrete region (for instance, 3×3 pixels) in a CT image, the different parameters obtained can be assembled together to form a parametric (e.g., blood flow, F) map. This process is illustrated in Figure 1.6 in the case of computing kidney blood flow.

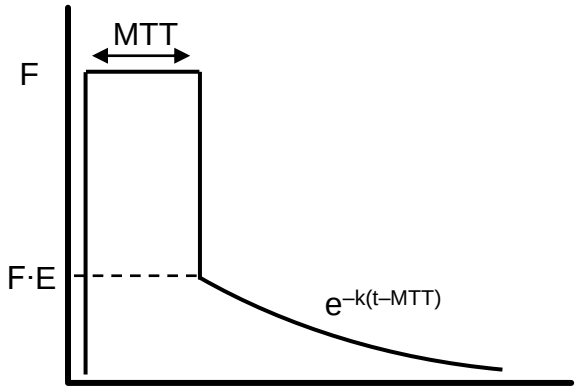

Figure 1.5: Johnson-Wilson model blood flow-scaled impulse residue function. F = blood flow, E = extraction efficiency, MTT = mean transit time, T_0 = contrast arrival time, k = F·E / V_e = efflux rate constant. Adapted from *CT imaging of angiogenesis* by Lee, Purdie and Stewart (Q J Nucl Med, Vol 41, p171-187, 2003).[131]

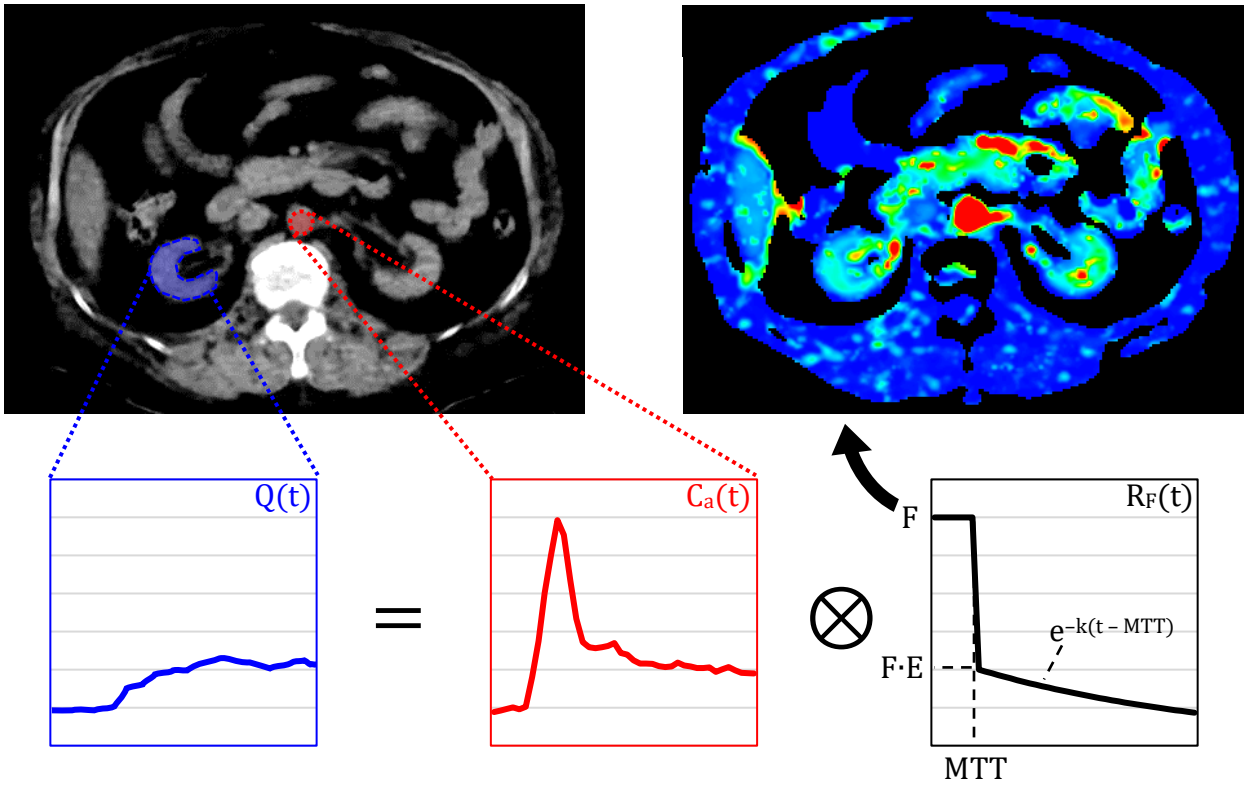

Figure 1.6: Application of tracer kinetic modelling to the computation of physiologic parameters (e.g., renal blood flow). From the dynamic series CT images, the baseline subtracted arterial TDC is deconvolved from each baseline subtracted tissue TDC (i.e., individual tissue curve for each 3×3 pixel block in the CT image) to estimate model (functional) parameters of the flow-scaled impulse residue function (based on non-linear least squares curve fitting), yielding parametric maps (such as blood flow).

1.7.4 CTP Imaging of Liver Perfusion

As discussed in the previous section, measurements of the arterial and the tissue time-density curve are required in order to perform deconvolution and extract functional parameters related to tissue perfusion. While the tissue enhancement (CT density change) of most organs (including the kidneys) results from the inflow of contrast from arteries (i.e., $C_a(t)$ measured from aorta), enhancement of liver parenchyma results from the combined inflow from the hepatic artery and portal vein.[132] However, the portal vein

TDC, $C_{PV}(t)$, cannot be approximated by that of the hepatic artery, $C_{HA}(t)$. There is an inherent delay between contrast agent delivery through the arterial and portal routes: while hepatic arterial blood branches off and arrives directly from the abdominal aorta, portal venous blood is delayed and diluted as it passes through and drains from the splanchnic organs. Owing to these aspects of the liver's blood supply, quantification of hepatic perfusion can be separated into the hepatic arterial and portal venous components by splitting up the arterial input function into two parts:

$$Q(t) = C_a(t) \otimes R_F(t) = [\alpha \cdot C_{HA}(t) + (1-\alpha) \cdot C_{PV}(t)] \otimes R_F(t)$$

Here, α is the hepatic perfusion index (also known as the hepatic arterial fraction), which is the ratio of hepatic artery perfusion to total liver perfusion (i.e., sum of hepatic artery and portal vein perfusion) and is computed as an additional parameter during deconvolution.[132]

1.8 Motivation and Objectives of Thesis

Millions of people around the world are afflicted by CKD. While HD is an effective treatment for those who progress to ESRD, it inflicts recurrent circulatory stress during each treatment session, thereby perpetuating a host of comorbidities in this patient population. The quantitative characterization of these hemodynamic perturbations (including GFR measurement) may inform the development of effective adjunctive treatments to potentially slow RRF loss and mitigate endotoxemia.

Because HD is typically administered in a clinical setting, performing hemodynamic measurements using non-invasive and minimally disruptive methodology, such as advanced functional imaging, is highly desirable. Being able to assess the effects of HD-

induced circulatory stress on multi-organ hemodynamics during live HD sessions can provide novel insights into how certain complications develop in this patient population, and how these developments may be slowed or stopped. This thesis will describe the application of CTP imaging to ESRD patients on HD in order to explore the effects of this treatment modality on renal and hepatic blood flow and function.

This thesis is divided into three research projects (chapters 2, 3 and 4) with the following objectives:

- Project 1: effects of HD on kidney blood flow, and relationship to RRF loss
    - Examine how HD affects renal perfusion
    - Explore the relationship between changes in renal perfusion and myocardial dysfunction (a hallmark of HD-induced circulatory stress) during HD
    - Investigate whether cooling can protect the kidneys from HD-induced circulatory stress
- Project 2: effects of HD liver blood flow and function, and relationship to endotoxemia
    - Examine how HD affects hepatic perfusion and function
    - Explore the relationship between changes in hepatic perfusion and endotoxin levels during HD
    - See if cooling can maintain liver hemodynamics and limit systemic exposure to endotoxin
- Project 3: measuring GFR in HD patients using CTP
    - Develop methodology for CTP-based GFR assessment
    - Explore the feasibility of using CTP imaging to quantify GFR in HD patients
    - Assess how GFR changes over the course of HD

1.9 References

1. Hill NR, Fatoba ST, Oke JL, et al. Global Prevalence of Chronic Kidney Disease - A Systematic Review and Meta-Analysis. *PLoS One*. 2016;11:e0158765.

2. GBD Chronic Kidney Disease Collaboration. Global, regional, and national burden of chronic kidney disease, 1990–2017: a systematic analysis for the Global Burden of Disease Study 2017. *Lancet*. 2020;395:709-733.

3. Canadian Institute for Health Information. Annual Statistics on Organ Replacement in Canada: Dialysis, Transplantation and Donation, 2009 to 2018. 2019;

4. Manns B, McKenzie SQ, Au F, et al. The Financial Impact of Advanced Kidney Disease on Canada Pension Plan and Private Disability Insurance Costs. *Can J Kidney Health Dis*. 2017;4:1-11.

5. Lameire N, Van Biesen W, Vanholder R. Did 20 Years of Technological Innovations in Hemodialysis Contribute to Better Patient Outcomes? *Clin J Am Soc Nephrol*. 2009;4:S30-S40.

6. McIntyre CW. Recurrent Circulatory Stress: The Dark Side of Dialysis. *Semin Dialysis*. 2010;23:449-451.

7. Man NK, Zingraff J, Jungers P. Long-term Hemodialysis. Dordrecht, Netherlands: Kluwer Academic Publishers, 1995.

8. Stevens LA, Huang C, Levey AS, *Measurement and Estimation of Kidney Function*, in *Chronic Kidney Disease, Dialysis, and Transplantation - A Companion to Brenner and Rector's The Kidney*, J. Himmelfarb and M.H. Sayegh, Editors. 2010, Saunders Elsevier: Philadelphia, PA, USA. p. 22-38.

9. Schnermann JB, Sayegh SI. Kidney Physiology. Philadelphia, PA, USA: Lippincott-Raven, 1998.

10. Haraldsson B, Nystrom J, Deen WM. Properties of the Glomerular Barrier and Mechanisms of Proteinuria. *Physiol Rev*. 2008;88:451-487.

11. Kumar J. Pathophysiology of ischemic acute tubular necrosis. *Clin Queries: Nephrol*. 2012;1:18-26.

12. Shafi T, Levey AS. Measurement and Estimation of Residual Kidney Function in Dialysis Patients. *Adv Chronic Kidney Dis*. 2018;25:93-104.

13. Levey AS, Inker LA. Assessment of Glomerular Filtration Rate in Health and Disease: A State of the Art Review. *Clin Pharmacol Ther*. 2017;102:405-419.

14. Grenier N, Quaia E, Prasad PV, et al. Radiology Imaging of Renal Structure and Function by Computed Tomography, Magnetic Resonance Imaging, and Ultrasound. *Semin Nucl Med*. 2011;41:45-60.

15. Read S, Allen C, Hare C. Applications of Computed Tomography in Renal Imaging *Nephron Clin Pract*. 2006;103:c29-c36.

16. Dawson P, Peters M. Dynamic Contrast Bolus Computed Tomography for the Assessment of Renal Function. *Invest Radiol*. 1993;28:1039-1042.

17. Bokacheva L, Rusinek H, Zhang JL, et al. Assessment of Renal Function with Dynamic Contrast Enhanced MR Imaging. *Magn Reson Imaging Clin N Am*. 2008;16:597-611.

18. Bellomo R, Ronco C, Kellum JA, et al. Acute renal failure – definition, outcome measures, animal models, fluid therapy and information technology needs: the Second International Consensus Conference of the Acute Dialysis Quality Initiative (ADQI) Group. *Crit Care*. 2004;8:R204-R212.

19. Lopes JA, Jorge S. The RIFLE and AKIN classifications for acute kidney injury: a critical and comprehensive review. *Clin Kidney J*. 2013;6:8-14.

20. Khwaja A. KDIGO Clinical Practice Guidelines for Acute Kidney Injury. *Nephron Clin Pract*. 2012;120:c179-c185.

21. Lattanzio MR, Kopyt NP. Acute Kidney Injury: New Concepts in Definition, Diagnosis, Pathophysiology, and Treatment. *J Am Osteopath Assoc*. 2009;109:13-19.

22. Basile DP, Anderson MD, Sutton TA. Pathophysiology of Acute Kidney Injury. *Compr Physiol*. 2012;2:1303-1353.

23. Davenport MS, Perazella MA, Yee J, et al. Use of Intravenous Iodinated Contrast Media in Patients with Kidney Disease: Consensus Statements from the American College of Radiology and the National Kidney Foundation. *Radiology*. 2020;0:1-9.

24. McDonald RJ, McDonald JS, Bida JP, et al. Intravenous Contrast Material-induced Nephropathy: Causal or Coincident Phenomenon? *Radiology*. 2013;267:106-119.

25. Shafi T, Coresh J, *Chronic Kidney Disease: Definition, Epidemiology, Cost, and Outcomes*, in *Chronic Kidney Disease, Dialysis, and Transplantation - A Companion to Brenner and Rector's The Kidney*, J. Himmelfarb and M.H. Sayegh, Editors. 2010, Saunders Elsevier: Philadelphia, PA, USA. p. 3-21.

26. Williams ME, Stanton RC, *Diabetic Kidney Disease: Current Challenges*, in *Chronic Kidney Disease, Dialysis, and Transplantation - A Companion to Brenner and Rector's The Kidney*, J. Himmelfarb and M.H. Sayegh, Editors. 2010, Saunders Elsevier: Philadelphia, PA, USA. p. 39-56.

27. Hill GS. Hypertensive nephrosclerosis. *Curr Opin Nephrol Hypertens*. 2008;17:266-270.

28. Khosla N, Kalaitzidis R, Bakris G, *Hypertensive Kidney Disease*, in *Chronic Kidney Disease, Dialysis, and Transplantation - A Companion to Brenner and Rector's The Kidney*, J. Himmelfarb and M.H. Sayegh, Editors. 2010, Saunders Elsevier: Philadelphia, PA, USA. p. 57-67.

29. Beaulieu MC, Curtis BM, Levin A, *The Role of the Chronic Kidney Disease Clinic*, in *Chronic Kidney Disease, Dialysis, and Transplantation - A Companion to Brenner and Rector's The Kidney*, J. Himmelfarb and M.H. Sayegh, Editors. 2010, Saunders Elsevier: Philadelphia, PA, USA. p. 75-86.

30. Young BA, *Timing and Initiation and Modality Options for Renal Replacement Therapy*, in *Chronic Kidney Disease, Dialysis, and Transplantation - A Companion to Brenner and Rector's The Kidney*, J. Himmelfarb and M.H. Sayegh, Editors. 2010, Saunders Elsevier: Philadelphia, PA, USA. p. 265-274.

31. Gill JS, Johnston O, *Chronic Kidney Disease and the Kidney Transplant Recipient*, in *Chronic Kidney Disease, Dialysis, and Transplantation - A Companion to Brenner and Rector's The Kidney*, J. Himmelfarb and M.H. Sayegh, Editors. 2010, Saunders Elsevier: Philadelphia, PA, USA. p. 636-640.

32. Galach M, Werynski A, Lindholm B, et al, *Representations of Peritoneal Tissue – Mathematical Models in Peritoneal Dialysis*, in *Progress in Peritoneal Dialysis*, R. Krediet, Editor. 2011, In-Tech: Rijeka, Croatia. p. 1-22.

33. Heimburger O, *Peritoneal Physiology*, in *Chronic Kidney Disease, Dialysis, and Transplantation - A Companion to Brenner and Rector's The Kidney*, J. Himmelfarb and M.H. Sayegh, Editors. 2010, Saunders Elsevier: Philadelphia, PA, USA. p. 387-404.

34. Chaudhary K, Sangha H, Khanna R. Peritoneal Dialysis First: Rationale. *Clin J Am Soc Nephrol*. 2011;6:447-456.

35. Dixon BS, Dember LM, *Vascular Access*, in *Chronic Kidney Disease, Dialysis, and Transplantation - A Companion to Brenner and Rector's The Kidney*, J. Himmelfarb and M.H. Sayegh, Editors. 2010, Saunders Elsevier: Philadelphia, PA, USA. p. 303-319.

36. Yeun JY, Depner TA, *Principles of Hemodialysis*, in *Chronic Kidney Disease, Dialysis, and Transplantation - A Companion to Brenner and Rector's The Kidney*, J. Himmelfarb and M.H. Sayegh, Editors. 2010, Saunders Elsevier: Philadelphia, PA, USA. p. 277-302.

37. Movilli E, Gaggia P, Zubani R, et al. Association between high ultrafiltration rates and mortality in uraemic patients on regular haemodialysis. A 5-year prospective observational multicentre study. *Nephrol Dial Transplant*. 2007;22:3547-3552.

38. Liangos O, Jaber BL, *Acute Complications Associated with Hemodialysis*, in *Chronic Kidney Disease, Dialysis, and Transplantation - A Companion to Brenner and Rector's The Kidney*, J. Himmelfarb and M.H. Sayegh, Editors. 2010, Saunders Elsevier: Philadelphia, PA, USA. p. 354-369.

39. Chaignon M, Chen WT, Tarazi RC, et al. Effect of Hemodialysis on Blood Volume Distribution and Cardiac Output. *Hypertension*. 1981;3:327-332.

40. Buchanan C, Mohammed A, Cox E, et al. Intradialytic Cardiac Magnetic Resonance Imaging to Assess Cardiovascular Responses in a Short-Term Trial of Hemodiafiltration and Hemodialysis. *J Am Soc Nephrol*. 2017;28:1269-1277.

41. Chesterton LJ, Selby NM, Fialova J, et al. Categorization of the hemodynamic response to hemodialysis: The importance of baroreflex sensitivity. *Hemodial Int*. 2010;14:18-28.

42. Shoji T, Tsubakihara Y, Fujii M, et al. Hemodialysis-associated hypotension as an independent risk factor for two-year mortality in hemodialysis patients. *Kidney Int*. 2004;66:1212-1220.

43. Weiner DE, Sarnak MJ, *Cardiovascular Disease in Patients with Chronic Kidney Disease*, in *Chronic Kidney Disease, Dialysis, and Transplantation - A Companion to Brenner and Rector's The Kidney*, J. Himmelfarb and M.H. Sayegh, Editors. 2010, Saunders Elsevier: Philadelphia, PA, USA. p. 128-144.

44. McIntyre CW. Haemodialysis-induced myocardial stunning in chronic kidney disease - a new aspect of cardiovascular disease. *Blood Purif*. 2010;29:105-110.

45. Mondillo S, Galderisi M, Mele D, et al. Speckle-Tracking Echocardiography: A New Technique for Assessing Myocardial Function. *J Ultrasound Med*. 2011;30:71-83.

46. McIntyre CW, Burton JO, Selby NM, et al. Hemodialysis-Induced Cardiac Dysfunction Is Associated with an Acute Reduction in Global and Segmental Myocardial Blood Flow. *Clin J Am Soc Nephrol*. 2008;3:19-26.

47. Selby NM, Burton JO, Chesterton LJ, et al. Dialysis-Induced Regional Left Ventricular Dysfunction Is Ameliorated by Cooling the Dialysate. *Clin J Am Soc Nephrol*. 2006;1:1216-1225.

48. Burton JO, Jefferies HJ, Selby NM, et al. Hemodialysis-Induced Cardiac Injury: Determinants and Associated Outcomes. *Clin J Am Soc Nephrol*. 2009;4:914-920.

49. Dasselaar JJ, Slart RHJA, Knip M, et al. Haemodialysis is associated with a pronounced fall in myocardial perfusion. *Nephrol Dial Transplant*. 2009;24:604-610.

50. Cukor D, Rosenthal DS, Kimmel PL, *Depression and Neurocognitive Function in Chronic Kidney Disease*, in *Chronic Kidney Disease, Dialysis, and Transplantation - A Companion to Brenner and Rector's The Kidney*, J. Himmelfarb and M.H. Sayegh, Editors. 2010, Saunders Elsevier: Philadelphia, PA, USA. p. 218-230.

51. McIntyre CW, Goldsmith DJ. Ischemic brain injury in hemodialysis patients: which is more dangerous, hypertension or intradialytic hypotension? *Kidney Int*. 2015;87:1109-1115.

52. Polinder-Bos HA, Garcia DV, Kuipers J, et al. Hemodialysis Induces an Acute Decline in Cerebral Blood Flow in Elderly Patients. *J Am Soc Nephrol*. 2018;29:1317-1325.

53. Findlay MD, Dawson J, Dickie DA, et al. Investigating the Relationship between Cerebral Blood Flow and Cognitive Function in Hemodialysis Patients. *J Am Soc Nephrol*. 2019;30:147-158.

54. MacEwen C, Sutherland S, Daly J, et al. Relationship between Hypotension and Cerebral Ischemia during Hemodialysis. *J Am Soc Nephrol*. 2017;28:2511-2520.

55. Nakatani T, Naganuma T, Uchida J, et al. Silent Cerebral Infarction in Hemodialysis Patients. *Am J Nephrol*. 2003;23:86-90.

56. Anan F, Shimomura T, Imagawa M, et al. Predictors for silent cerebral infarction in patients with chronic renal failure undergoing hemodialysis. *Metabolism*. 2007;56:593-598.

57. Kamata T, Hishida A, Takita T, et al. Morphologic Abnormalities in the Brain of Chronically Hemodialyzed Patients without Cerebrovascular Disease. *Am J Nephrol*. 2000;20:27-31.

58. Prohovnik I, Post J, Uribarri J, et al. Cerebrovascular effects of hemodialysis in chronic kidney disease. *J Cereb Blood Flow Metab*. 2007;27:1861-1869.

59. Lamar M, Catani M, Price CC, et al. The impact of region-specific leukoaraiosis on working memory deficits in dementia. *Neuropsychologia*. 2008;46:2597-2601.

60. Kim C, Lee H, Kim D, et al. High Prevalence of Leukoaraiosis in Cerebral Magnetic Resonance Images of Patients on Peritoneal Dialysis. *Am J Kidney Dis*. 2007;50:98-107.

61. Hsieh T, Chang J, Chuang H, et al. End-Stage Renal Disease: In Vivo Diffusion-Tensor Imaging of Silent White Matter Damage. *Radiology*. 2009;252:518-525.

62. Eldehni MT, Odudu A, McIntyre CW. Randomized Clinical Trial of Dialysate Cooling and Effects on Brain White Matter. *J Am Soc Nephrol*. 2015;26:957-965.

63. Eldehni MT, Odudu A, McIntyre CW. Brain white matter microstructure in end-stage kidney disease, cognitive impairment, and circulatory stress. *Hemodial Int*. 2019;23:356-365.

64. Leypoldt JK, Culleton BF, Cheung AK, *Hemodialysis Adequacy*, in *Chronic Kidney Disease, Dialysis, and Transplantation - A Companion to Brenner and Rector's The Kidney*, J. Himmelfarb and M.H. Sayegh, Editors. 2010, Saunders Elsevier: Philadelphia, PA, USA. p. 320-334.

65. Saran R, Bragg-Gresham JL, Levin NW, et al. Longer treatment time and slower ultrafiltration in hemodialysis: Associations with reduced mortality in the DOPPS. *Kidney Int*. 2006;69:1222-1228.

66. Garg AX, Suri RS, Eggers P, et al. Patients receiving frequent hemodialysis have better health-related quality of life compared to patients receiving conventional hemodialysis. *Kidney Int*. 2017;91:746-754.

67. Krane V, Krieter DH, Olschewski M, et al. Dialyzer Membrane Characteristics and Outcome of Patients With Type 2 Diabetes on Maintenance Hemodialysis. *Am J Kidney Dis*. 2007;49:267-275.

68. McIntyre CW, Lambie SH, Fluck RJ. Biofeedback controlled hemodialysis (BF-HD) reduces symptoms and increases both hemodynamic tolerability and dialysis adequacy in non-hypotension prone stable patients. *Clin Nephrol*. 2003;60:105-112.

69. Selby NM, Lambie SH, Camici PG, et al. Occurrence of Regional Left Ventricular Dysfunction in Patients Undergoing Standard and Biofeedback Dialysis. *Am J Kidney Dis*. 2006;47:830-841.

70. Ronco C, Brendolan A, Milan M, et al. Impact of biofeedback-induced cardiovascular stability on hemodialysis tolerance and efficiency. *Kidney Int*. 2000;58:800-808.

71. Selby NM, McIntyre CW. Peritoneal Dialysis Is Not Associated with Myocardial Stunning. *Periton Dialysis Int*. 2011;31:27-33.

72. Marron B, Remon C, Perez-Fontan M, et al. Benefits of preserving residual renal function in peritoneal dialysis. *Kidney Int*. 2008;73:S42-S51.

73. Tomai F, Crea F, Chiariello L, et al. Ischemic Preconditioning in Humans: Models, Mediators, and Clinical Relevance. *Circulation*. 1999;100:559-563.

74. Gassanov N, Nia AM, Caglayan E, et al. Remote Ischemic Preconditioning and Renoprotection: From Myth to a Novel Therapeutic Option? *J Am Soc Nephrol*. 2014;25:216-224.

75. Crowley LE, McIntyre CW. Remote ischaemic conditioning—therapeutic opportunities in renal medicine. *Nat Rev Nephrol*. 2013;9:739-746.

76. Salerno FR, Crowley LE, Odudu A, et al. Remote Ischemic Preconditioning Protects Against Hemodialysis-Induced Cardiac Injury. *Kidney Int Rep*. 2020;5:99-103.

77. Selby NM, McIntyre CW. A systematic review of the clinical effects of reducing dialysate fluid temperature. *Nephrol Dial Transplant*. 2006;21:1883-1898.

78. Mustafa RA, Bdair F, Akl EA, et al. Effect of Lowering the Dialysate Temperature in Chronic Hemodialysis: A Systematic Review and Meta-Analysis. *Clin J Am Soc Nephrol*. 2016;11:442-457.

79. Chesterton LJ, Selby NM, Burton JO, et al. Cool dialysate reduces asymptomatic intradialytic hypotension and increases baroreflex variability. *Hemodial Int*. 2009;13:189-196.

80. Beerenhout CH, Noris M, Kooman JP, et al. Nitric Oxide Synthetic Capacity in Relation to Dialysate Temperature. *Blood Purif*. 2004;22:203-209.

81. Moore EM, Nichol AD, Bernard SA, et al. Therapeutic hypothermia: Benefits, mechanisms and potential clinical applications in neurological, cardiac and kidney injury. *Injury*. 2011;42:843-854.

82. Hsu S-F, Niu K-C, Lin C-L, et al. Brain cooling causes attenuation of cerebral oxidative stress, systemic inflammation, activated coagulation, and tissue ischemia/injury during heatstroke. *Shock*. 2006;26:210-220.

83. Jefferies HJ, Burton JO, McIntyre CW. Individualised dialysate temperature improves intradialytic haemodynamics and abrogates haemodialysis-induced myocardial stunning, without compromising tolerability. *Blood Purif*. 2011;32:63-68.

84. Odudu A, Eldehni MT, McGann GP, et al. Randomized Controlled Trial of Individualized Dialysate Cooling for Cardiac Protection in Hemodialysis Patients. *Clin J Am Soc Nephrol*. 2015;10:1408-1417.

85. Lautt WW. Hepatic Circulation: Physiology and Pathophysiolog. San Rafael, CA, USA: Morgan & Claypool Life Sciences, 2010.

86. McIntyre CW, Crowley LE. Dying to Feel Better: The Central Role of Dialysis–Induced Tissue Hypoxia. *Clin J Am Soc Nephrol*. 2016;11:549-551.

87. Hawker F. Critical Care Management: The Liver. London, UK: Saunders, 1993.

88. van der Wal WM, Noordzij M, Dekker FW, et al. Full loss of residual renal function causes higher mortality in dialysis patients; findings from a marginal structural model. *Nephrol Dial Transplant*. 2011;26:2978-2983.

89. Jansen MAM, Hart AAM, Korevaar JC, et al. Predictors of the rate of decline of residual renal function in incident dialysis patients. *Kidney Int*. 2002;62:1046-1053.

90. Shafi T, Jaar BG, Plantinga LC, et al. Association of Residual Urine Output with Mortality, Quality of Life, and Inflammation in Incident Hemodialysis Patients: The CHOICE (Choices for Healthy Outcomes in Caring for End-Stage Renal Disease) Study. *Am J Kidney Dis*. 2010;56:348-358.

91. Wang A-M, Lai K-N. The importance of residual renal function in dialysis patients. *Kidney Int*. 2006;69:1726-1732.

92. Shemin D, Bostom AG, Laliberty P, et al. Residual Renal Function and Mortality Risk in Hemodialysis Patients. *Am J Kidney Dis*. 2001;38:85-90.

93. Bargman JM, Thorpe KE, Churchill DN. Relative Contribution of Residual Renal Function and Peritoneal Clearance to Adequacy of Dialysis: A Reanalysis of the CANUSA Study. *J Am Soc Nephrol*. 2001;12:2158-2162.

94. National Kidney Foundation: KDOQI clinical practice guidelines and clinical practice recommendations: Hemodialysis adequacy, peritoneal dialysis adequacy and vascular access: Update 2006. *Am J Kidney Dis*. 2006;48:S1-S322.

95. Obi Y, Streja E, Rhee CM, et al. Incremental Hemodialysis, Residual Kidney Function, and Mortality Risk in Incident Dialysis Patients: A Cohort Study. *Am J Kidney Dis*. 2016;68:256-265.

96. Moist LM, Port FK, Orzol SM, et al. Predictors of Loss of Residual Renal Function among New Dialysis Patients. *J Am Soc Nephrol*. 2000;11:556-564.

97. Mathew AT, Fishbane S, Obi Y, et al. Preservation of residual kidney function in hemodialysis patients: reviving an old concept. *Kidney Int*. 2016;90:262-271.

98. Lysaght MJ, Vonesh EF, Gotch F, et al. The influence of dialysis treatment modality on the decline of remaining renal function. *Trans Am Soc Artif Intern Organs*. 1991;37:598-604.

99. Nolan JP. Endotoxin, Reticuloendothelial Function, and Liver Injury. *Hepatol*. 1981;1:458-465.

100. Jacob AI, Goldberg PK, Bloom N, et al. Endotoxin and bacteria in portal blood. *Gastroenterology*. 1977;72:1268-1270.

101. Prytz H, Holst-Christensen J, Korner B, et al. Portal venous and systemic endotoxaemia in patients without liver disease and systemic endotoxaemia in patients with cirrhosis. *Scand J Gastroenterol*. 1976;11:

102. Ruiter DJ, van der Meulen J, Brouwer A, et al. Uptake by liver cells of endotoxin following its intravenous injection. *Lab Invest*. 1981;45:38-45.

103. McIntyre CW, Harrison LE, Eldehni MT, et al. Circulating endotoxemia: a novel factor in systemic inflammation and cardiovascular disease in chronic kidney disease. *Clin J Am Soc Nephrol*. 2011;6:133-141.

104. Ibrahim M, Behairy M, El-Ashry M, et al. Cardiovascular risk of circulating endotoxin level in prevalent hemodialysis patients. *Egypt Heart J*. 2018;70:27-33.

105. Krasity BC, Troll JV, Lehnert EM, et al. Structural and Functional Features of a Developmentally Regulated Lipopolysaccharide-Binding Protein. *mBio*. 2015;6:e01193-15.

106. Reyes-Bahamonde J, Raimann JG, Thijssen S, et al. Fluid Overload and Inflammation—A Vicious Cycle. *Semin Dialysis*. 2012;26:31-35.

107. Friedlander MA, Hilbert CM, Wu YC, et al. Role of Dialysis Modality in Responses of Blood Monocytes and Peritoneal Macrophages to Endotoxin Stimulation *Am J Kidney Dis*. 1993;22:11-23.

108. Diebel L, Kozol R, Wilson R, et al. Gastric intramucosal acidosis in patients with chronic kidney failure. *Surgery*. 1993;113:520-526.

109. Yu AW, Nawab ZM, Barnes W, et al. Splanchnic erythrocyte content decreases during hemodialysis: a new compensatory mechanism for hypovolemia. *Kidney Int*. 1997;51:1986-1990.

110. Jakob SM, Rvokenen E, Vuolteenaho O, et al. Splanchnic perfusion during hemodialysis: evidence for marginal tissue perfusion. *Crit Care Med*. 2001;29:1393-1398.

111. Khanna A, Rossman JE, Fung HL, et al. Intestinal and hemodynamic impairment following mesenteric ischemia/reperfusion. *J Surg Res*. 2001;99:114-119.

112. Kotanko P, Carter M, Levin NW. Intestinal bacterial microflora—a potential source of chronic inflammation in patients with chronic kidney disease. *Nephrol Dial Transplant*. 2006;21:2057-2060.

113. Davenport A. Measuring residual renal function in dialysis patients: can we dispense with 24-hour urine collection? *Kidney Int*. 2016;89:978-980.

114. Shafi T, Mullangi S, Toth-Manikowski SM, et al. Residual Kidney Function: Implications in the Era of Personalized Medicine. *Semin Dialysis*. 2017;30:241-245.

115. Mathew AT, Obi Y, Rhee CM, et al. Incremental dialysis for preserving residual kidney function— Does one size fit all when initiating dialysis? *Semin Dialysis*. 2018;31:343-352.

116. National Kidney Foundation: KDOQI clinical practice guideline for hemodialysis adequacy: 2015 update. *Am J Kidney Dis*. 2015;66:884-930.

117. Sandilands EA, Dhaun N, Dear JW, et al. Measurement of renal function in patients with chronic kidney disease. *Br J Clin Pharmacol*. 2013;76:504-515.

118. Filler G, Cuellar CR, Medeiros M. Overcoming the limitations of glomerular filtration rate estimation by using a novel rapid bedside measurement? *Ann Transl Med*. 2018;6:312.

119. Boele-Schutte E, Gansevoort RT. Measured GFR: not a gold, but a gold-plated standard. *Nephrol Dial Transplant*. 2017;32:ii180-ii184.

120. Tsushima Y, Blomley MJK, Kusano S, et al. Use of Contrast-Enhanced Computed Tomography to Measure Clearance Per Unit Renal Volume: A Novel Measurement of Renal Function and Fractional Vascular Volume. *Am J Kidney Dis*. 1999;33:754-760.

121. Deniffel D, Boutelier T, Labani A, et al. Computed Tomography Perfusion Measurements in Renal Lesions Obtained by Bayesian Estimation, Advanced Singular-Value Decomposition Deconvolution, Maximum Slope, and Patlak Models: Intermodel Agreement and Diagnostic Accuracy of Tumor Classification. *Invest Radiol*. 2018;53:477-485.

122. Chang J, Kim S, Jung J, et al. Assessment of glomerular filtration rate with dynamic computed tomography in normal Beagle dogs. *J Vet Sci*. 2011;12:393-399.

123. Sommer FG. Can Single-Kidney Glomerular Filtration Rate Be Determined with Contrast-enhanced CT? *Radiology*. 2007;242:325-326.

124. Yuan X, Zhang J, Tang K, et al. Determination of Glomerular Filtration Rate with CT Measurement of Renal Clearance of Iodinated Contrast Material versus 99mTc-DTPA Dynamic Imaging “Gates” Method: A Validation Study in Asymmetrical Renal Disease. *Radiology*. 2017;282:552-560.

125. Crone C. The Permeability of Capillaries in Various Organs as Determined by Use of the (Indicator Diffusion’ Method. *Acta Physiol Scand*. 1963;58:292-305.

126. Kalender WA. Computed Tomography: Fundamentals, System Technology, Image Quality, Applications. Munich, Germany: Publicis, 2011.

127. Miles KA, *Image acquisition and contrast enhancement protocols for CT perfusion*, in *Multidetector Computed Tomography in Oncology: CT Perfusion Imaging*, K.A. Miles, C. Cuenod, and J. Husband, Editors. 2007, Informa Healthcare: London, UK. p. 47-60.

128. Lee T, Stewart E, *Scientific basis and validation*, in *Multidetector Computed Tomography in Oncology: CT Perfusion Imaging*, K.A. Miles, C. Cuenod, and J. Husband, Editors. 2007, Informa Healthcare: London, UK. p. 15-46.

129. Larson KB, Markham J, Raichle ME. Tracer-Kinetic Models for Measuring Cerebral Blood Flow Using Externally Detected Radiotracers. *J Cereb Blood Flow Metab*. 1987;7:443-463.

130. St. Lawrence KS, Lee T-Y. An Adiabatic Approximation to the Tissue Homogeneity Model for Water Exchange in the Brain: I. Theoretical Derivation *J Cereb Blood Flow Metab*. 1998;18:1365-1377.

131. Lee T-Y, Purdie TG, Stewart E. CT Imaging of Angiogenesis. *Q J Nucl Med*. 2003;47:171-187.

132. Cuenod C, Fournier L, Balvay D, et al, *CT perfusion of liver metastases and early detection of micrometastases*, in *Multidetector Computed Tomography in Oncology: CT Perfusion Imaging*, K.A. Miles, C. Cuenod, and J. Husband, Editors. 2007, Informa Healthcare: London, UK. p. 173-196.

CHAPTER 2

2 Renal Perfusion during Hemodialysis: Intradialytic Blood Flow Decline and Effects of Dialysate Cooling

Residual renal function confers survival in patients with end-stage renal disease but declines after initiating hemodialysis. We used CT perfusion imaging to explore whether hemodialysis-induced circulatory stress causes renal ischemia, which could help explain residual renal function loss in this patient population.

The contents of this chapter were adapted from an original research manuscript entitled “Renal Perfusion during Hemodialysis: Intradialytic Blood Flow Decline and Effects of Dialysate Cooling”, which was published in the *Journal of the American Society of Nephrology* in 2019 and co-authored by Raanan Marants, Elena Qirjazi, Claire Grant, Ting-Yim Lee and Christopher McIntyre. The permissions to reproduce this manuscript are provided in Appendix E.

2.1 Introduction

Most patients on incident hemodialysis (HD) are not completely anuric.[1,2] The presence and preservation of even minimal amounts[3-6] of residual renal function (RRF) after HD initiation is associated with better control of serum phosphate, hypervolemia, and hypertension, improved nutrition, less anemia, higher middle molecule clearance, and improved survival.[7-12] Although the importance of long-term RRF maintenance is recognized,[13] RRF characteristically declines after HD initiation, necessitating more aggressive fluid removal in subsequent HD sessions.[14,15] This decline is linked to poorer outcomes and increased mortality.[12,16]

Observational studies have found that age, chronic kidney disease (CKD) cause, bioincompatible dialysis membranes, and elevated blood pressure (BP) are associated with RRF decline.[9,17,18] Larger epidemiologic studies have confirmed these findings and shown that hemodynamic instability during HD (i.e., intradialytic hypotension, IDH) is independently associated with RRF loss.[14,19]

Intradialytic circulatory stress is associated with reduced perfusion in multiple vulnerable organs.[20] Recurring subclinical ischemic injury over many HD sessions is linked to increased morbidity and mortality. One strategy that reduces IDH frequency (an independent predictor of mortality[14]) and ameliorates HD-induced circulatory stress is dialysate cooling (DC).[21,22] This intervention does not adversely affect HD efficiency, is generally well tolerated, and can be widely implemented at no additional cost.[23] Studies have found that myocardial and cerebral perfusion can be preserved using DC, providing protection against injury and longer-term organ dysfunction.[22,24,25]

Several authors have speculated that HD causes recurrent renal ischemic insults, which may cause irreversible injury leading to RRF loss.[10,11,26] However, trials to date have not focused on measuring HD-induced renal ischemia or describing its relationship with RRF loss, preventing the evaluation of potential preservation interventions. We therefore conducted a pilot study of whole organ kidney perfusion, measured serially during HD using computed tomography (CT) perfusion imaging, to measure intradialytic renal perfusion and test two hypotheses: first, that HD is associated with acute renal perfusion decline, and second, that DC ameliorates HD-induced changes in renal hemodynamics. Confirming quantitatively that HD does in fact result in decreased renal perfusion (DRP) will represent the first crucial step toward the pathophysiologic

characterization of HD-mediated RRF loss in patients with end-stage renal disease (ESRD).

2.2 Methods

2.2.1 Patients

Thirty patients (19 men) in total from the London Health Sciences Centre Regional Renal Program were enrolled in two experiments (see Study Design below), after giving their written informed consent. Adult patients established on HD for at least 3 months and who had low RRF (<250 mL/day) were eligible. This group of patients with already low RRF was selected to limit any potential effects of contrast-induced nephropathy. Exclusion criteria included active infection/ malignancy, pregnancy, breast feeding, planned pregnancy, diabetic with hypoglycemia during HD within the past 2 months, and known allergy to iodinated contrast agent. These experiments were approved by the University of Western Ontario Health Sciences Research Ethics Board and were conducted in compliance with the approved protocols, Good Clinical Practice Guidelines, and all applicable regulatory requirements.

2.2.2 Study Design

Two back-to-back pilot experiments were conducted and then the results were combined. In the first experiment, 14 patients were recruited to undergo a single session of standard dialysate temperature (36.5°C) HD. In the second experiment, 16 patients were recruited to undergo two sessions of HD: one session of standard dialysate temperature HD and another of cooled dialysate temperature (35.0°C) HD. Patients

involved in the second experiment were randomly assigned to receive either standard or cooled HD first in a two-visit crossover study design, thereby acting as their own controls.

Combined findings from the two experiments were divided into “standard HD” (14+16=30 standard HD patients) and “standard versus cooled HD” (16 standard and cooled HD patients) and analyzed accordingly. All patients underwent uninterrupted HD in the CT scanner room. Analysis of the imaging data from the crossover experiment was performed with the operator blinded to allocation. Patients, dialysis unit staff, and the investigator at the experiment visit were not blinded to the intervention, but were not involved in the imaging data analysis.

2.2.3 Dynamic CT Image Acquisition and Analysis

CT perfusion imaging was performed on a GE Healthcare Revolution 256-slice CT scanner at three times during each HD session: immediately before, 3 hours into (i.e., peak stress, defined from previous studies of HD-induced myocardial injury), and 15 minutes after dialysis. For the intradialytic scan, patients were transferred to the CT bed without interrupting their HD treatment. After iodinated contrast agent injection (at a rate of 5 mL/s, followed by a 30 mL saline flush), dynamic contrast-enhanced CT scanning of a 16 cm section of the abdomen was performed without breath hold. The type of contrast agent, iopamidol (Isovue 370; Bracco Imaging), was identical in all patients for both standard and cooled HD sessions, and was administered at a dose of 1 mL/kg of pre-HD patient weight (up to a maximum dose of 70 mL).

Scan ranges were optimized to encompass as much of both kidneys as possible by performing a non-contrast localization scan prior to each CT perfusion scan. The

section was divided into 32 slices of 5 mm thickness each, and was scanned 42 times at 2.8 second intervals using 120 kV and 22.4 mAs, for a duration of approximately 2 minutes. Images were reconstructed using 100% Adaptive Statistical Iterative Reconstruction (GE Healthcare) to reduce image noise, and then registered using nonrigid registration (GE Healthcare) to minimize breathing motion among images of the dynamic scan. Registered images were analyzed using CT Perfusion 4D software (GE Healthcare). An aortic region of interest (ROI) was selected for generation of renal perfusion (i.e., blood flow) maps (this process is described in section 1.7.3). Next, ROIs were manually drawn over the kidneys in the blood flow maps to encompass medullar and cortical areas. Kidney ROIs were reviewed and verified by three experienced (>10 years) radiologists. Then, perfusion values were averaged over the selected slices to determine mean whole kidney blood flow values.

DRP was defined as either (1) a drop in blood flow at peak stress ≥2 SEM (SEM of the patient group), or (2) a drop in blood flow at both peak stress ≥1 SEM and after HD ≥1 SEM.

2.2.4 Echocardiography Analysis of Myocardial Stunning

Myocardial response to HD was assessed to provide a reference to another critical organ known to be vulnerable to HD-induced circulatory stress. Echocardiography was performed by trained investigators before commencing and 15 minutes before the end of HD, using commercially available equipment (1.5–3.6 MHz M4S probe, Vivid-iq; GE Healthcare). Standard apical two- and four-chamber views were recorded for offline digital

analysis with a semi-automated computer program (EchoPac; GE Healthcare) using two-dimensional speckle tracking software.

Images were anonymized and analyzed in random order by the same trained investigators (E.Q. and C.G.). Three cardiac cycles at each time point were analyzed to derive segmental (12 left ventricular segments) and global longitudinal strain. Myocardial stunning (MS) was defined as a reduction in longitudinal strain of >20% in two or more segments of the left ventricle caused by regional wall motion abnormalities (RWMAs). The number of left ventricular segments exhibiting a reduction in strain of >20% was also recorded.

2.2.5 Statistical Analyses

Kidney perfusion has never been assessed previously in the context of HD and inadequate data exist to perform a meaningful sample size calculation. As the initial proof-of-principle study for hypothesis generation, a sample size of approximately 15 patients per pilot experiment is not powered for analysis of the data with inferential statistics. However, the proposed sample size has been selected on a pragmatic basis and is comparable with published norms[22,27,28] and recommendations.[29,30]

Statistical analysis was performed using SPSS, version 25.0 (IBM, Chicago, IL). Data were analyzed using repeated measures ANOVA with post hoc t tests (with Bonferroni correction) and patient baseline-adjusted ANCOVA to detect differences between groups. Associations between variables were assessed using the Pearson product-moment correlation coefficient, and the McNemar test was used to detect

differences between proportions. Two-tailed P values <0.05 were considered statistically significant.

2.3 Results

2.3.1 Clinical Characteristics of Study Population

Thirty patients (19 men) aged 40–84 years were enrolled in two back-to-back experiments. However, one patient could not return for the second visit of the crossover experiment and was excluded from the analysis, resulting in 29 standard HD patients, 15 of which also underwent cooled HD. The median dialysis vintage was 5.3 years (range, 0.8–46 years). Ten patients had known coronary artery disease, seven had congestive heart failure, four had peripheral vascular disease, 15 had diabetes, and 25 had hypertension. Dialysis session length ranged from 2 to 4 hours (median, 3.5 hours) and ultrafiltration (UF) ranged from 0 to 41 mL/kg (median 23 mL/kg). Table 2.1 presents the summary of patient baseline characteristics.

Table 2.1: Baseline characteristics of first project study population.

Characteristics	Mean (Range)[a]
n (standard HD, cooled HD)	29 (29,15)
Age	64 (40–84)
Men, n (%)	19 (66)
Dialysis vintage, years	5.3 (0.8–46)
Coronary artery disease, n (%)	10 (34)
Congestive heart failure, n (%)	7 (24)
Peripheral vascular disease, n (%)	4 (14)
Diabetes, n (%)	15 (52)
Hypertension, n (%)	25 (86)
Length of HD session, hours	3.5 (2.0–4.0)
UF, mL/kg	23.3 (0.0–40.9)

[a]Unless otherwise specified.

2.3.2 Renal Perfusion

Baseline renal perfusion and renal hemodynamic response to HD differed between both kidneys to a measurable extent for many patients. Therefore, perfusion data analysis was on the basis of individual kidneys among all patients.

2.3.2.1 Standard HD

Perfusion was measured in all 29 patients, resulting in computed values for 57 kidneys (one patient had a solitary kidney). Average baseline per kidney perfusion was 33.2±2.9 mL/min/100g (mean±SEM) and correlated with dialysis vintage (r=-0.35;

P<0.01). At peak stress, average per kidney perfusion dropped to 81.6%±4.8% of baseline (Figures 2.1 and 2.2A). After HD, average per kidney perfusion recovered to 95.1%±5.2% of baseline (Figure 2.2A). After repeated measures ANOVA, post hoc analysis revealed that the intradialytic renal perfusion drop was statistically significant compared with pre- and post-HD (P<0.005). Acute DRP during HD was observed in 37 out of 57 kidneys (65%), where average per kidney perfusion dropped to 61.4%±3.6% of baseline during peak stress. For the remaining 20 kidneys (35%), average per kidney perfusion increased to 119.9%±5.2% of baseline at peak stress (Figure 2.2A).

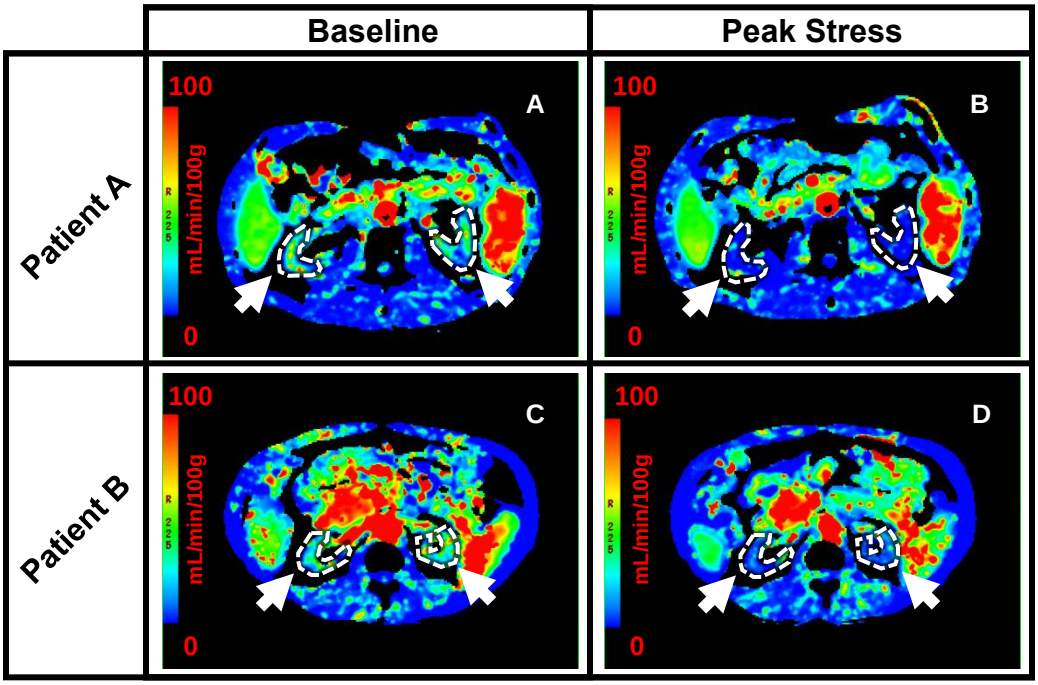

Figure 2.1: HD-induced decrease in kidney blood flow visualized with parametric renal perfusion maps. Renal blood flow at baseline (A and C) and 3 hours into dialysis (B and D) for two patients (top and bottom rows). Kidneys have been identified (white arrows and dotted contours) for both patients.

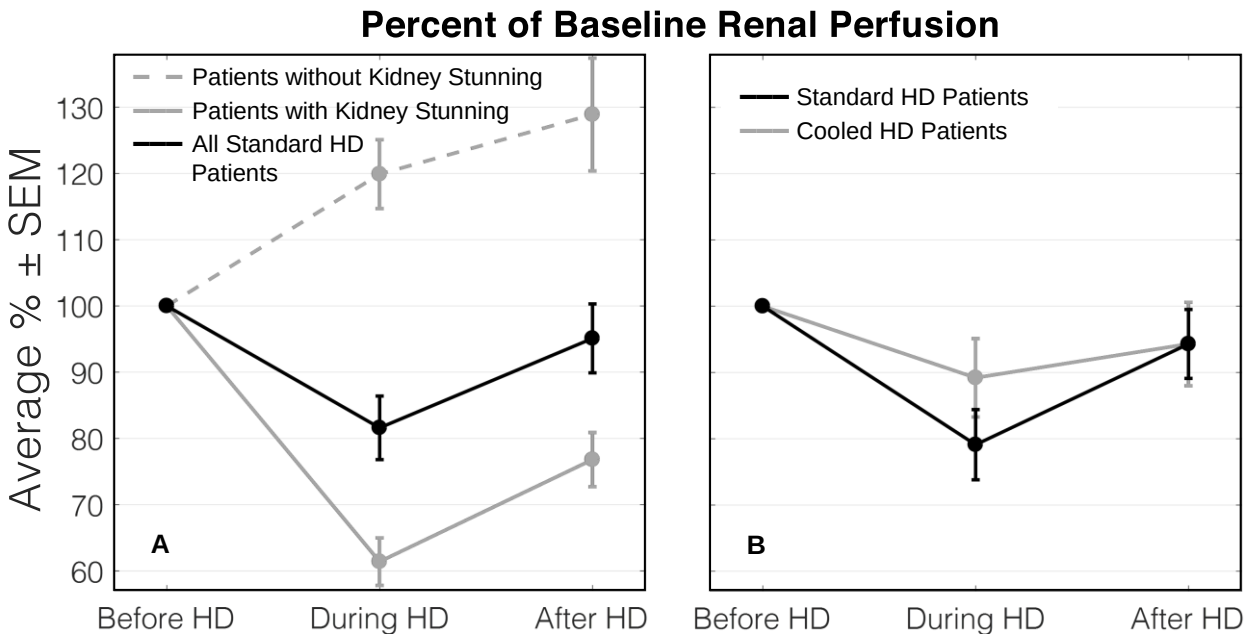

Figure 2.2: Plots of changes in renal perfusion during standard and cooled HD. Renal perfusion significantly declined during standard HD but not during cooled HD. Percent of baseline per kidney perfusion before, 3 hours into, and after dialysis, where results are given as average±SEM. (A) In 29 standard HD patients (57 kidneys), the drop in renal perfusion during HD was statistically significant compared with pre- and post-HD blood flow values ($P<0.005$). (B) In 15 standard and cooled HD patients (30 kidneys each), there was a smaller decline in renal perfusion during cooled HD (not statistically significant) compared with standard HD.

2.3.2.2 Standard versus Cooled HD

Perfusion was measured in all 15 crossover patients, resulting in 30 paired values under standard and cooled HD conditions. Average per kidney perfusion dropped to 79.1%±5.3% and 89.2%±5.9% of baseline at peak stress during standard and cooled HD, respectively (Figure 2.2B). Session-specific, patient baseline-adjusted ANCOVA revealed that the decline in intradialytic renal perfusion between dialysis treatments was not different ($F(1,57)=1.814$; $P=0.18$). Average per kidney perfusion recovered to 94.3% of

baseline after both standard and cooled HD. DRP was observed in 20 out of 30 kidneys (67%) during standard HD and 15 out of 30 kidneys (50%) during cooled HD (not significantly different). In those kidneys, however, the perfusion decline (37% below baseline) was the same for both dialysate temperatures.

2.3.3 Relationship to Cardiac Injury

2.3.3.1 Standard HD

A total of 24 out of 29 patients (83%) exhibited MS. The degree of stunning correlated with DRP ($r=-0.33$; $P<0.05$) (Figure 2.3A). The McNemar test showed that during HD, MS incidence (83%) was significantly higher ($P<0.05$) than DRP incidence (65%). Patients without MS were also protected from HD-induced DRP, where peak stress perfusion declined by 4.4%±13.5% relative to baseline (not statistically significant). This change in perfusion, however, was not significantly different from the 21%±5.0% drop in the MS patients according to patient baseline-adjusted ANCOVA ($F(1,52)=1.575$; $P=0.22$).

2.3.3.2 Standard versus Cooled HD

MS was observed in 13 out of 15 (87%) and 11 out of 15 (73%) patients during standard and cooled HD, respectively (not significantly different), where DC reduced, increased, and had no effect on the number of stunned myocardial segments in eight, five, and two patients, respectively. Although the degree of cardiac injury and severity of renal insult were not associated during standard HD, they were negatively correlated

during cooled HD (r=-0.36; P<0.05) (Figure 2.3B). For both HD subgroups, patients without MS experienced milder DRP.

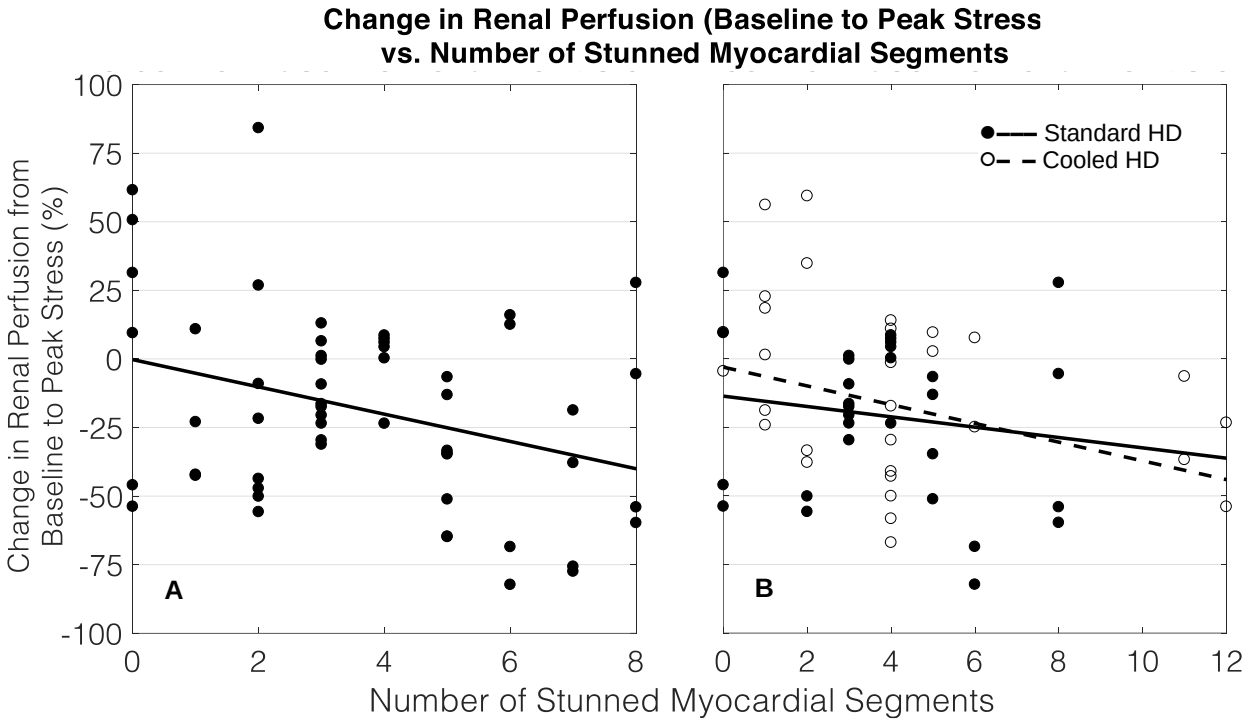

Figure 2.3: Plots of changes in renal perfusion versus the number of stunned myocardial segments during standard and cooled HD. Decreased renal perfusion was associated with an increased number of stunned myocardial segments during standard and cooled HD. Change in per kidney perfusion from baseline to peak stress (i.e., 3 hours into dialysis) versus the number of stunned myocardial segments measured with echocardiography. The dotted lines represent data trendlines. (A) In 29 standard HD patients (57 kidneys), there was a correlation between the degree of cardiac injury and severity of renal insult (r=-0.33; P<0.05). (B) In 15 standard and cooled HD patients (30 kidneys each), there was a correlation between the degree of cardiac injury and severity of renal insult during cooled HD (r=-0.36; P<0.05) but not during standard HD.

2.3.4 Relationship to Dialysis Stress Factors

2.3.4.1 Standard HD

Seven out of 29 patients (24%) experienced IDH (symptomatic and drop in systolic blood pressure (SBP) >200 mmHg). SBP and mean arterial pressure (MAP) dropped significantly during HD to 88.5% ($P<0.005$) and 91.2% ($P<0.05$) of baseline, respectively, before both recovering to 99% of baseline after HD. Although diastolic BP (DBP) behaved similarly, the intradialytic change to 95.6% of baseline was not significant. However, no correlations were found between BP changes and MS development and/or changes in renal perfusion.

Mean and total UF were associated with DRP ($r=-0.31$; $P<0.05$ and $r=-0.26$; $P=0.05$, respectively) and more stunned myocardial segments ($r=0.30$; $P<0.05$ and $r=0.27$; $P<0.05$, respectively) (Figure 2.4). DRP (in at least one kidney) and MS occurred in most patients. Comparing those patients who did experience DRP and stunning with those who did not, there was an association between patients who were taking β-blockers and DRP and stunning ($r=0.48$; $P<0.01$ for DRP and $r=0.54$; $P<0.005$ for MS). Also, there was a discrepancy in patient sex, where the male-to-female ratio was 12:9/7:1 for those who did/did not experience DRP and 15:9/4:1 for those who did/did not experience MS.

2.3.4.2 Standard versus Cooled HD

Three out of 15 patients experienced IDH during both HD sessions, and ten out of 15 patients experienced an SBP drop (.20 mm Hg) during standard HD compared with eight out of 15 during cooled HD (not significantly different). Session-specific, patient baseline-adjusted ANCOVA revealed that BP changes during HD between dialysis

treatments was not statistically significant ($F(1,26)=2.814$ and $P=0.11$; $F(1,26)=0.582$ and $P=0.45$; $F(1,26)=0.382$ and $P=0.54$ for SBP, DBP, and MAP, respectively). During standard HD, changes in SBP and MAP correlated with MS ($r=-0.36$; $P=0.05$ and $r=-0.38$; $P<0.05$, respectively). During cooled HD, these associations persisted ($r=-.45$; $P<0.05$ and $r=-0.43$; $P<0.05$ for SBP and MAP, respectively), and new associations emerged between BP changes and the number of stunned myocardial segments ($r=-0.44$; $P<0.05$ and $r=-0.40$; $P<0.05$ for DBP and MAP, respectively) and absolute changes in renal perfusion ($r=0.47$; $P<0.05$ for DBP).

In terms of thermal symptoms, two out of 15 patients reported feeling cold and/or were shivering during standard HD compared with six out of 15 (two same, four new) during cooled HD (not significantly different).

During standard HD, UF metrics were not associated with DRP or severity of myocardial injury. During cooled HD, UF metrics remained uncorrelated to DRP but were negatively associated with the number of stunned myocardial segments ($r=-0.41$; $P<0.05$ for mean and total UF).

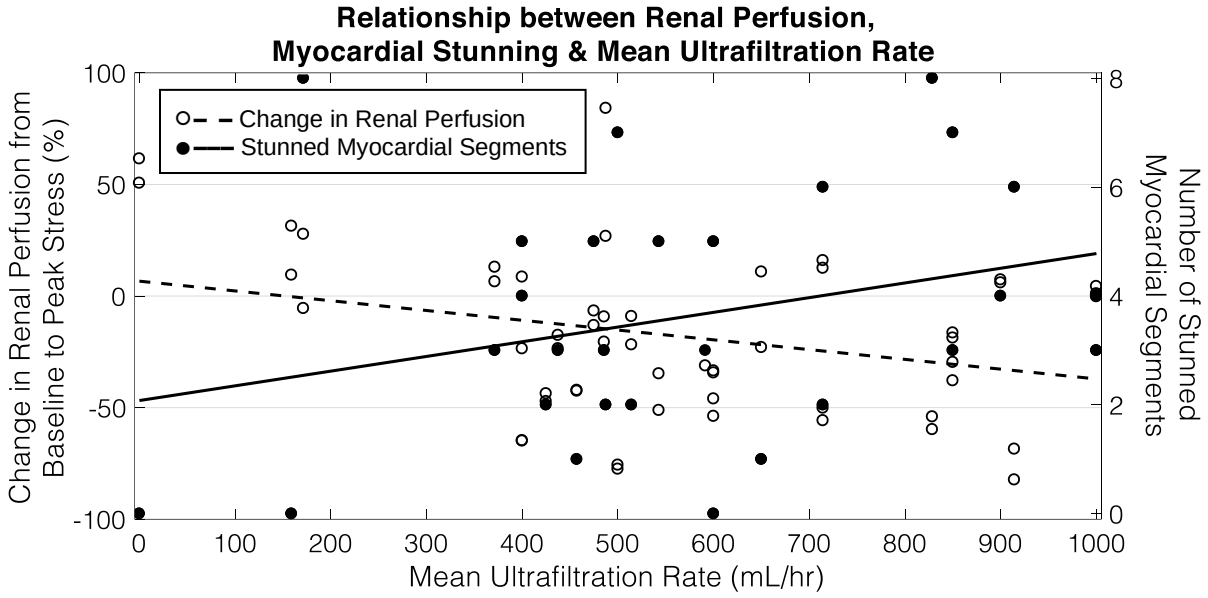

Figure 2.4: Plot of changes in renal perfusion and the number of stunned myocardial segments versus the mean UF rate during standard HD. Decreased renal perfusion and an increased number of stunned myocardial segments were both associated with higher mean ultrafiltration rates during standard HD. Change in per kidney perfusion from baseline to peak stress (open circles) and number of stunned myocardial segments (solid circles) versus mean UF rate for 29 standard HD patients (57 kidneys). The dotted and solid lines represent data trendlines for the renal perfusion and MS data, respectively. The mean UF rate was associated with a larger drop in renal perfusion from baseline to peak stress ($r=-0.31$; $P<0.05$) and a greater number of stunned myocardial segments ($r=0.30$; $P<0.05$).

2.4 Discussion

This study demonstrated that renal perfusion decreased during dialysis, even in the absence of significant hypotension, contemporaneously with MS. In addition, DRP and MS were minimized with DC (although not to a statistically significant extent). These important findings may provide a pathophysiologic explanation and potentially preventative intervention for the characteristic rapid decline of RRF in patients on HD.

2.4.1 Renal Perfusion

Although absolute renal perfusion does not directly represent kidney function, it is a major factor in determining GFR and urine output. As such, perfusion values measured for this study act as surrogate measures of renal function.

2.4.1.1 Standard HD

Average per kidney perfusion dropped to 81.6% of baseline during HD and 21 out of 29 patients (72%) experienced intradialytic DRP in at least one kidney. This reduction in perfusion represents a potential ischemic insult, which is repeated during recurring dialysis sessions and could result in cumulative renal tissue damage and a subsequent RRF reduction. This mechanism is reinforced by the inverse correlation between baseline renal perfusion (RRF surrogate) and dialysis vintage. Perfusion values for patients in our study (<105 mL/min/100g, average baseline of 33.2±2.9 mL/min/100g) were markedly reduced compared with normal control (typical range, 200–500 mL/min/100g) and earlier stage CKD values (approximately 140–300 mL/min/100g) measured in other studies.[31-35]

Recovery of perfusion to 95%of baseline after HD suggests that HD-induced DRP resolves after UF ends and hypovolemia is relieved. The role of HD-mediated hemodynamic instability and transient renal ischemia in progressive RRF decline in patients on HD has been alluded to previously.[10,11,26,36,37] However, this is the first study to directly measure intradialytic renal perfusion and confirm that DRP represents the first key step toward characterizing RRF loss in patients on HD.

Patients with ESRD who are undergoing HD three to four times weekly are subjected to recurrent circulatory stress, suggesting repeated episodes of DRP.

Interestingly, Ronco *et al*.[38] list the combination of hypoperfusion, prolonged hypovolemia, and presence of comorbidities as key factors resulting in subclinical, prerenal AKI. Together with our perfusion results, these aforementioned factors are present during HD sessions of patients with ESRD. Thus, renal tubular damage due to repetitive, intradialytic ischemic AKI may contribute to kidney injury resulting in long-term RRF reduction.

2.4.1.2 Standard versus Cooled HD

DC helped ameliorate HD-induced DRP, where the cooled subgroup experienced a smaller decline in renal perfusion at peak stress and had fewer kidneys with DRP compared with the standard subgroup, although neither findings were statistically significant. Along with other studies that illustrated the protective effects of DC on the brain[25] and heart,[24] this study's findings demonstrate the global hemodynamic effect of HD and the protective potential of DC.

When considering only kidneys with DRP, the change in perfusion from baseline to peak stress was the same for both dialysate temperatures. This suggests that although DC reduces DRP incidence, it does not reduce the magnitude of renal ischemia. However, because of the difference in the overall number of kidneys with DRP, the decline in average per kidney perfusion at peak stress was larger (not statistically significant) for standard HD. These results are consistent with those of a similarly designed study by Selby *et al*.,[22] which assessed myocardial function. They found that although patients undergoing standard HD developed more RWMAs compared with cooled HD, the RWMA magnitude (i.e., percentage shortening fraction) was equal between both HD treatments.

2.4.2 Relationship to Cardiac Injury

2.4.2.1 Standard HD

HD causes transient ischemia in multiple vulnerable vascular beds.[20,39,40] In the heart, demonstrable injury manifests as MS,[41] which was measured with echocardiography and observed in 83% of patients. In non-stunning patients, intradialytic perfusion changes were lessened compared with all patients collectively. This reinforces the notion that MS is a hallmark of HD-induced systemic circulatory stress[28,42] and suggests that its presence potentiates DRP. The magnitude of MS, characterized by the number of stunned segments, was associated with DRP severity, as well as with higher mean and total UF. These results suggest that HD-specific factors contributing to DRP (e.g., aggressive UF, circulating endotoxins, IDH, etc.) are the same as those responsible for intradialytic myocardial injury.[42-44]

2.4.2.2 Standard versus Cooled HD

Additional intradialytic cardiac dysfunction may potentiate renal injury. Therefore, for patients with minimal urine output, RRF preservation could be achieved by lessening the circulatory stress of HD via hemodynamic-protective strategies. Techniques such as DC[23] and ischemic preconditioning,[45] which have shown potential for attenuating the burden of dialysis upon the heart[24,27] and brain,[25] may also protect renal parenchyma from recurring intradialytic ischemic insults.

In this study, DC seemed to help ameliorate intradialytic myocardial injury. Fewer patients experienced MS during cooled HD and more patients received benefit from the intervention than harm in terms of severity of myocardial injury (i.e., lowering the number

of stunned segments with cooling). However, neither of these outcomes were statistically significant. These findings are consistent with results of similarly designed studies that characterized and compared myocardial injury during standard versus cooled HD.[22,24,27] However, certain shortcomings in the results of those studies (e.g., no difference in left ventricular ejection fraction between standard and cooled HD groups[24,27]) and our work suggests that although DC is a favorable intervention in terms of feasibility and effectiveness, it may be worthwhile to combine it with other interventions (e.g., biofeedback dialysis[46-48]) to ameliorate HD-induced circulatory stress and myocardial injury.

2.4.3 Relationship to Dialysis Stress Factors

2.4.3.1 Standard HD

The continual drop in RRF over many HD sessions necessitates more fluid removal (i.e., higher UF) to account for increased interdialytic hypervolemia. However, higher UF causes greater hemodynamic stress[49] and increases IDH incidence, an independent predictor of RRF decline.[36,50] This coincides with our findings, where DRP severity was associated with mean and total UF (r=0.31; P,0.05 and r=0.26; P=0.05, respectively), suggesting that UF-induced ischemic injury may be a key factor in progressive RRF loss in patients on HD. This establishes a vicious cycle of HD-induced RRF decline, followed by a necessitated increase in UF, followed again by RRF decline, in keeping with the observed rapid decline shortly after HD initiation.

RRF declines faster with HD compared with peritoneal dialysis.[19,26] Although factors such as more gradual shifts in volume and higher biocompatibility play a role in

greater RRF preservation in peritoneal dialysis relative to HD,[51] another key element is dialysis-induced MS as a marker of global circulatory stress. MS incidence is much lower in peritoneal dialysis[52] compared with HD, suggesting renal perfusion could be better maintained during treatment and long-term RRF loss may be slowed as a result.

The observed renal hemodynamic response of patients to HD-induced circulatory stress was heterogenous, similar to other studies of the heart[43] and brain.[53] Most patients exhibited DRP, but some instead demonstrated increased perfusion. Although the cause of this heterogeneity in response is unknown, it is well recognized[54] and likely due to the status of patients' circulatory compensatory mechanisms. Most patients on HD have impaired compensatory mechanisms (chronotropic incompetence,[55,56] β-blocker use,[57] reduced baroreflex sensitivity[54]), increasing their vulnerability to UF-induced hypovolemia and IDH, whereas patients with more intact mechanisms are better able to compensate for HD-induced circulatory stress. In addition, CKD-related factors, such as increased fluid volume retention, altered sympathetic nervous system activity, endothelial dysfunction, oxidative stress, inflammation, and increased arterial stiffness, may contribute to varying BP response to circulatory stress.[58] This may be why no association was observed between BP changes and MS development and/or changes in renal perfusion, despite significant declines in intradialytic SBP and MAP.

There was an association between MS and DRP, and patients taking β-blockers (but not other antihypertensives). The blockade of b-adrenergic receptors in the heart may weaken compensatory mechanisms to offset HD-induced circulatory stress. This mechanism is unique to β-blockers[57] and likely the cause of the observed correlation.

The discrepancy in sex between patients who did versus did not experience MS and DRP was apparent in another study that examined HD-induced myocardial injury,[42] where the male-to-female ratio was 28:17 for patients who exhibited RWMAs and 19:6 for those who did not. In a study assessing stress cardiomyopathy (i.e., acute emotional stress leading to MS), 95% of patients were female.[59] The authors cite several studies on myocardial injury with similar sex-related trends, but the biologic mechanisms behind this discrepancy are unknown.

2.4.3.2 Standard versus Cooled HD

DC did not demonstrate any statistically significant benefit in terms of controlling intradialytic BP compared with standard HD. However, patients were not subjected to continuous BP monitoring but only episodic checks (e.g., imaging timepoints). It is therefore entirely possible that there were BP differences between standard and cooled HD that could not be assessed. Also, DC has other effects to improve response to ischemic injury that go beyond just increasing peripheral vasoconstriction to limit hypotension[60] (e.g., increasing ischemic tolerance with moderate hypothermia and effects on the splanchnic circulation helping to support circulatory volume[61,62]). In addition, changes in SBP, DBP, and MAP were variably associated with MS and renal perfusion changes for standard and cooled HD. The combination of impaired compensatory mechanisms and increased BP variability may be the cause of these inconsistent findings.

During cooled HD, correlations between renal perfusion and UF were abolished, whereas correlations between myocardial injury and UF were reversed. Although these findings may have been because of a lower relative sample size, they support the idea

that DC better maintains hemodynamic stability during UF.[63,64] Therefore, HD effectiveness could be improved by using DC to more easily achieve patient-specific UF requirements.

Four out of 15 patients (27%) were shivering and/or reported feeling cold only during cooled HD. Other studies found similar[22,65] and higher[63] temperature-related symptom incidence. Jefferies *et al*.[27] used patient-individualized body temperature dialysate (i.e., 0.5°C below core temperature) to improve DC tolerability, where only one out of 11 patients reported cold-related symptoms. This individualized intervention was subsequently applied to a larger cohort of 73 patients, with no cooling-related adverse events reported.[24,25]

2.4.4 Limitations

This early phase study has several limitations. Patients received a radiation dose of approximately 8 mSv during each CT perfusion scan. Considering that radiation-induced cancer manifestation typically takes decades,[66] and HD patients are generally older and have a low five-year survival rate,[67] patients' lifespans are not expected to be affected in any significant way. In addition, only patients with urine output <250 mL/24 hours were examined to limit contrast-induced nephropathy. As a result, the study focused on patients with low baseline RRF, and this group may be predisposed to ischemic injury. However, this was proof-of-principle work and further studies are needed in patients with higher RRF, including patients on incident HD.

There appeared to be no significant artifactual effect of contrast media on renal perfusion. First, using further exposure to contrast, we demonstrated almost complete

recovery in average perfusion after HD. Second, contrast agent administration was low risk (low intravenous dose). Third, crossover experiment patients underwent the same HD treatments but exhibited improved renal hemodynamics with DC (despite identical contrast exposure). In addition, we have previously demonstrated testosterone-dependent reduction in renal perfusion, with recovery after discontinuation (using the same small contrast load).[35]

These were pilot experiments with a modest total sample size of 29 patients. Thus, generalizing the findings to the general population should be withheld until a larger, randomized, controlled trial is conducted. However, these experiments included detailed, multimodal imaging measurements, where both inter- and intra-patient variations were assessed. Further studies are required to examine the direct effects of standard and cooled HD upon renal perfusion in individuals with higher RRF, and to longitudinally follow patients on incident HD with respect to declining RRF.

2.5 Conclusion

In conclusion, recurrent HD-induced renal ischemia lays the groundwork toward pathophysiologically explaining the previously observed relationship between time spent on dialysis and declining RRF. In addition, although amelioration of the decline in renal perfusion by DC did not reach statistical significance, this intervention, which has already been applied in the protection of the brain and heart from HD-induced injury, may provide protection from recurrent kidney injury.

2.6 References

1. Kjaergaard KD, Jensen JD, Peters CD, et al. Preserving residual renal function in dialysis patients: an update on evidence to assist clinical decision making. *NDT Plus*. 2011;4:225-230.

2. van der Wal WM, Noordzij M, Dekker FW, et al. Full loss of residual renal function causes higher mortality in dialysis patients; findings from a marginal structural model. *Nephrol Dial Transplant*. 2011;26:2978-2983.

3. Churchill DN, Taylor DW, Keshaviah PR. Adequacy of Dialysis and Nutrition in Continuous Peritoneal Dialysis: Association with Clinical Outcomes. *J Am Soc Nephrol*. 1996;7:198-207.

4. Shemin D, Bostom AG, Laliberty P, et al. Residual Renal Function and Mortality Risk in Hemodialysis Patients. *Am J Kidney Dis*. 2001;38:85-90.

5. Bonomini V, Albertazzi A, Vangelista A, et al. Residual Renal Function and Effective Rehabilitation in Chronic Dialysis. *Nephron*. 1976;16:89-99.

6. Merkus MP, Jager KJ, Dekker FW, et al. Predictors of Poor Outcome in Chronic Dialysis Patients: The Netherlands Cooperative Study on the Adequacy of Dialysis. *Am J Kidney Dis*. 2000;35:69-79.

7. Vilar E, Wellsted D, Chandna SM, et al. Residual renal function improves outcome in incremental haemodialysis despite reduced dialysis dose. *Nephrol Dial Transplant*. 2009;24:2502-2510.

8. Vilar E, Farrington K. Emerging Importance of Residual Renal Function in End-Stage Renal Failure. *Semin Dialysis*. 2011;24:487-494.

9. Canaud B. Residual renal function: the delicate balance between benefits and risks. *Nephrol Dial Transplant*. 2008;23:1801-1805.

10. Wang A-M, Lai K-N. The importance of residual renal function in dialysis patients. *Kidney Int*. 2006;69:1726-1732.

11. Mathew AT, Fishbane S, Obi Y, et al. Preservation of residual kidney function in hemodialysis patients: reviving an old concept. *Kidney Int*. 2016;90:262-271.

12. Shafi T, Jaar BG, Plantinga LC, et al. Association of Residual Urine Output with Mortality, Quality of Life, and Inflammation in Incident Hemodialysis Patients: The CHOICE (Choices for Healthy Outcomes in Caring for End-Stage Renal Disease) Study. *Am J Kidney Dis*. 2010;56:348-358.

13. National Kidney Foundation: KDOQI clinical practice guidelines and clinical practice recommendations: Hemodialysis adequacy, peritoneal dialysis adequacy and vascular access: Update 2006. *Am J Kidney Dis*. 2006;48:S1-S322.

14. Jansen MAM, Hart AAM, Korevaar JC, et al. Predictors of the rate of decline of residual renal function in incident dialysis patients. *Kidney Int*. 2002;62:1046-1053.

15. Rottembourg J, Issad B, Gallego J, et al. Evolution of residual renal function in patients undergoing maintenance haemodialysis or continuous ambulatory peritoneal dialysis. *Proc Eur Dial Transplany Assoc*. 1983;19:397-403.

16. Obi Y, Streja E, Rhee CM, et al. Incremental Hemodialysis, Residual Kidney Function, and Mortality Risk in Incident Dialysis Patients: A Cohort Study. *Am J Kidney Dis*. 2016;68:256-265.

17. van Stone JC. The Effect of Dialyzer Membrane and Etiology of Kidney Disease on the Preservation of Residual Renal Function in Chronic Hemodialysis Patients. *ASAIO J*. 1995;41:M713-M716.

18. Menon MK, Naimark DM, Bargman JM, et al. Long-term blood pressure control in a cohort of peritoneal dialysis patients and its association with residual renal function. *Nephrol Dial Transplant*. 2001;16:2207-2213.

19. Moist LM, Port FK, Orzol SM, et al. Predictors of Loss of Residual Renal Function among New Dialysis Patients. *J Am Soc Nephrol*. 2000;11:556-564.

20. McIntyre CW. Recurrent Circulatory Stress: The Dark Side of Dialysis. *Semin Dialysis*. 2010;23:449-451.

21. Toth-Manikowski SM, Sozio SM. Cooling dialysate during in-center hemodialysis: Beneficial and deleterious effects. *World J Nephrol*. 2016;5:166-171.

22. Selby NM, Burton JO, Chesterton LJ, et al. Dialysis-Induced Regional Left Ventricular Dysfunction Is Ameliorated by Cooling the Dialysate. *Clin J Am Soc Nephrol*. 2006;1:1216-1225.

23. Selby NM, McIntyre CW. A systematic review of the clinical effects of reducing dialysate fluid temperature. *Nephrol Dial Transplant*. 2006;21:1883-1898.

24. Odudu A, Eldehni MT, McGann GP, et al. Randomized Controlled Trial of Individualized Dialysate Cooling for Cardiac Protection in Hemodialysis Patients. *Clin J Am Soc Nephrol*. 2015;10:1408-1417.

25. Eldehni MT, Odudu A, McIntyre CW. Randomized Clinical Trial of Dialysate Cooling and Effects on Brain White Matter. *J Am Soc Nephrol*. 2015;26:957-965.

26. Lysaght MJ, Vonesh EF, Gotch F, et al. The influence of dialysis treatment modality on the decline of remaining renal function. *Trans Am Soc Artif Intern Organs*. 1991;37:598-604.

27. Jefferies HJ, Burton JO, McIntyre CW. Individualised dialysate temperature improves intradialytic haemodynamics and abrogates haemodialysis-induced myocardial stunning, without compromising tolerability. *Blood Purif*. 2011;32:63-68.

28. Burton JO, Jefferies HJ, Selby NM, et al. Hemodialysis-Induced Repetitive Myocardial Injury Results in Global and Segmental Reduction in Systolic Cardiac Function. *Clin J Am Soc Nephrol*. 2009;4:1925-1931.

29. Julious SA. Sample size of 12 per group rule of thumb for a pilot study. *Pharm Stat*. 2005;4:287-291.

30. Whitehead AL, Julious SA, Cooper CL, et al. Estimating the sample size for a pilot randomised trial to minimise the overall trial sample size for the external pilot and main trial for a continuous outcome variable. *Stat Methods Med Res*. 2016;25:1057-1073.

31. Artz NS, Sadowski EA, Wentland AL, et al. Arterial Spin Labeling MRI for Assessment of Perfusion in Native and Transplanted Kidneys. *Magn Reson Imaging*. 2011;29:74-82.

32. Khatir DS, Pedersen M, Jespersen B, et al. Evaluation of Renal Blood Flow and Oxygenation in CKD Using Magnetic Resonance Imaging. *Am J Kidney Dis*. 2015;66:402-411.

33. Rossi C, Artunc F, Martirosian P, et al. Histogram Analysis of Renal Arterial Spin Labeling Perfusion Data Reveals Differences Between Volunteers and Patients With Mild Chronic Kidney Disease. *Invest Radiol*. 2012;47:490-496.

34. Gillis KA, McComb C, Patel RK, et al. Non-Contrast Renal Magnetic Resonance Imaging to Assess Perfusion and Corticomedullary Differentiation in Health and Chronic Kidney Disease. *Nephron*. 2016;133:183-192.

35. Filler G, Ramsaroop A, Stein R, et al. Is Testosterone Detrimental to Renal Function? *Kidney Int Rep*. 2016;1:306-310.

36. Sjolund J, Anton DG, Bayes LY, et al. Diuretics, Limited Ultrafiltration, and Residual Renal Function in Incident Hemodialysis Patients: A Case Series. *Semin Dialysis*. 2016;29:410-415.

37. Daugirdas JT. Pathophysiology of Dialysis Hypotension: An Update. *Am J Kidney Dis*. 2001;38:S11-S17.

38. Ronco C, Kellum JA, Haase M. Subclinical AKI is still AKI. *Crit Care*. 2012;16:1-4.

39. McIntyre CW, Burton JO, Selby NM, et al. Hemodialysis-Induced Cardiac Dysfunction Is Associated with an Acute Reduction in Global and Segmental Myocardial Blood Flow. *Clin J Am Soc Nephrol*. 2008;3:19-26.

40. McIntyre CW, Goldsmith DJ. Ischemic brain injury in hemodialysis patients: which is more dangerous, hypertension or intradialytic hypotension? *Kidney Int*. 2015;87:1109-1115.

41. McIntyre CW. Haemodialysis-induced myocardial stunning in chronic kidney disease - a new aspect of cardiovascular disease. *Blood Purif*. 2010;29:105-110.

42. Burton JO, Jefferies HJ, Selby NM, et al. Hemodialysis-Induced Cardiac Injury: Determinants and Associated Outcomes. *Clin J Am Soc Nephrol*. 2009;4:914-920.

43. Dasselaar JJ, Slart RHJA, Knip M, et al. Haemodialysis is associated with a pronounced fall in myocardial perfusion. *Nephrol Dial Transplant*. 2009;24:604-610.

44. Dorairajan S, Chockalingam A, Misra M. Myocardial stunning in hemodialysis: What is the overall message? *Hemodial Int*. 2010;14:447-450.

45. Crowley LE, McIntyre CW. Remote ischaemic conditioning—therapeutic opportunities in renal medicine. *Nat Rev Nephrol*. 2013;9:739-746.

46. McIntyre CW, Lambie SH, Fluck RJ. Biofeedback controlled hemodialysis (BF-HD) reduces symptoms and increases both hemodynamic tolerability and dialysis adequacy in non-hypotension prone stable patients. *Clin Nephrol*. 2003;60:105-112.

47. Ronco C, Brendolan A, Milan M, et al. Impact of biofeedback-induced cardiovascular stability on hemodialysis tolerance and efficiency. *Kidney Int*. 2000;58:800-808.

48. Selby NM, Lambie SH, Camici PG, et al. Occurrence of Regional Left Ventricular Dysfunction in Patients Undergoing Standard and Biofeedback Dialysis. *Am J Kidney Dis*. 2006;47:830-841.

49. Bos WJW, Bruin S, van Olden RW, et al. Cardiac and Hemodynamic Effects of Hemodialysis and Ultrafiltration. *Am J Kidney Dis*. 2000;35:819-826.

50. Saran R, Bragg-Gresham JL, Levin NW, et al. Longer treatment time and slower ultrafiltration in hemodialysis: Associations with reduced mortality in the DOPPS. *Kidney Int*. 2006;69:1222-1228.

51. Marron B, Remon C, Perez-Fontan M, et al. Benefits of preserving residual renal function in peritoneal dialysis. *Kidney Int*. 2008;73:S42-S51.

52. Selby NM, McIntyre CW. Peritoneal Dialysis Is Not Associated with Myocardial Stunning. *Periton Dialysis Int*. 2011;31:27-33.

53. Polinder-Bos HA, Garcia DV, Kuipers J, et al. Hemodialysis Induces an Acute Decline in Cerebral Blood Flow in Elderly Patients. *J Am Soc Nephrol*. 2018;29:1317-1325.

54. Chesterton LJ, Selby NM, Fialova J, et al. Categorization of the hemodynamic response to hemodialysis: The importance of baroreflex sensitivity. *Hemodial Int*. 2010;14:18-28.

55. Carreira MAMQ, Nogueira AB, Pena FM, et al. Detection of Autonomic Dysfunction in Hemodialysis Patients Using the Exercise Treadmill Test: The Role of the

Chronotropic Index, Heart Rate Recovery, and R-R Variability. *PLoS One*. 2015;10:1-11.

56. Klein DA, Katz DH, Beussink-Nelson L, et al. Association of Chronic Kidney Disease with Chronotropic Incompetence in Heart Failure with Preserved Ejection Fraction. *Am J Cardiol*. 2015;116:1093–1100.

57. Gorre F, Vandekerckhove H. Beta-blockers: focus on mechanism of action. Which beta-blocker, when and why? *Acta Cardiol*. 2010;65:565-570.

58. Velasquez MT, Beddhu S, Nobakht E, et al. Ambulatory Blood Pressure in Chronic Kidney Disease: Ready for Prime Time? *Kidney Int Rep*. 2016;1:94-104.

59. Wittstein IS, Thiemann DR, Lima JAC, et al. Neurohumoral Features of Myocardial Stunning Due to Sudden Emotional Stress. *N Engl J Med*. 2005;352:539-548.

60. McGuire S, Horton EJ, Renshaw D, et al. Hemodynamic Instability during Dialysis: The Potential Role of Intradialytic Exercise. *Biomed Res Int*. 2018;2018:1-11.

61. Yu AW, Ing TS, Zabaneh RI, et al. Effect of dialysate temperature on central hemodynamics and urea kinetics. *Kidney Int*. 1995;48:237-243.

62. Yu AW, Lai KN. Dialysis hypotension and splanchnic circulation. *Int J Artif Organs*. 1998;21:774-777.

63. Dheenan S, Henrich WL. Preventing dialysis hypotension: A comparison of usual protective maneuvers. *Kidney Int*. 2001;59:1175-1181.

64. Azar AT. Effect of Dialysate Temperature on Hemodynamic Stability among Hemodialysis Patients. *Saudi J Kidney Dis Transpl*. 2009;20:596-603.

65. Rezki H, Salam N, Addou K, et al. Comparison of prevention methods of intradialytic hypotension. *Saudi J Kidney Dis Transplant*. 2007;18:361-364.

66. Ferrero A, Takahashi N, Vrtiska TJ, et al. Understanding, justifying, and optimizing radiation exposure for CT imaging in nephrourology. *Nat Rev Urol*. 2019;16:231-244.

67. Canadian Institute for Health Information. Annual Statistics on Organ Replacement in Canada: Dialysis, Transplantation and Donation, 2009 to 2018. 2019;

CHAPTER 3

3 Exploring the Link between Hepatic Perfusion and Systemic Endotoxemia in Hemodialysis Patients

The liver normally receives and clears gut-derived endotoxin but hemodialysis patients have elevated levels of circulating endotoxin. We used CT perfusion imaging to assess whether hemodialysis-induced circulatory stress disrupts hepatic perfusion and function, which could negatively affect the liver's control of endotoxemia.

The contents of this chapter were adapted from an original research manuscript entitled "Exploring the Link between Hepatic Perfusion and Systemic Endotoxemia in Hemodialysis Patients: A Randomized Crossover Study", which was submitted for publication in *Kidney International* in 2020 and co-authored by Raanan Marants, Elena Qirjazi, Fiona Li, Ka-Bik Lai, Cheuk-Chun Szeto, Philip Li, Ting-Yim Lee and Christopher McIntyre.

3.1 Introduction

Hemodialysis (HD) induces circulatory stress which causes mesenteric ischemia, leading to disrupted gut mucosal structure and function.[1,2] The resulting increase in translocated endotoxin (gut-derived proinflammatory mediators) correlates with a multitude of hemodynamic and cardiovascular complications.[3] The liver normally receives endotoxin from the gut via portal vein blood[4] and under healthy conditions, clears it before it reaches systemic circulation.[5] However, increased endotoxin has been found in HD patients compared to the general population and to early stage chronic kidney disease

(CKD) patients,[3] suggesting that HD may disrupt liver hemodynamics and function, allowing more gut-derived products to reach the systemic circulation.

Multiple organs develop subclinical ischemia due to intradialytic circulatory stress.[6] Functional imaging studies in the heart,[7,8] brain[9] and kidneys[10] have demonstrated these ischemic insults can be attenuated using dialysate cooling (DC),[11] providing intradialytic hemodynamic protection and minimization of chronic organ dysfunction. However, the liver's dual blood supply may allow it to potentially respond differently to HD-induced circulatory stress.[12] Previous work by our group and others has shown that liver hemodynamics and water content are not significantly affected by HD.[12-14] Even so, these studies have not assessed changes in the fractional supply (from portal vein or hepatic artery) and how it is related to endotoxemia in HD patients, or the effect of potentially protective interventions.

Therefore, we conducted an exploratory study of liver perfusion and excretory function using computed tomography (CT) perfusion imaging to measure hepatic arterial and portal venous blood flow derived separately from the hepatic artery and portal vein, respectively, during HD. By assessing intradialytic hepatic perfusion and function, we aimed to test the hypothesis that HD disrupts liver hemodynamics and drives endotoxemia. In addition, we intended to explore whether DC ameliorates HD-induced changes in liver hemodynamics and limits systemic exposure to endotoxin.

3.2 Methods

3.2.1 Patients

Patients from the London Health Sciences Centre Regional Renal Program (London, Ontario, Canada) were enrolled in the study after giving informed consent. Adult patients with HD vintage ≥3 months and low residual renal function (<250 mL/day to limit any potential effects of contrast-induced nephropathy) were eligible. Major exclusion criteria included: chronic liver or intestinal disease (excluding irritable bowel syndrome), previous liver transplant or resection, trans-jugular portosystemic shunt insertion, active infection/malignancy, current or planned pregnancy, breast feeding, uncontrolled diabetes mellitus (defined as recorded hypoglycemia during HD within the last 2 months) or known allergy to iodinated contrast agent.

3.2.2 Study Design

In this crossover study, patients underwent one standard (36.5°C) and one cooled (35.0°C) dialysate temperature HD session. Other than dialysate temperature, sessions were identical. The session order was randomly assigned, with patients acting as their own controls. The randomization list (in blocks of four) was generated by a London Health Sciences Centre Kidney Clinical Research Unit medical statistician and revealed to the investigator for allocating subjects to the appropriate study group. A washout period ≥7 days between sessions was scheduled to ensure no significant carry-over effects.[15] During these sessions, we collected baseline characteristics and blood work, assessed hepatic function (clearance of indocyanine green), and acquired CT liver perfusion imaging. This was a single-blinded study, where patients, HD unit staff and the

investigator were not blinded to the intervention, but imaging analysis was performed with the operator blinded to allocation.

This study was approved by the University of Western Ontario Health Sciences Research Ethics Board and was conducted in compliance with the approved protocols, Good Clinical Practice Guidelines, the Declaration of Helsinki, and all applicable regulatory requirements. The study was registered at ClinicalTrials.gov (NCT02997774).

3.2.3 CT Perfusion Imaging

CT liver perfusion imaging was performed on a GE Healthcare (Waukesha, WI) Revolution 256-slice CT scanner just before, 3 hours into (i.e., peak intradialytic stress), and 15 minutes post discontinuation of both HD sessions. Patients were moved to the CT bed for the intradialytic scan without interrupting HD treatment. Dynamic contrast-enhanced CT scanning of a 16 cm section of the abdomen was performed, without breath-hold, following iodinated contrast agent injection (at a rate of 5 mL/s, followed by a 30 mL saline flush). Scan regions were optimized to include as much of the liver as possible by performing a non-contrast localization scan prior to each CT perfusion scan, and were divided into 32 slices of 5 mm thickness each. This region was scanned 42 times at 2.8 s intervals using 120 kV and 22.4 mAs for a duration of approximately 2 minutes. Iopamidol (Isovue 370, Bracco Imaging) at 1 mL/kg of pre-HD patient weight (up to a maximum dose of 70 mL) was used as contrast agent in both HD sessions. Image noise was reduced using 100% ASIR (Adaptive Statistical Iterative Reconstruction, GE Healthcare) and liver motion from breathing between scans was minimized using non-rigid registration (GE Healthcare).

CT Perfusion 4D software (GE Healthcare) was used to analyze the registered images as follows: aortic and portal venous regions of interest (ROIs) were selected for generation of arterial and venous input functions, respectively. Next, model-based deconvolution[16] was used to compute liver perfusion and the corresponding hepatic arterial fraction, yielding total liver, hepatic arterial and portal venous perfusion maps. A region was then manually drawn in the perfusion maps of each slice to encompass the liver, where blood flow and blood volume thresholds of 200 mL/min/100g and 80 mL/100g, respectively (determined from prior sensitivity analysis), were imposed to remove non-parenchymal blood vessels from the region, yielding a liver parenchyma ROI. A ROI size-weighted average of the resulting perfusion values over all liver-containing slices was performed to obtain mean values (in mL/min/100g) of total, hepatic arterial and portal venous perfusion for the whole liver.

3.2.4 Quantification of Perfusion Heterogeneity

Based on previous work,[12,13] we hypothesized that HD may cause heterogeneous redistribution of liver perfusion, despite overall perfusion being maintained (Figure 3.1). Total liver perfusion heterogeneity was quantified using an in-house MATLAB (MathWorks, Natick, MA) program based on an algorithm developed by Brooks and Grigsby.[17] For this work, the algorithm quantified the magnitude of perfusion gradation between all pixel-pair combinations in all liver ROIs.

A ROI size-weighted average of the heterogeneity values over all the ROIs was performed to obtain a mean perfusion heterogeneity value for the whole liver. A summary of this procedure is presented in Figure 3.2.

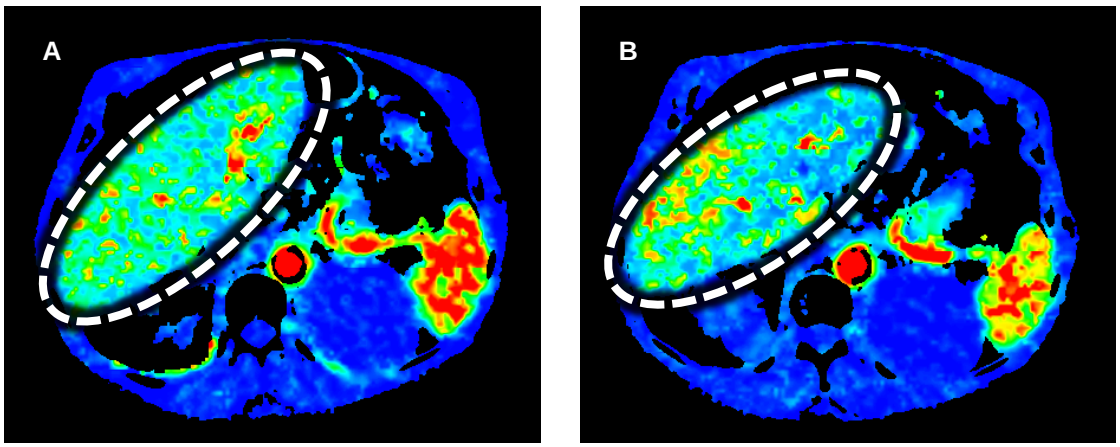

Figure 3.1: Insensitivity of global mean to changes in spatial perfusion heterogeneity visualized with hepatic perfusion maps. Total liver perfusion at baseline (A) and 3 hours into hemodialysis (B) for a patient. Liver parenchyma is outlined with dotted contours. Despite there being no measurable change in average liver perfusion between the two time-points, liver perfusion heterogeneity increased by approximately 25%.

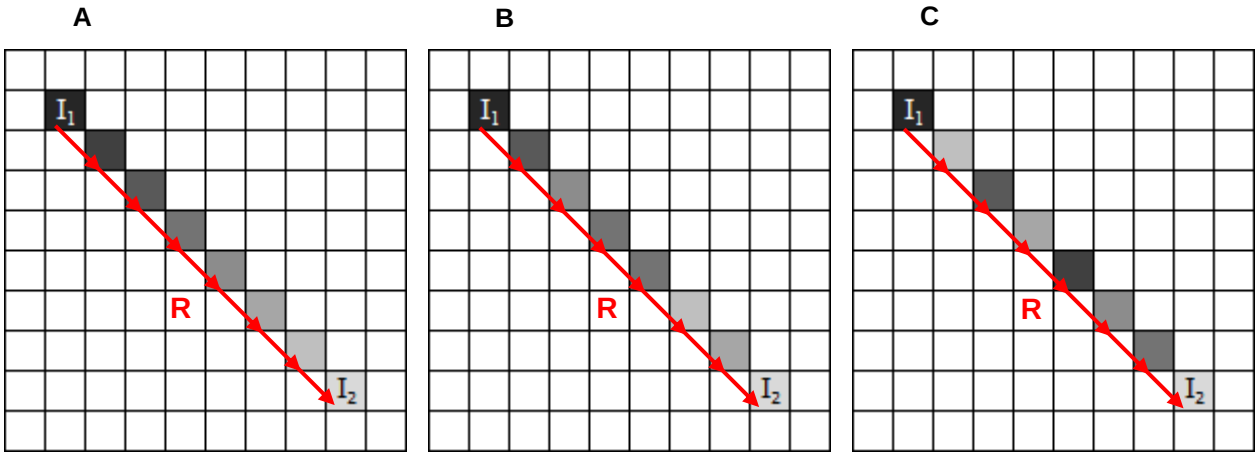
A
B
C
I_1
R
I_2

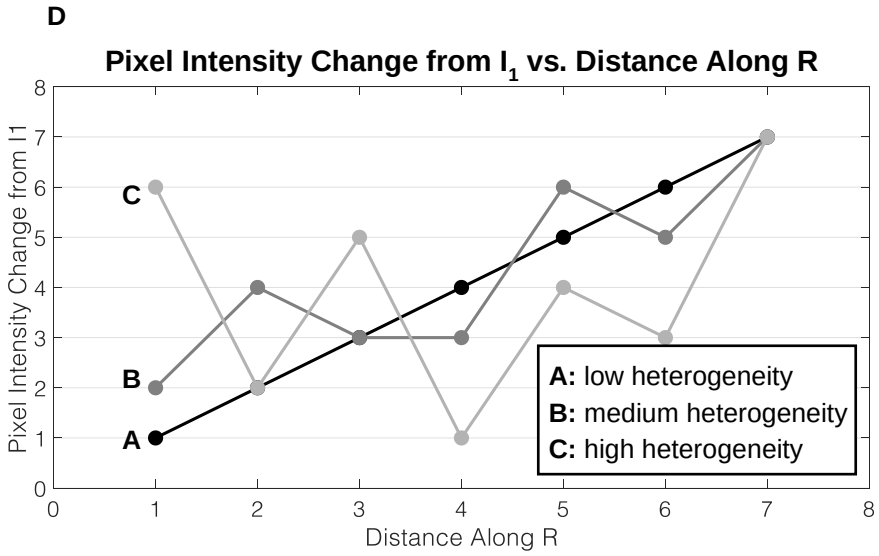
D
Pixel Intensity Change from I_1 vs. Distance Along R
Pixel Intensity Change from I1
Distance Along R
C
B
A
A: low heterogeneity
B: medium heterogeneity
C: high heterogeneity

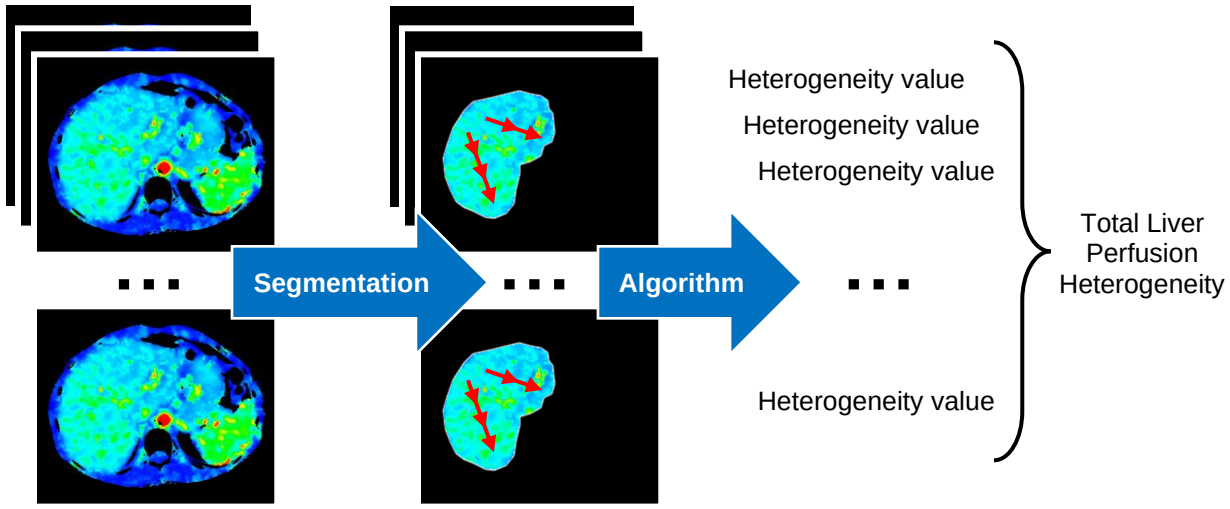
E
Segmentation
Algorithm
Heterogeneity value
Heterogeneity value
Heterogeneity value
Heterogeneity value
Total Liver Perfusion Heterogeneity

Figure 3.2: Theoretical basis of heterogeneity quantification algorithm and application of the algorithm in this study's workflow. The heterogeneity quantification algorithm computes the magnitude of pixel intensity (e.g., perfusion) gradation between all pixel-pair combinations of the liver in every slice. An example of heterogeneity quantification for a single pixel-pair (pixels 1 and 2, with intensities of I_1 and I_2, respectively, separated by distance R) is shown in the case of (A) low, (B) medium, and (C) high heterogeneity. (D) Plot of pixel intensity change from I_1 versus distance along R for case A, B, and C. (E) Following the generation of liver perfusion maps, manually drawn regions of interest were used to segment the liver parenchyma for all relevant slices. Next, the heterogeneity quantification algorithm was applied (red arrows) to all non-zero pixel-pairs within each resulting region, yielding a perfusion heterogeneity value for each region (i.e., for each slice). A region of interest size-weighted average of the heterogeneity values over the selected slices was performed to obtain a mean perfusion heterogeneity value for the whole liver.

3.2.5 Assessment of Hepatic Excretory Function

Indocyanine green (ICG) is a synthetic dye that is solely taken up by hepatocytes and excreted in bile,[18] where ICG clearance from blood reflects excretory liver function. Pulsed-dye densitometry (PDD; DDG devices, Nihon Kohden, Japan) provides a real-time, non-invasive measurement of blood ICG concentration using optical light at two wavelengths: 805 nm for peak optimal ICG absorption and 890 nm for minimal absorption.[19] Detection of ICG in the blood is based on the fractional change in optical absorption between the two wavelengths, where heartbeat-induced blood vessel pulsations lead to optical path length changes.[20] As a result, PDD measures ICG clearance from blood, which reflects excretory liver function. While ICG has historically also been used to assess liver blood flow, this application has methodological challenges[21,22] and was forgone in favor of using CT perfusion imaging in this work.

PDD was acquired for approximately 15 minutes following a single ICG bolus injection through a peripheral cannula by attaching a finger probe to the patient, measuring ICG concentration in blood over time with every heartbeat. These measurements were performed just before and 3 hours into every HD session. A biexponential fit, based on an open two-compartment model of ICG uptake and excretion, was applied to the data in order to extrapolate past the 15-minute point and more accurately determine the clearance.[23] The ICG clearance rate (mL/min) was calculated as the quotient of the ICG dose (mg) and the area under the ICG concentration vs. time curve (mg·min/mL).

3.2.6 Quantification of Endotoxin Levels

Serum lipopolysaccharide endotoxin quantification was performed using a Limulus Amebocyte assay (Cambrex, Verviers, Belgium). Following collection in London, all serum samples were shipped to and assayed at the Prince of Wales Hospital in Hong Kong, and endotoxin quantification was performed as described previously[24] to ensure comparability with results generated from our previous studies of endotoxin (all of which were analyzed in the same lab). Briefly, samples were diluted to 20% with endotoxin-free water and heated to 70°C for 10 minutes to inactivate plasma proteins. The manufacturer's protocol was used to quantify serum lipopolysaccharide. Samples with lipopolysaccharide level below the detection limit of 0.01 endotoxin units (EU)/mL were taken as 0 EU/mL. Samples were run in duplicate and the background noise was subtracted.

3.2.7 Statistical Analysis

Liver perfusion and excretory function were scarcely assessed previously in the context of HD and insufficient data exist to support performing a meaningful sample size calculation. This was an initial proof-of-principle study for hypothesis generation, with a sample size not powered for inferential statistical analysis. However, the sample size is comparable with previously published norms[7,10,25,26] and recommendations,[27,28] and was chosen on a partly pragmatic basis.

All statistical analyses were performed using SPSS, version 25.0 (IBM, Chicago, IL). Repeated measure ANOVA with Bonferroni-corrected post-hoc t-tests, and patient baseline-adjusted ANCOVA, were used to detect differences between groups and subgroups. Pearson's product-moment correlation coefficient was used to determine associations between variables, and McNemar's test was used to detect differences between proportions. Two-tailed P values <0.05 were considered statistically significant. Results are presented as mean ± standard error of the mean, unless otherwise specified.

3.3 Results

3.3.1 Clinical Characteristics of Study Population

Sixteen patients (ten male) aged 45-84 years were enrolled in this study. One patient was unable to return for the second session and was excluded from analysis. Fifteen patients completed the study, and Table 3.1 presents the summary of patient baseline characteristics, including age, sex, HD treatment details and comorbidities. This patient cohort was the same as the project 1 cooled HD cohort.

Table 3.1: Baseline characteristics of second project study population.

Characteristics	Mean (Range)[a]
n	15
Age	63 (45–84)
Men, n (%)	10 (67)
Dialysis Vintage (years)	3.0 (0.8–25.4)
Length of Hemodialysis Session (hours)	3.6 (3.1–4.2)
Ultrafiltration (mL/kg)	23.3 (6.1–40.9)
Coronary Artery Disease, n (%)	5 (33)
Congestive Heart Failure, n (%)	3 (20)
Peripheral Vascular Disease, n (%)	3 (20)
Diabetes, n (%)	9 (60)
Hypertension, n (%)	14 (93)

[a]Unless otherwise specified.

3.3.2 Hepatic Perfusion

Average baseline total liver perfusion was 82.7±3.7 mL/min/100g, with an average hepatic arterial fraction of 22.6%. Average total liver, hepatic arterial and portal venous perfusion changed to 106.7%±5.4%, 101.3%±11.2% and 111.1%±5.1% of baseline at peak HD stress, and 105.6%±3.7%, 102.7%±9.6% and 109.1%±6.0% of baseline after HD, respectively. None of these changes were statistically significant, but portal vein perfusion showed the greatest trend towards changing during HD (P=0.14, Figure 3.3A). Perfusion heterogeneity increased by 12.5%±4.4% (P=0.038) and 17.8%±3.7% (P=0.001) with respect to baseline during and after HD, respectively (Figure 3.4A). There

was an association between intradialytic changes in perfusion heterogeneity and total liver perfusion (r=0.70, P=0.003).

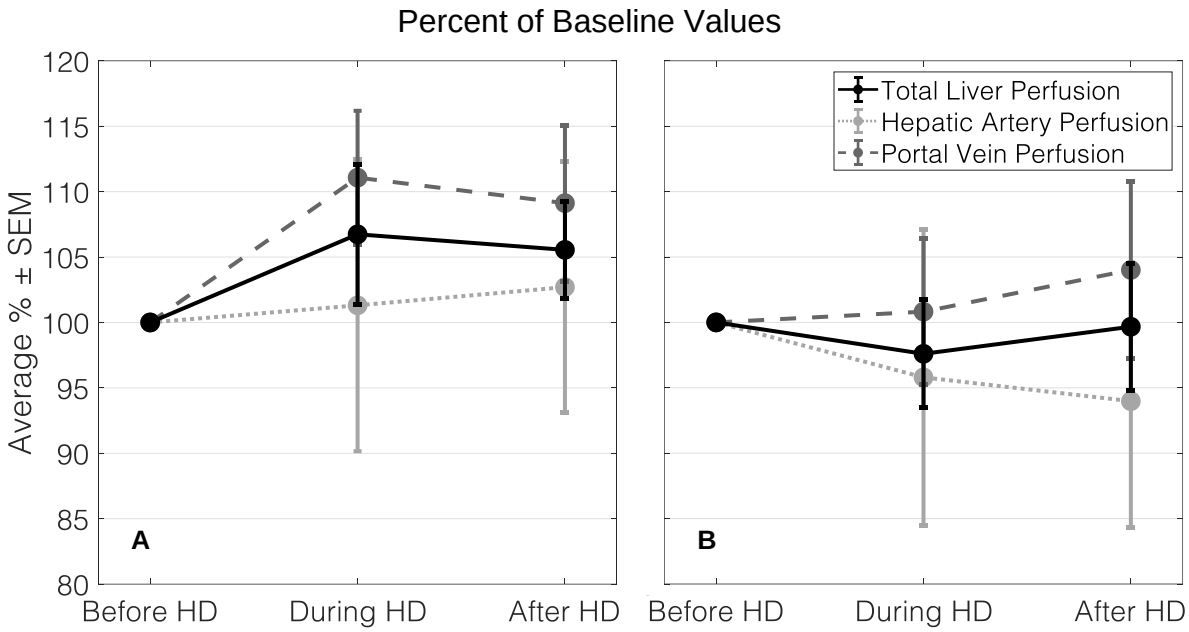

Figure 3.3: Plots of relative hepatic perfusion to baseline before, 3 hours into and after standard HD (A) and cooled HD (B). There were no significant changes in total liver, hepatic artery and portal vein perfusion over the course of either standard or cooled HD. However, portal vein perfusion demonstrated the greatest trend towards increasing during standard HD (P=0.14). Results are given as average ± standard error of the mean (SEM).

3.3.3 Hepatic Excretory Function

The ICG clearance rate dropped by 14.5%±5.3% (P=0.016) with respect to baseline during HD (Figure 3.4A). Changes in ICG clearance rate correlated with changes in total liver perfusion (r=0.55, P=0.034) and showed an associative trend with changes in perfusion heterogeneity (r=0.49, P=0.06) during HD. See Appendix A for a summary of relative changes in liver enzymes from pre- to post-HD (Table A1).

3.3.4 Endotoxin Levels

Average baseline endotoxin levels were 0.292±0.0156 EU/mL and correlated with dialysis vintage (r=0.58, P=0.024). Endotoxin increased by 19%±9.1% (P=0.15) and 28.4%±9.9% (P=0.037) with respect to baseline during HD and after HD, respectively (Figure 3.4A). Increased post-HD endotoxin correlated with the presence of congestive heart failure (r=0.52, P=0.046) but not with ultrafiltration (UF) metrics (UF volume, mean and maximum UF rates).

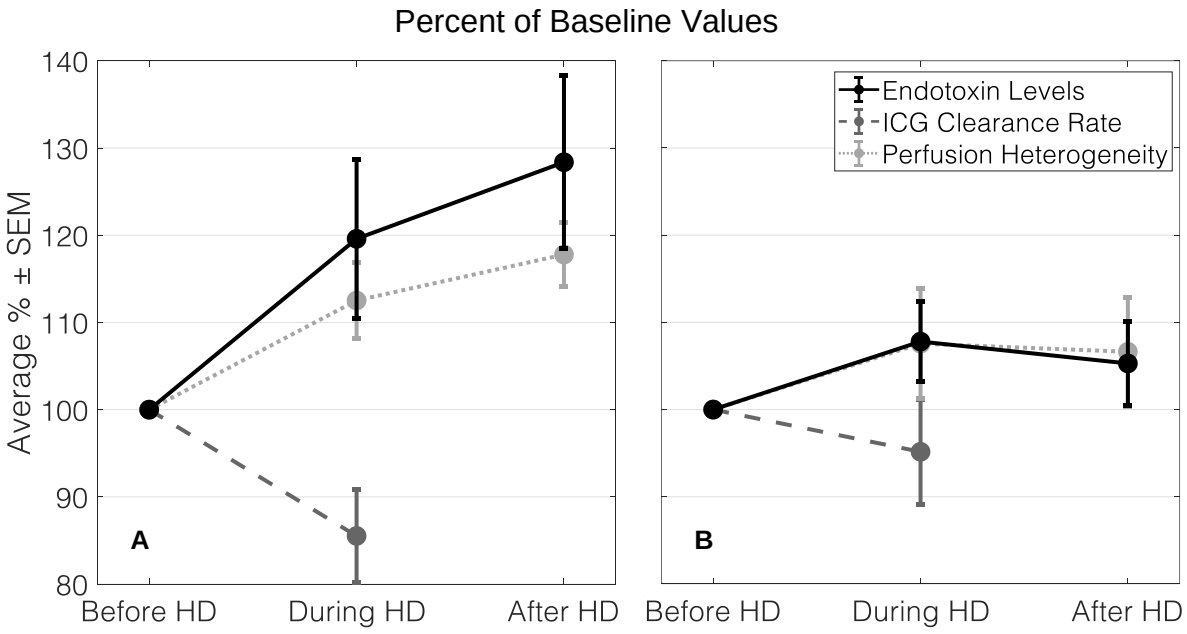

Figure 3.4: Plots of relative endotoxin levels, ICG clearance rate, and hepatic perfusion heterogeneity to baseline before, 3 hours into and after standard HD (A) and cooled HD (B). ICG clearance rate (P=0.016) and perfusion heterogeneity (P=0.038) significantly changed during standard HD and endotoxin levels (P=0.037) significantly changed after standard HD. None of these changes were statistically significant with cooled HD. Results are given as average ± standard error of the mean (SEM).

3.3.5 Effects of Dialysate Cooling

In contrast to standard HD, changes from baseline of all hepatic perfusion, hepatic excretory function, and endotoxin data during and after cooled HD were not statistically significant (Figures 3.3B and 3.4B). Although DC appeared to mitigate the hemodynamic and functional HD-induced changes that were observed for standard HD, session-specific, patient baseline-adjusted ANCOVA revealed that the changes in perfusion (total, hepatic arterial, portal venous), perfusion heterogeneity, ICG clearance rate, and endotoxin level between dialysis treatments were not statistically significantly different.

3.3.6 Intradialytic Blood Pressure and Adverse Events

Three patients experienced intradialytic hypotension (IDH) during both HD sessions, while ten experienced a systolic blood pressure drop >20 mm Hg during standard HD compared with eight during cooled HD (P=0.69). Intradialytic changes in blood pressure between dialysis treatments were not statistically significant according to session-specific, patient baseline-adjusted ANCOVA ($F(1,26)=2.814$ and $P=0.11$; $F(1,26)=0.582$ and $P=0.45$; $F(1,26)=0.382$ and $P=0.54$ for systolic blood pressure, diastolic blood pressure, and mean arterial pressure, respectively). During standard HD, increased endotoxin levels demonstrated an associative trend with the maximum reduction in mean arterial pressure ($r=0.47$, $P=0.08$). In terms of adverse events from DC, only thermal symptoms were reported: six patients reported feeling cold or experienced shivering during cooled HD, compared to two during standard HD (P=0.13).

3.3.7 Exploratory Analysis of Hepatic Perfusion Heterogeneity

Patients were divided into those with and without an increase in total liver perfusion heterogeneity during standard HD (defined as an increase in perfusion heterogeneity at peak dialytic stress ≥2 SEM of the patient group), yielding eight and seven patients with and without increased perfusion heterogeneity, respectively.

The subgroup of patients with increased perfusion heterogeneity had improved intradialytic ICG clearance (average decrease from baseline of 9.9%) and better maintenance of post-HD endotoxin levels (average increase from baseline of 18.8%) compared to the subgroup without increased perfusion heterogeneity (average decrease in ICG clearance from baseline of 18.2%, average increase in endotoxin levels from baseline of 39.3%). In addition, the subgroup of patients with increased perfusion heterogeneity received less benefit from DC in terms of the aforementioned functional measures (average decrease in ICG clearance from baseline of 10.9%, average increase in endotoxin levels from baseline of 8.4%), as compared to the subgroup without increased perfusion heterogeneity, who did appear to benefit from DC (average increase in ICG clearance from baseline of 2.1%, average increase in endotoxin levels from baseline of 1.7%).

Nevertheless, subgroup-specific, patient baseline-adjusted ANCOVAs were run for the aforementioned subgroup comparisons, revealing that none of the changes in ICG clearance or endotoxin levels between subgroups were significantly different. A summary of these findings, as well a comparison to these results for all patients collectively, is shown in Figure 3.5.

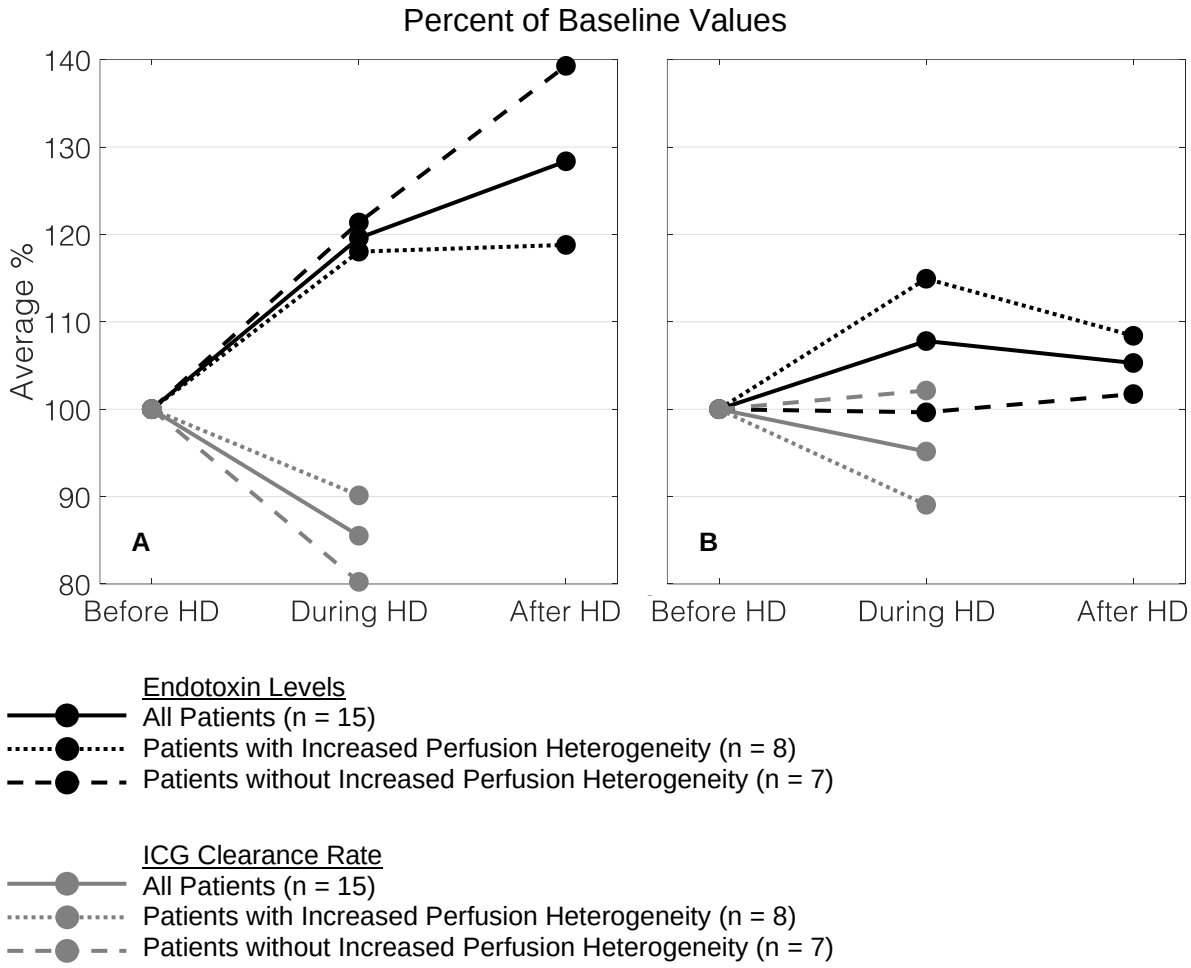

Figure 3.5: Plots of relative endotoxin levels and ICG clearance rate to baseline before, 3 hours into and after standard HD (A) and cooled HD (B) for patients with (n=8) and without (n=7) increased perfusion heterogeneity, and all patients (n=15). Increased perfusion heterogeneity during HD seemed to affect endotoxin levels and ICG clearance rate. (A) For standard HD, patients with increased perfusion heterogeneity appeared to have better intradialytic ICG clearance and improved maintenance of post-HD endotoxin levels compared to the subgroup of patients without increased perfusion heterogeneity (not statistically significant). (B) For cooled HD, the opposite was true (not statistically significant).

3.4 Discussion

This is the first study to demonstrate that redistribution of liver perfusion and attenuation of hepatic function occur together during HD. In addition, this is the first time

DC has been applied to prevent liver injury and endotoxemia. The important findings of this work may help to better understand how HD negatively affects the liver and results in the exacerbation of endotoxemia in maintenance HD patients, while also providing preliminary evidence for a potentially preventative intervention to limit systemic toxin exposure during HD and over the long-term.

3.4.1 Effects of Hemodialysis on Hepatic Perfusion, Hepatic Excretory Function and Endotoxemia

In this work, hepatic perfusion was measured using CT perfusion imaging, an approach which has been previously validated.[29] Overall liver perfusion did not significantly change during HD. While there is a paucity of data regarding intradialytic liver perfusion measurements, our findings are consistent with prior work.[12,13] These findings likely resulted from the liver's dual blood supply system which may have protected it from subclinical perfusion shifts associated with reduction in hepatic arterial flow,[30] although further work is needed to elucidate details of this mechanism. In addition, intradialytic portal vein perfusion showed the greatest trend towards changing, rising to 111% of baseline during HD. As portal venous blood is toxin-laden,[4] this finding suggests that HD-induced circulatory stress may increase endotoxin influx from the gut to the liver following translocation, and may be responsible for the trend towards increasing endotoxin levels during HD.

Liver perfusion heterogeneity was also assessed in this study, as significant perfusion changes may occur in small discrete liver regions and this signal would be lost if averaged over the entire liver volume (balanced by other areas shunting increased

blood flow). There are various approaches to quantify medical image heterogeneity (i.e., texture analysis[31,32]), and while each analysis technique has its advantages and applications, we chose to implement the algorithm developed by Brooks and Grigsby[17] due to its intuitiveness and ease of implementation with respect to our data. This algorithm yields a single statistic per image, providing a simple, quantitative method of comparing images based on heterogeneity. We observed with this algorithm a significant increase in hepatic perfusion heterogeneity during HD. While never studied in the context of HD, liver perfusion heterogeneity has been assessed for various types of liver injury,[33-35] consistently demonstrating a relationship with hepatic injury. In addition, changes in liver excretory function (i.e., ICG clearance rate) were related to changes in hepatic perfusion and perfusion heterogeneity in this work.

Previous studies (including in dialysis patients[36,37]) performed ICG-based measurements of hepatic function,[38] which in this work, was assessed by measuring the ICG clearance rate with the optical PDD technique. Because clearance of ICG and endotoxin occurs fully[18] and partially[39] within hepatocytes, respectively, and given that our patients had minimal residual renal function and a likely higher reliance on hepatic clearance, the ICG clearance rate therefore represents a suitable surrogate measure of hepatic endotoxin clearance.

Excretory liver function significantly declined during HD, as measured with PDD-based ICG clearance. Previous work has demonstrated that decreased ICG clearance following hepatic injury is linked to increased production of reactive oxygen intermediates and neutrophil elastase,[40] and occurs together with increased expression of endothelin-1,[41] all of which mediate liver cell injury and/or dysfunction.[40,42,43] In addition, endotoxin

itself has also been shown to induce oxidative stress[44,45] and attenuate ICG clearance.[46,47] Raised levels of these and other inflammatory mediators have been characterized in ESRD and HD patients,[3,44,45,48-51] suggesting that the liver is susceptible to recurrent HD-induced circulatory stress via inflammatory mediators which negatively affect hepatic function and cause hepatic injury (see Appendix A, Table A1).

We have previously demonstrated that renal perfusion significantly declines at peak dialytic stress,[10] representing repetitive, intradialytic episodes of ischemic acute kidney injury.[52] The potential negative relationship between kidney injury and the liver's clearance function has been previously discussed in the context of acute kidney injury[53,54] and ESRD,[13,55] and may be an important additional factor contributing to HD-induced hepatic dysfunction and increased endotoxemia.

In this work, endotoxin was quantified using a Limulus Amebocyte assay in a manner described previously.[24] Although the sensitivity of this technique has been criticized,[56] we have taken measures to establish internal consistency of our current measurements to ensure that our findings were not artefactual. Firstly, serum samples were collected before, during and after HD, yielding three endotoxin measurements per patient per study visit. As these samples were stored, shipped, and analyzed identically to one another, any potential issues with endotoxin quantification methodology would affect all three samples equally (save for minor fluctuations). Therefore, while the absolute measures of endotoxin may not be completely accurate, the relative changes in endotoxin from baseline levels (which we present and focus on) still hold true and provide scientific value. Secondly, the endotoxin quantification methodology used in this work is the same as what was done in our group's previous studies.[3,57-59] Given our familiarity and expertise

with this methodology, along with the convincing, positive results it has enabled us to produce previously (e.g., endotoxin levels in HD patients correlate with negative clinical outcomes and reduced survival[3]), we felt confident applying it to the current study as well.

The baseline endotoxin levels measured in this work (0.29 EU/mL) are consistent with findings in other studies of dialysis patients.[56,60] Endotoxin levels trended towards increasing during HD, and increased markedly from baseline after HD. This escalation has been attributed to increased endotoxin translocation from mesenteric injury and compromised gut mucosal permeability,[1,2] which is repeated during recurring dialysis sessions. This mechanism is reinforced by the strong correlation observed between baseline endotoxin levels and dialysis vintage. In addition, other than an associative trend between increased endotoxin levels and maximum reduction in mean arterial pressure during HD, we did not find evidence of HD-induced circulatory stress (i.e., UF metrics and IDH) being linked to endotoxemia, differing from the results of other studies.[3,59] This suggests (a) that in our patients, endotoxemia was driven more by liver hemodynamic and excretory functional changes than by direct effects of circulatory stress (i.e., UF metrics and IDH), and (b) that more generally, it may be the combination of direct effects of circulatory stress together with changes in hepatic hemodynamics and excretory function which contribute to increased endotoxin levels characteristically seen in HD patients.

Based on the results of this study (italicized items below), we propose the following pathway by which HD perpetuates endotoxemia in ESRD patients:

1: Mesenteric ischemia (due to HD-induced circulatory stress) disrupts gut mucosal structure and function, and increases bowel wall permeability.

2: Endotoxin more readily translocates across the intestinal barrier.

3: More endotoxin arrives to the liver from the gut via portal vein perfusion, which trends towards increasing during HD.

4: Decreased ICG clearance rate during HD represents compromised hepatic excretory function, likely due to increasing levels of endotoxin and other inflammatory mediators.

5: Further increase in post-HD endotoxin levels, likely resulting from the combination of more endotoxin arriving to the liver and lowered hepatic clearance function.

6: Recurrent cycles over many HD sessions lead to higher circulating endotoxin levels in ESRD patients.

3.4.2 Initial Description of Dialysate Cooling Effects

We demonstrated that DC did not negatively affect liver hemodynamics and function, or worsen endotoxemia, and may even have helped improve these metrics compared to standard HD, albeit this was not statistically significant. This is plausible because cooling potentiates better maintenance of organ perfusion due to peripheral vasoconstriction,[61] increased baroreflex sensitivity variability,[62] and reduced IDH.[62,63] Also, in the context of therapeutic hypothermia, cooling mitigates organ injury via several potential mechanisms of action (e.g., reducing inflammation, attenuating oxidative stress, decreasing free radical production), demonstrating effectiveness in multiple organs.[64,65] Therefore, it is reasonable to assume that DC-induced maintenance of liver perfusion and mitigation of hepatic injury could result in improved control of endotoxin levels. However, the beneficial changes of DC observed in this study were not statistically significantly different compared to changes during standard HD, and further work is needed to

demonstrate the protective potential of DC for preserving hepatic function and mitigating endotoxemia.

The DC results of this work corroborate with findings of similarly designed studies assessing myocardial injury[7,8,25] and renal ischemia[10] during cooled HD. The effectiveness of DC was not universal in those studies (e.g., no difference in left ventricular ejection fraction between standard and cooled HD groups,[8,25] no difference between decreased kidney perfusion between standard and cooled HD groups[10]) or in our work. In addition, four of our 15 patients (27%) experienced cold-related symptoms (e.g., shivering, feeling cold) during cooled HD only, which is consistent with the incidence of temperature-related symptoms reported in other studies.[7,66,67] These findings suggest although DC shows promise as an intradialytic intervention, combining cooling with other interventions (e.g., ischemic preconditioning[68,69]) and/or implementing other cooling techniques (e.g., DC based on pre-HD body temperature[8,25]) may more effectively ameliorate HD-induced circulatory stress and cooling-related symptoms.

3.4.3 Exploratory Analysis of Hepatic Perfusion Heterogeneity

Patients were divided into those with and without an increase in total liver perfusion heterogeneity during HD (due to well described association with hepatic injury[33-35]). Patients with increased perfusion heterogeneity had smaller relative increases in endotoxin levels post-HD and smaller relative decreases in ICG clearance during HD compared to patients without increased heterogeneity. Although these findings were not statistically significant (potentially due to small subgroup sizes) they suggest that increased heterogeneity may represent protection from hepatic injury, or a consequence

of it. Mehrabi *et al*.[33] speculated that “increased heterogeneity of liver perfusion … probably can be seen as a basic physiological reaction to trauma”, which in this context is HD-induced circulatory stress. Regardless of interpretation, increased heterogeneity was linked to increased perfusion, suggesting that higher levels of perfusion are required to redistribute blood flow and to increase perfusion heterogeneity. More studies are needed to better elucidate the relationship of perfusion heterogeneity with liver function during HD.

DC had intriguing and potentially important effects on patients when split into those with and without an increase in total liver perfusion heterogeneity during HD, although these results did not reach statistical significance. Patients with increased perfusion heterogeneity seemed to receive less benefit from cooling in terms of controlling endotoxin levels and maintaining ICG clearance. However, patients without increased heterogeneity appeared to benefit greatly from DC. As postulated earlier, it may be that increased intradialytic liver perfusion heterogeneity represents some form of intrinsic hepatic functional protection, and since cooling reduces the changes in heterogeneity, it acts to effectively attenuate this heterogeneity-based protective effect. Interestingly, DC and increased perfusion heterogeneity may be two competing protective effects which work to preserve liver function and limit endotoxemia.

3.4.4 Limitations

There are several limitations associated with this early phase study. First, our study did not examine the relationship between changes in ICG clearance and cardiac output during HD, which may have had significant effects on hepatic function measurements.

Second, this was a pilot study with a limited sample size of 15 patients, and generalization of findings should be withheld until a larger, randomized controlled trial is performed. However, this study incorporated imaging and functional measurements for assessment of both inter- and intra-patient variations. Third, only patients with low baseline renal function (urine output <250 mL/24 hours) were assessed to minimize the risk of contrast-induced nephropathy damaging significant residual renal function, and this patient group may be predisposed to hepatic injury. However, this was a proof-of-principle study, and future experiments are required to examine the direct effects of standard and cooled HD upon endotoxemia and liver hemodynamics in individuals with higher residual renal function, and to longitudinally follow patients new to HD with respect to increasing endotoxin levels.

3.5 Conclusion

In summary, HD-induced circulatory stress resulted in redistribution of liver perfusion and attenuation of hepatic excretory function. Endotoxin levels peaked after HD, and higher endotoxin levels in end-stage renal disease patients may result from the combination of two intradialytic effects: decreased hepatic clearance of endotoxin, and a trend towards increased toxin-laden portal vein perfusion to the liver. In addition, although mitigation of endotoxin via improved maintenance of hepatic perfusion and function with DC did not reach statistical significance, this intervention, which has already been applied in the protection of the brain, heart and kidneys from HD-induced injury, warrants further study on its protective effects from endotoxemia.

3.6 References

1. Diebel L, Kozol R, Wilson R, et al. Gastric intramucosal acidosis in patients with chronic kidney failure. *Surgery*. 1993;113:520-526.

2. Khanna A, Rossman JE, Fung HL, et al. Intestinal and hemodynamic impairment following mesenteric ischemia/reperfusion. *J Surg Res*. 2001;99:114-119.

3. McIntyre CW, Harrison LE, Eldehni MT, et al. Circulating endotoxemia: a novel factor in systemic inflammation and cardiovascular disease in chronic kidney disease. *Clin J Am Soc Nephrol*. 2011;6:133-141.

4. Jacob AI, Goldberg PK, Bloom N, et al. Endotoxin and bacteria in portal blood. *Gastroenterology*. 1977;72:1268-1270.

5. Caridis DT, Reinhold RB, Woodruff PWH. Endotoxemia in man. *Lancet*. 1972;299:1381-1386.

6. McIntyre CW. Recurrent Circulatory Stress: The Dark Side of Dialysis. *Semin Dialysis*. 2010;23:449-451.

7. Selby NM, Burton JO, Chesterton LJ, et al. Dialysis-Induced Regional Left Ventricular Dysfunction Is Ameliorated by Cooling the Dialysate. *Clin J Am Soc Nephrol*. 2006;1:1216-1225.

8. Odudu A, Eldehni MT, McGann GP, et al. Randomized Controlled Trial of Individualized Dialysate Cooling for Cardiac Protection in Hemodialysis Patients. *Clin J Am Soc Nephrol*. 2015;10:1408-1417.

9. Eldehni MT, Odudu A, McIntyre CW. Randomized Clinical Trial of Dialysate Cooling and Effects on Brain White Matter. *J Am Soc Nephrol*. 2015;26:957-965.

10. Marants R, Qirjazi E, Grant CJ, et al. Renal Perfusion during Hemodialysis: Intradialytic Blood Flow Decline and Effects of Dialysate Cooling. *J Am Soc Nephrol*. 2019;30:1086-1095.

11. Toth-Manikowski SM, Sozio SM. Cooling dialysate during in-center hemodialysis: Beneficial and deleterious effects. *World J Nephrol*. 2016;5:166-171.

12. Grant CJ, Huang SS, McIntyre CW. Hepato-splanchnic circulatory stress: An important effect of hemodialysis. *Semin Dialysis*. 2019;32:237-242.

13. Leblanc M, Roy LF, Villeneuve J-P, et al. Liver Blood Flow in Chronic Hemodialysis Patients. *Nephron*. 1996;73:396-402.

14. Grant CJ, Wade TP, McKenzie CA, et al. Effect of ultrafiltration during hemodialysis on hepatic and total-body water: an observational study. *BMC Nephrol*. 2018;19:1-8.

15. Maheshwari V, Lau T, Samavedham L, et al. Effect of cool vs. warm dialysate on toxin removal: rationale and study design. *BMC Nephrol*. 2015;16:1-5.

16. St. Lawrence KS, Lee T-Y. An Adiabatic Approximation to the Tissue Homogeneity Model for Water Exchange in the Brain: I. Theoretical Derivation *J Cereb Blood Flow Metab*. 1998;18:1365-1377.

17. Brooks FJ, Grigsby PW. Quantification of heterogeneity observed in medical images. *BMC Med Imaging*. 2013;13:1-12.

18. Wheeler HO, Cranston WI, Meltzer JI. Hepatic uptake and biliary excretion of indocyanine green in the dog. *Proc Soc Exp Biol Med*. 1958;99:11-14.

19. Goy RW, Chiu JW, Loo CC. Pulse dye densitometry: a novel bedside monitor of circulating blood volume. *Ann Acad Med Singapore*. 2001;30:192-198.

20. Iijima T, Aoyagi T, Iwao Y, et al. Cardiac output and circulating blood volume analysis by pulse dye-densitometry. *J Clin Monit*. 1997;13:81-89.

21. Skak C, Keiding S. Methodological problems in the use of indocyanine green to estimate hepatic blood flow and ICG clearance in man. *Liver*. 1987;7:155-162.

22. Keiding S. Hepatic clearance and liver blood flow. *J Hepatol*. 1987;4:393-398.

23. Imamura H, Sano K, Sugawara Y, et al. Assessment of hepatic reserve for indication of hepatic resection: decision tree incorporating indocyanine green test. *J Hepatobiliary Pancreat Surg*. 2005;12:16-22.

24. Brenchley JM, Price DA, Schacker TW, et al. Microbial translocation is a cause of systemic immune activation in chronic HIV infection. *Nat Med*. 2006;12:1365-1371.

25. Jefferies HJ, Burton JO, McIntyre CW. Individualised dialysate temperature improves intradialytic haemodynamics and abrogates haemodialysis-induced myocardial stunning, without compromising tolerability. *Blood Purif*. 2011;32:63-68.

26. Burton JO, Jefferies HJ, Selby NM, et al. Hemodialysis-Induced Repetitive Myocardial Injury Results in Global and Segmental Reduction in Systolic Cardiac Function. *Clin J Am Soc Nephrol*. 2009;4:1925-1931.

27. Julious SA. Sample size of 12 per group rule of thumb for a pilot study. *Pharm Stat*. 2005;4:287-291.

28. Whitehead AL, Julious SA, Cooper CL, et al. Estimating the sample size for a pilot randomised trial to minimise the overall trial sample size for the external pilot and main trial for a continuous outcome variable. *Stat Methods Med Res*. 2016;25:1057-1073.

29. Stewart EE, Chen X, Hadway J, et al. Hepatic perfusion in a tumor model using DCE-CT: an accuracy and precision study. *Phys Med Biol*. 2008;53:4249-4267.

30. Eipel C, Abshagen K, Vollmar B. Regulation of hepatic blood flow: The hepatic arterial buffer response revisited. *World J Gastroenterol*. 2010;16:6046-6057.

31. Haralick RM, Shanmugam K, Dinstein I. Textural Features for Image Classification. *IEEE T Syst Man Cyb*. 1973;SMC-3:610-621.

32. Reed TR, du Buf JMH. A Review of Recent Texture Segmentation and Feature Extraction Techniques. *CVGIP-Imag Understan*. 1993;57:359-372.

33. Mehrabi A, Golling M, Jahnke C, et al. Characterization of hepatic parenchymous perfusion heterogeneity and regional flow kinetics after porcine liver transplantation. *Microvasc Res*. 2003;65:78-87.

34. Mayumi T, Chan CK, Clemens MG, et al. Zonal heterogeneity of hepatic injury following shock/resuscitation: relationship of xanthine oxidase activity to localization of neutrophil accumulation and central lobular necrosis. *Shock*. 1996;5:324-332.

35. Martin DR, Seibert D, Yang M, et al. Reversible Heterogeneous Arterial Phase Liver Perfusion Associated With Transient Acute Hepatitis: Findings on Gadolinium-Enhanced MRI. *J Magn Reson Imaging*. 2004;20:838-842.

36. Mitra S, Chamney P, Greenwood R, et al. Serial Determinations of Absolute Plasma Volume with Indocyanine Green during Hemodialysis. *J Am Soc Nephrol*. 2003;14:2345-2351.

37. Ribitsch W, Schneditz D, Franssen CFM, et al. Increased Hepato-Splanchnic Vasoconstriction in Diabetics during Regular Hemodialysis. *PLoS One*. 2015;10:1-14.

38. Vos JJ, Wietasch KG, Absalom AR, et al. Green light for liver function monitoring using indocyanine green? An overview of current clinical applications. *Anaesthesia*. 2014;69:1364-1376.

39. Freudenberg MA, Freudenberg N, Galanos C. Time course of cellular distribution of endotoxin in liver, lungs and kidneys of rats. *Brit J Exp Pathol*. 1982;63:56-65.

40. Plevris JN, Jalan R, Bzeizi KI, et al. Indocyanine green clearance reflects reperfusion injury following liver transplantation and is an early predictor of graft function. *J Hepatol*. 1999;30:142-148.

41. Kubulus D, Mathes A, Reus E, et al. Endothelin-1 contributes to hemoglobin glutamer-200-mediated hepatocellular dysfunction after hemorrhagic shock. *Shock*. 2009;32:179-189.

42. Sadler KM, Walsh TS, Garden OJ, et al. Comparison of hepatic artery and portal vein reperfusion during orthotopic liver transplantation. *Transplantation*. 2001;72:1680-1684.

43. Bzeizi KI, Jalan R, Plevris JN, et al. Primary Graft Dysfunction After Liver Transplantation: From Pathogenesis to Prevention. *Liver Transplant Sur*. 1997;3:137-148.

44. Locatelli F, Canaud B, Eckardt K-U, et al. Oxidative stress in end-stage renal disease: an emerging threat to patient outcome. *Nephrol Dial Transplant*. 2003;18:1272-1280.

45. Morena M, Delbosc S, Dupuy A-M, et al. Overproduction of reactive oxygen species in end-stage renal disease patients: A potential component of hemodialysis-associated inflammation. *Hemodial Int*. 2005;9:37-46.

46. Beno DWA, Uhing MR, Goto M, et al. Endotoxin-induced reduction in biliary indocyanine green excretion rate in a chronically catheterized rat model. *Am J Physiol Gastrointest Liver Physiol*. 2001;280:G858-G865.

47. Okabe A, Hirota M, Kimura Y, et al. Functional Disturbance of Biliary Indocyanine Green Excretion in Rat Cerulein Pancreatitis Followed by Endotoxemia: Role of the Prime and the Second Attack. *J Pancreas*. 2003;4:178-183.

48. Khatib-Massalha E, Michelis R, Trabelcy B, et al. Free circulating active elastase contributes to chronic inflammation in patients on hemodialysis. *Am J Physiol Renal*. 2018;314:F203–F209.

49. Stefanidis I, Wurth P, Mertens PR, et al. Plasma Endothelin-1 in Hemodialysis Treatment – the Influence of Hypertension. *J Cardiovasc Pharmacol*. 2004;44:S43-S48.

50. Tridon A, Albuisson E, Deteix P, et al. Leukotriene B4 in Hemodialysis. *Artif Organs*. 1990;14:387-390.

51. Jörres A, Jörres D, Gahl GM, et al. Leukotriene release from neutrophils of patients on hemodialysis with cellulose membranes. *Int J Artif Organs*. 1992;15:84-88.

52. Ronco C, Kellum JA, Haase M. Subclinical AKI is still AKI. *Crit Care*. 2012;16:1-4.

53. Lane K, Dixon JJ, MacPhee IAM, et al. Renohepatic crosstalk: does acute kidney injury cause liver dysfunction? *Nephrol Dial Transplant*. 2013;28:1634-1647.

54. Dixon JJ, Lane K, MacPhee IAM, et al. Xenobiotic Metabolism: The Effect of Acute Kidney Injury on Non-Renal Drug Clearance and Hepatic Drug Metabolism. *Int J Mol Sci*. 2014;15:2538-2553.

55. Hou Y-C, Liu W-C, Liao M-T, et al. Long-Term and Short-Term Effects of Hemodialysis on Liver Function Evaluated Using the Galactose Single-Point Test. *Sci World J*. 2014;2014:1-6.

56. Wong J, Zhang Y, Patidar A, et al. Is Endotoxemia in Stable Hemodialysis Patients an Artefact? Limitations of the Limulus Amebocyte Lysate Assay and Role of (1→3)-β-D Glucan. *PLoS One*. 2016;11:e0164978.

57. John SG, Owen PJ, Harrison LEA, et al. The Impact of Antihypertensive Drug Therapy on Endotoxemia in Elderly Patients with Chronic Kidney Disease. *Clin J Am Soc Nephrol*. 2011;6:2389-2394.

58. Harrison LEA, Burton JO, Szeto C, et al. Endotoxaemia in Haemodialysis: A Novel Factor in Erythropoetin Resistance? *PLoS One*. 2012;7:e40209.

59. Jefferies HJ, Crowley LE, Harrison LE, et al. Circulating Endotoxaemia and Frequent Haemodialysis Schedules. *Nephron Clin Pract*. 2014;128:141-146.

60. Wong J, Vilar E, Farrington K. Endotoxemia in End-Stage Kidney Disease. *Semin Dialysis*. 2014;28:59-78.

61. Mahida BH, Dumler F, Zasuwa G, et al. Effect of Cooled Dialysate on Serum Catecholamines and Blood Pressure Stability. *Trans Am Soc Artif Intern Organs*. 1983;29:384-389.

62. Chesterton LJ, Selby NM, Burton JO, et al. Cool dialysate reduces asymptomatic intradialytic hypotension and increases baroreflex variability. *Hemodial Int*. 2009;13:189-196.

63. Cruz DN, Mahnensmith RL, Brickel HM, et al. Midodrine and Cool Dialysate Are Effective Therapies for Symptomatic Intradialytic Hypotension. *Am J Kidney Dis*. 1999;33:920-926.

64. Moore EM, Nichol AD, Bernard SA, et al. Therapeutic hypothermia: Benefits, mechanisms and potential clinical applications in neurological, cardiac and kidney injury. *Injury*. 2011;42:843-854.

65. Hsu S-F, Niu K-C, Lin C-L, et al. Brain cooling causes attenuation of cerebral oxidative stress, systemic inflammation, activated coagulation, and tissue ischemia/injury during heatstroke. *Shock*. 2006;26:210-220.

66. Rezki H, Salam N, Addou K, et al. Comparison of prevention methods of intradialytic hypotension. *Saudi J Kidney Dis Transplant*. 2007;18:361-364.

67. Dheenan S, Henrich WL. Preventing dialysis hypotension: A comparison of usual protective maneuvers. *Kidney Int*. 2001;59:1175-1181.

68. Park J, Ann SH, Chung HC, et al. Remote ischemic preconditioning in hemodialysis: a pilot study. *Heart Vessels*. 2014;29:58-64.

69. Salerno FR, Crowley LE, Odudu A, et al. Remote Ischemic Preconditioning Protects Against Hemodialysis-Induced Cardiac Injury. *Kidney Int Rep*. 2020;5:99-103.

CHAPTER 4

4 Measuring Glomerular Filtration Rate in End-Stage Renal Disease Patients on Hemodialysis using CT Perfusion Imaging

Accurate assessment of residual renal function in end-stage renal disease patients is critical for adjusting the hemodialysis prescription but no clinical method exists currently which can accurately and efficiently measure glomerular filtration rate in these patients. Using CT perfusion imaging, we developed and applied a novel glomerular filtration rate measurement approach in hemodialysis patients which has the potential to become an accessible clinical renal function assessment technique in this population.

The contents of this chapter were adapted from an original research manuscript entitled “Measuring Glomerular Filtration Rate in End-Stage Renal Disease Patients on Hemodialysis using CT Perfusion Imaging”, which was submitted for publication in *Radiology* in 2020 and co-authored by Raanan Marants, Christopher McIntyre, and Ting-Yim Lee.

4.1 Introduction

The current clinical protocol for measuring kidney function (i.e., glomerular filtration rate, GFR) in end-stage renal disease (ESRD) patients on hemodialysis (HD) is cumbersome, time-consuming and inaccurate.[1-3] This is problematic because adjusting HD prescription based on changes in a patient’s residual renal function (RRF) is an important aspect of clinical care[4] that is difficult to address and often disregarded.[1,3] If it were possible to readily and rapidly obtain accurate GFR measurements, RRF-based HD prescription adjustments may have yielded better outcomes for ESRD patients.

Presently, there is no way to accurately measure GFR in ESRD, which is commonly assessed using population-based equations (using demographic information and serum creatinine/urea levels) or urine/plasma sampling of endogenous/exogenous markers.[2] While these approaches represent the current gold standard in nephrology practice, they have important limitations to consider,[2] including:

- Population-based equation accuracy decreases with kidney disease progression
- Endogenous marker levels directly affected by HD and fluctuate during HD cycle
- Impossible to perform single-kidney GFR assessment

These limitations may be overcome with imaging-based GFR measurement. While many previous studies have explored such methodologies in animal and human subjects,[5,6] these techniques have never been applied to ESRD and/or HD patients. In this technical development, we propose using computed tomography perfusion (CTP) imaging to measure GFR in HD patients. If appropriately implemented, we believe that CTP imaging has the potential to become an accessible clinical GFR measurement method in ESRD patients on HD, providing a rapid, reliable and accurate measurement of kidney function.

4.2 Methods

4.2.1 Patients and Study Design

Patients from the London Health Sciences Centre Regional Renal Program (London, ON) were enrolled after giving informed consent. Adult patients with HD vintage ≥3 months and low RRF (<250 mL/day to limit any potential effects of contrast-induced nephropathy) were eligible. Exclusion criteria included: active infection/malignancy,

pregnancy, breast feeding, planned pregnancy, diabetic with hypoglycemia during HD within the last 2 months or known allergy to iodinated contrast agent.

In this crossover study, patients underwent one standard (36.5°C) and one cooled (35.0°C) dialysate temperature HD session. During both sessions, HD was administered using a Fresenius 5008 machine (Waltham, MA) with a high-flux polysulfone membrane. Session order was randomly assigned, with patients acting as their own controls. A washout period ≥7 days between sessions was scheduled to prevent significant carry-over effects. During each session, we collected baseline characteristics and blood work, and acquired CT renal perfusion imaging. Patients, hemodialysis unit staff and the investigator were not blinded to the intervention, but imaging analysis was performed with the operator blinded to allocation. This study was approved by the University of Western Ontario Health Sciences Research Ethics Board and was conducted in compliance with the approved protocol, Good Clinical Practice Guidelines and all applicable regulatory requirements.

4.2.2 CT Perfusion Imaging

CT renal perfusion imaging was performed on a GE Healthcare (Waukesha, WI) Revolution 256-slice CT scanner before, during (i.e., peak intradialytic stress), and after HD for both sessions. Patients were moved to the CT bed for the intradialytic scan without interrupting HD treatment. Iopamidol (Isovue 370, Bracco Imaging), at 1 mL/kg of pre-HD patient weight (up to a maximum dose of 70 mL), was the non-ionic, low-osmolar iodinated contrast agent used for both sessions.

Dynamic contrast-enhanced CT scanning of a 16 cm long abdominal region, selected to include as much of both kidneys as possible, was performed without breath-hold following contrast agent injection into an antecubital vein at 5 mL/s injection rate. The selected region was divided into 32 slices of 5 mm thickness each and scanned 42 times at 2.8 s intervals using 120 kV and 22.4 mAs for a duration of approximately 2 minutes. Image noise was reduced using 100% Adaptive Statistical Iterative Reconstruction (GE Healthcare). Reconstructed images were co-registered with non-rigid transformation (GE Healthcare) to minimize kidney misregistration from breathing motion.

The registered images were analyzed with the CT Perfusion 4D software (GE Healthcare). An aortic region of interest (ROI) was selected for generation of arterial input function (AIF, $C_a(t)$) from the registered dynamic images. Next, the AIF was deconvolved from the time-density curve of each 3×3 kidney voxel, Q(t), based on the Johnson-Wilson model of contrast distribution in kidney[7] to compute various functional parameters, yielding parametric maps of renal perfusion (F) and permeability-surface area product (PS)[8] for all slices containing the kidneys. In the deconvolution process, the parameters of the Johnson-Wilson model – F, K, k and MTT – were iteratively changed to minimize the sum of squared deviations of the convolution of the blood flow-scaled impulse residue function, $R_F(t)$, with $C_a(t)$ from Q(t) as shown in Figure 4.1.

4.2.3 GFR Quantification

To improve corticomedullary differentiation for accurate cortical delineation, the second quarter of the dynamic series CT images (i.e., timepoints 11-21 of 42) were summed together for each slice. This timepoint range was chosen to maximize contrast

enhancement in the cortex (i.e., cortical phase), which occurs in early timepoints (e.g., 1-10) for healthy kidneys but occurs later in diseased kidneys.[9,10] Next, a dynamic threshold was applied separately for each slice of each kidney of every patient, and was chosen by anatomically matching the segmented cortical region to the contrast-enhancement cortex of the summed image as closely as possible (see Figure 4.2). This process yielded a segmented cortical ROI which was superimposed onto the corresponding F and PS parametric maps for all relevant slices. The GFR was then computed as follows:

$$GFR_{pixel,i} = K \cdot M = (F \cdot E) \cdot (V \cdot D) = \left[F \cdot \left(1 - e^{-\frac{PS}{F}}\right)\right] \cdot [(A \cdot T) \cdot D]$$

K = filtration rate constant, M = pixel mass

F = perfusion, E = extraction efficiency

V = pixel volume, D = tissue density

PS = permeability-surface area product

A = pixel area, T = slice thickness

$$GFR_{slice} = \sum_{i=1}^{N_p} GFR_{pixel,i}$$

N_p = number of cortical pixels in image slice

$$GFR_{kidney} = BSA \cdot \sum_{i=1}^{N_s} GFR_{slice,i}$$

N_s = number of image slices in kidney

BSA = 1.73m^2 / patient's body surface area

For this work, A = (0.88 mm)^2, T = 5 mm and D = 1.050 g/mL[11] in all cases.

A

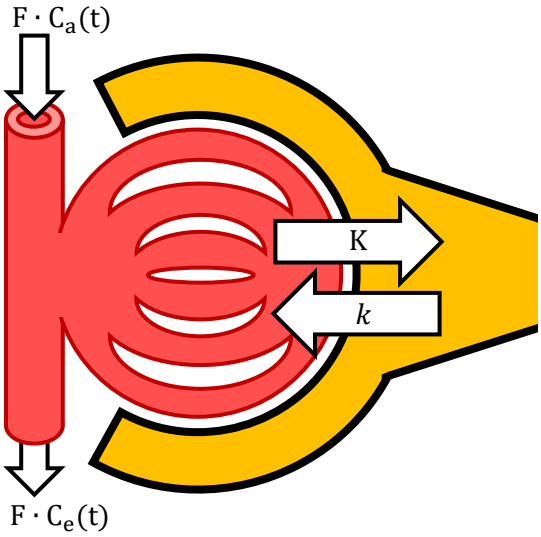

B

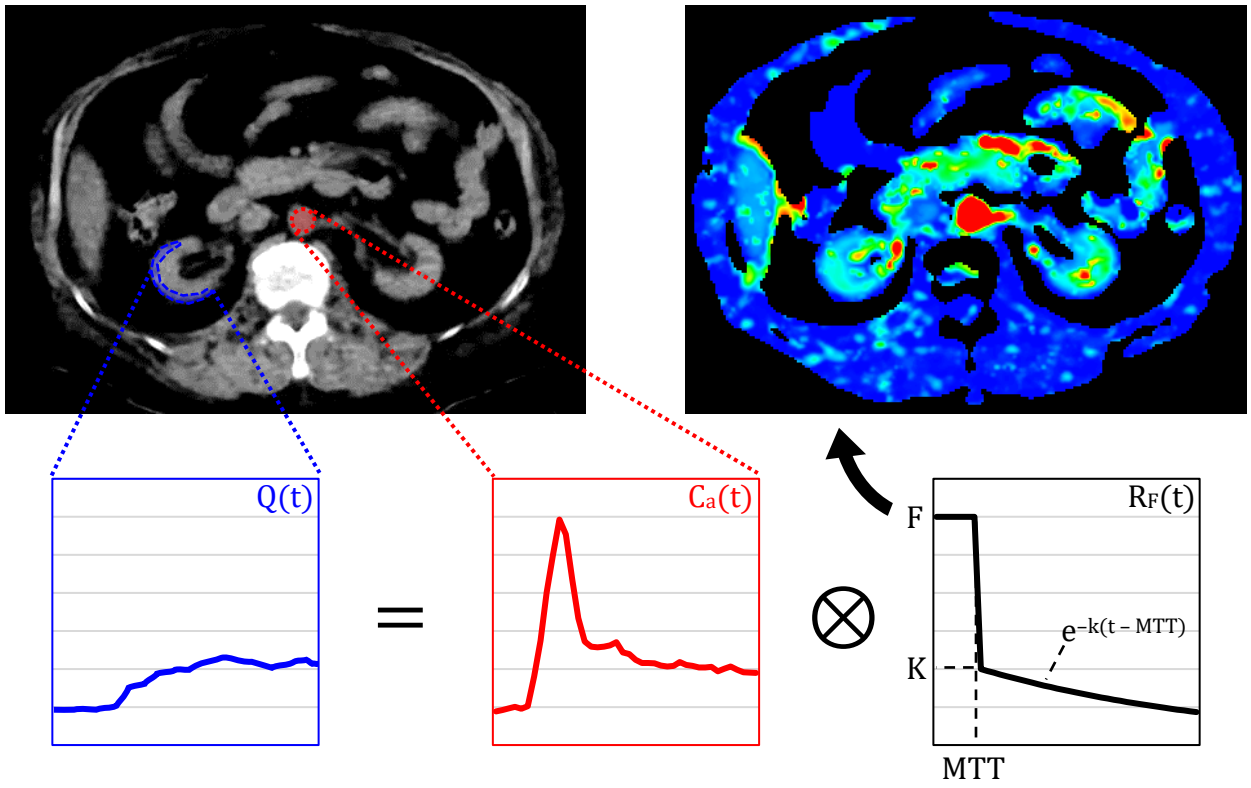

Figure 4.1: GFR measurement by analyzing CTP images with a tracer kinetic model. (A) Schematic of Johnson-Wilson model applied to the glomerular capillaries (red region) and Bowman's capsule (yellow region) in the kidney. Contrast is delivered by perfusion (F) to the glomerulus and in the mean transit time

(MTT) it takes to travel from the afferent arteriole to the efferent arteriole, it is filtered through the glomerular barrier into the Bowman's capsule. The filtration process is governed by the influx (K) and efflux (k) rate constant. (B) From the dynamic series CT images, the arterial input function, $C_a(t)$, and each 3×3 pixel tissue time-density curve in the kidney, Q(t), were obtained. $C_a(t)$ is deconvolved from Q(t) to calculate the flow-scaled impulse residue function, $R_F(t)$, based on the Johnson-Wilson model, yielding parametric maps (e.g., perfusion, permeability-surface area product) which are used to compute GFR as explained in the text. The ⊗ symbol is the convolution operator.

4.2.4 Statistical Analysis

GFR has seldom been measured in HD patients previously; inadequate data exist for a meaningful sample size calculation. This was an initial proof-of-principle study to explore the feasibility of our methods, with a sample size not powered for inferential statistical analysis

Statistical analysis was performed using SPSS, version 25.0 (IBM, Chicago). Data were analyzed using primarily non-parametric statistical tests. Differences between groups and associations between variables were assessed using the Wilcoxon signed-rank test and the Spearman rank-order correlation coefficient, respectively. Associations between GFR and perfusion data were assessed (on a per kidney basis) using the Pearson product-moment correlation. Two-tailed P values <0.05 were considered statistically significant. Results are presented as the mean ± standard error of the mean (SEM), unless otherwise specified.

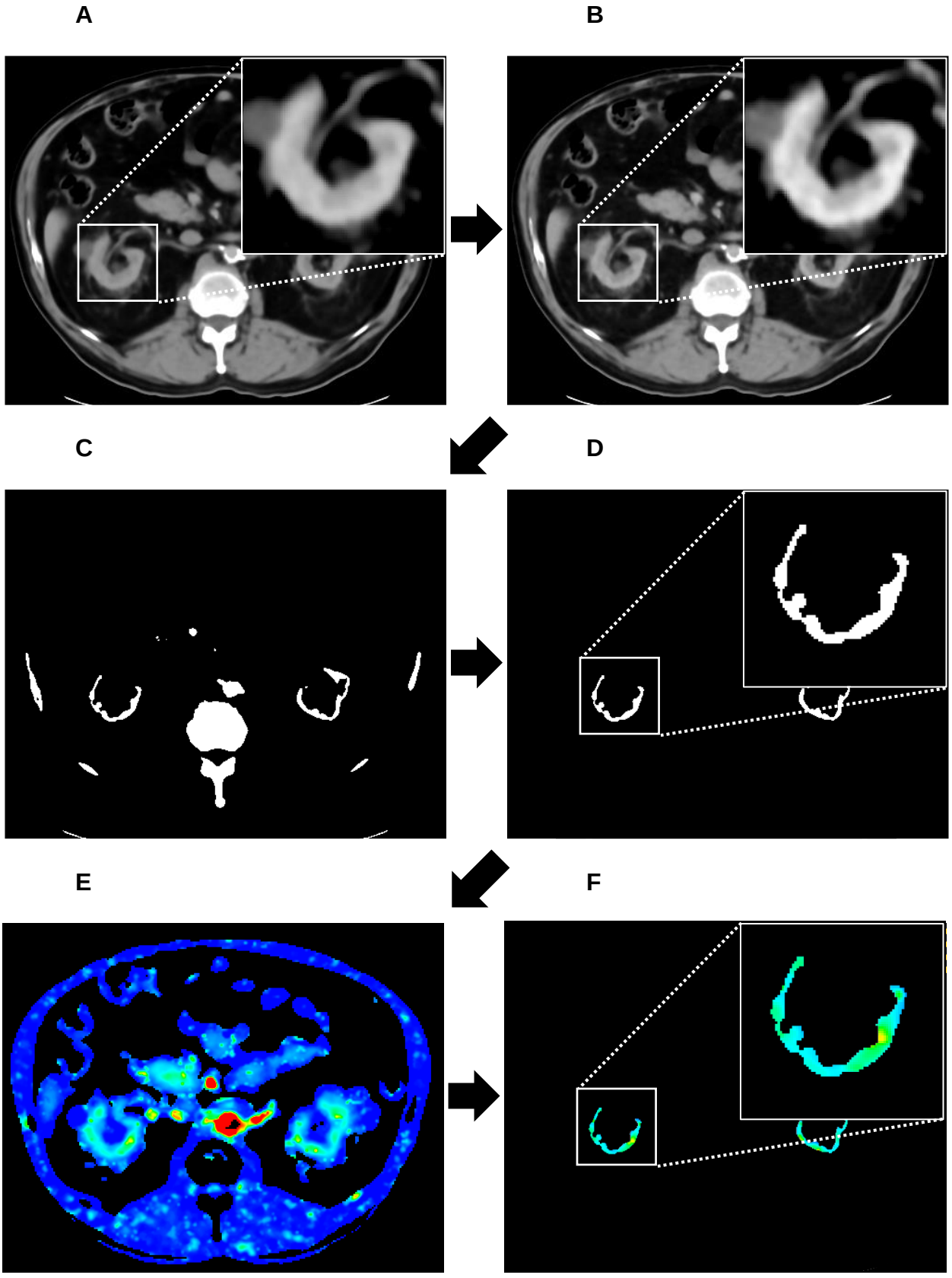
A
B
C
D
E
F

Figure 4.2: Image processing steps for CTP-based GFR measurement. (A) Average of entire dynamic series CT images with poor corticomedullary differentiation. (B) Summation of cortical phase timepoints (i.e., second quarter of dynamic series CT images) only, demonstrating a minor yet noticeable improvement in corticomedullary differentiation. (C) Application of dynamic threshold (anatomically matching the segmented cortical region to the contrast-enhanced cortex of the summed image as closely as possible), (D) allowing for creation of cortical region masks. (E) Cortical region masks were superimposed onto the perfusion and permeability-surface area product map, (F) yielding values that were used to calculate GFR (as described in section 4.2.3).

4.3 Results

Of the sixteen patients enrolled, ten were excluded from the analysis to measure GFR because either one or both kidneys was not completely captured in the CTP scanning. Six patients completed the study and were analyzed. A summary of patient baseline characteristics is presented in Table 4.1.

Of the six patients, only one was randomized to receive cooled HD during the first visit, while the other five all received standard HD during the first visit. Consequently, analyzing the results based on organizing the patients by HD type (i.e., standard HD or cooled HD) did not significantly alter any of the relevant findings or conclusions of this work. Therefore, the results will be presented based on organizing the patients by study visit (i.e., first or second visit). A summary of the patient-specific HD session details is shown in Table 4.2.

Table 4.1: Baseline characteristics of third project study population.

Characteristics	Mean (Range)[a]
n	6
Age	62 (45–84)
Men, n (%)	2 (33)
Dialysis Vintage (years)	3.3 (0.8–25.4)
Length of HD Session (hours)	3.5 (3.0–4.0)
UF (mL/kg)	21.3 (8.6–38.5)
Coronary Artery Disease, n (%)	1 (17)
Congestive Heart Failure, n (%)	1 (14)
Peripheral Vascular Disease, n (%)	2 (33)
Diabetes, n (%)	1 (17)
Hypertension, n (%)	5 (83)

[a]Unless otherwise specified.

Table 4.2: Patient-specific HD session details.

Patient Number	HD Type of Visit 1 / 2	Days Between Visits	HD Sessions Between Visits	HD Vintage (months)
1	Standard / Cooled	14	5	48
2	Standard / Cooled	14	5	14
3	Standard / Cooled	49	20	22
4	Standard / Cooled	35	14	9
5	Cooled / Standard	7	2	117
6	Standard / Cooled	7	2	302

Pre-HD GFR values are presented in Table 4.3. The average baseline left kidney, right kidney, and total GFR values for the first visit were 2.6±0.9, 1.7±0.5, and 4.3±1.0 mL/min/1.73m^2, respectively. The average baseline left kidney, right kidney, and total GFR values for the second visit were 2.6±1.1, 1.5±0.4, and 4.0±1.2 mL/min/1.73m^2, respectively. There were no significant differences between the corresponding GFR values between the two visits (2.6±0.9 to 2.6±1.1 mL/min/1.73m^2 for left kidney GFR, P=0.917; 1.7±0.5 to 1.5±0.4 mL/min/1.73m^2 for right kidney GFR, P=0.075; 4.3±1.0 to 4.0±1.2 mL/min/1.73m^2 for total GFR, P=0.345). These findings are summarized in Table 4.3. In addition, Figure 4.3 presents the changes in single-kidney and total GFR over the course of the two study visits. See Appendix B for a summary of GFR (Table B1), perfusion (Table B2) and extraction efficiency (Table B3) values for all patients.

Table 4.3: Average pre-HD GFR values. Results are presented for the left kidney, right kidney, and both kidneys for the first and second study visits.

	Mean Baseline GFR ± SEM (mL/min/1.73m^2)	
	Visit 1	**Visit 2**
Left Kidney	2.6 ± 0.9	2.6 ± 1.1
Right Kidney	1.7 ± 0.5	1.5 ± 0.4
Total	**4.3 ± 1.0**	**4.0 ± 1.2**

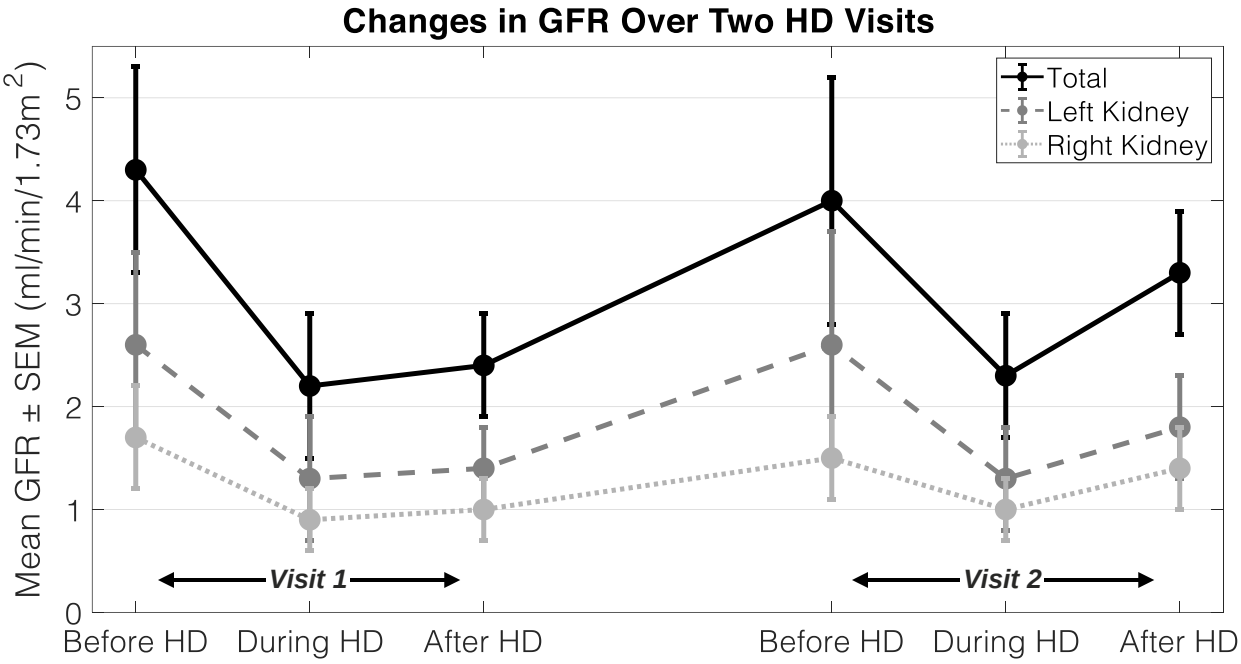

Figure 4.3: Changes in single-kidney and total GFR over the two HD visits, where GFR was assessed before, during and after HD for each visit. Right kidney, left kidney and total GFR values are represented by the light gray, dark gray, and black curves, respectively. The average baseline GFR was not significantly different between the first and second visit for the left kidney (P=0.917), right kidney (P=0.075), and total GFR (P=0.345). Results are given as average ± SEM (standard error of the mean).

4.4 Discussion

4.4.1 GFR

Among the two visits, average baseline total GFR ranged between 4 and 4.5 mL/min/1.73m^2, while average baseline single-kidney GFR ranged between 1 and 3 mL/min/1.73m^2. Overall, these values are physiologically reasonable and may accurately represent true RRF.

Measured GFR trended towards decreasing pre- to post-HD over the course of both visits. Firstly, These findings coincide with previous work which demonstrated that

renal function is maximal pre-HD and minimal post-HD.[12] Secondly, measured cortical perfusion (see Appendix B, Table B2) trended towards decreasing during HD over the course of both visits (consistent with first project[13]), while measured extraction efficiency (see Appendix B, Table B3) did not appear to change during HD over the course of both visits. These findings help to explain why GFR, which is directly proportional to the product of F and E, trended towards decreasing over the course of HD.

Szeto *el al*.[14] previously observed an RRF loss rate of -0.083±0.094 mL/min/month following continuous ambulatory peritoneal dialysis initiation in 645 ESRD patients. Combining this rate (which has been shown to be identical between HD with high-flux polysulfone membranes and continuous ambulatory peritoneal dialysis[15]) with our patients' baseline GFR measurements and dialysis vintages yields an average baseline GFR at dialysis initiation of approximately 11.7 mL/min/1.73m^2. This estimate is consistent with recent trends in Canadian patients' GFRs at HD initiation.[16]

4.4.2 Methodology

In this work, per pixel GFR was computed as the product of the filtration rate constant and pixel mass, where only cortical pixels were considered. The filtration rate constant describes the clearance constant of contrast from glomerular capillaries to Bowman's capsule in nephrons,[17] and the exclusive use of cortical pixels arises from the fact that glomerular filtration occurs entirely within the cortical segment of the nephron (i.e., in the renal corpuscle – glomerulus and Bowman's capsule).[18]

Previous studies that used imaging techniques to compute GFR have employed Patlak graphical analysis or various compartment modelling approaches.[5,6,17,19] However,

underlying assumptions behind these methodologies (e.g., negligible contrast transit time through blood vessels in tissues, negligible efflux of contrast from Bowman's capsule back to glomerulus) are likely violated in the case of ESRD/HD renal pathophysiology.[9,20] Conversely, the Johnson-Wilson model accounts for transit and potential bidirectional exchange in the renal corpuscle as contrast flows through the glomerulus.[7]

Renal structural and functional homogeneity, as well as corticomedullary differentiation, diminishes as kidney disease progresses.[17,21] Therefore, imaging the entire kidney (compared to a single slice) and augmenting cortical contrast enhancement (by summing cortical phase images) are necessary for avoiding single-slice extrapolation bias and improving cortical pixel delineation, respectively, allowing for accurate GFR measurement.

Our proposed CTP-based GFR measurement approach overcomes important shortcomings associated with current clinical GFR assessment. GFR measurement could be confounded by extra-renal clearance, as well as tubular secretion or reabsorption, of the GFR agent (including contrast) used for the measurement.[2] These confounding effects undermine the utility of commonly used GFR measurement methods, as well as endogenous and exogenous filtration markers. Standard clinical GFR measurement methods are based on measuring the blood or urine clearance of GFR agents. Since blood goes everywhere in the body, the removal mechanisms of these agents could be glomerular filtration, other extra-renal clearance routes as well as tubular mechanisms. In addition, while urine collection does ensure that one is measuring what is cleared by the glomerulus, creatinine and urea are secreted and reabsorbed, respectively, by the proximal tubule of the nephron, making GFR measurements based on urinary clearance

of these agents inaccurate. On the other hand, our CT-based method directly measures the removal of contrast in blood delivered to the afferent arterioles of glomeruli by limiting the analysis to the cortical region of the kidney, making this technique free of influence of extra-glomerular sources of clearance, as well as tubular secretion or reabsorption. The rapid scan time also ensures that F·E can be reliably estimated by the deconvolution method. Finally, CTP is a favorable imaging modality because it yields additional useful anatomical and functional information. This modality is also readily available and relatively inexpensive compared to magnetic resonance and nuclear medicine approaches.

4.4.3 Potential Weaknesses, Limitations and Concerns

We performed three contrast-enhanced scans for this work, but only one (pre-HD) would be necessary in a clinical setting. Previous work has shown that HD with high-flux polysulfone membranes clears contrast media[22] and that iopamidol in particular is cleared by HD,[23] suggesting that pre-HD CTP-based GFR quantification does not result in significant contrast agent retention. While contrast media have historically been discouraged from clinical use in kidney disease patients, recent reports have questioned the nephrotoxic nature of contrast media, where there has been no conclusive evidence of contrast-induced nephropathy in HD patients.[24]

Our approach carries a few additional limitations. Firstly, each GFR measurement requires a ~8 mSv dose CTP scan. However, CTP-based GFR measurement could be performed infrequently, limited to decisions regarding HD dosing/scheduling adjustments. In addition, the time needed for radiation-induced cancer manifestation[25] is much greater than HD patient life expectancy.[26] Secondly, we did not validate our findings against any

other GFR assessments. However, there is in fact no gold standard GFR assessment technique for ESRD patients on HD.[2] Thirdly, renal tissue density was assumed to be 1.050 g/cm3. While this value is for healthy tissue, there is no published ESRD kidney density data available. Finally, our approach is based on certain technical requirements, including hardware (CTP-capable scanner with sufficient coverage) and software requirements (noise reduction and motion correction); even though they are becoming more widely available.

4.5 Conclusion

The results of this work represent the first imaging-based assessment of GFR in HD patients. Using CT perfusion imaging, physiologically realistic GFR values were measured over the course of two HD sessions. These preliminary findings demonstrate the feasibility of this approach in terms of reliability and accuracy, and provide early evidence of the clinical potential that CT perfusion imaging has for GFR measurement in ESRD patients on HD.

4.6 References

1. Mathew AT, Fishbane S, Obi Y, et al. Preservation of residual kidney function in hemodialysis patients: reviving an old concept. *Kidney Int*. 2016;90:262-271.

2. Shafi T, Levey AS. Measurement and Estimation of Residual Kidney Function in Dialysis Patients. *Adv Chronic Kidney Dis*. 2018;25:93-104.

3. Davenport A. Measuring residual renal function in dialysis patients: can we dispense with 24-hour urine collection? *Kidney Int*. 2016;89:978-980.

4. European Best Renal Practice Guidelines for haemodialysis Part 1. *Nephrol Dial Transplant*. 2002;17:S1-S111.

5. Grenier N, Quaia E, Prasad PV, et al. Radiology Imaging of Renal Structure and Function by Computed Tomography, Magnetic Resonance Imaging, and Ultrasound. *Semin Nucl Med*. 2011;41:45-60.

6. Read S, Allen C, Hare C. Applications of Computed Tomography in Renal Imaging *Nephron Clin Pract*. 2006;103:c29-c36.

7. St. Lawrence KS, Lee T-Y. An Adiabatic Approximation to the Tissue Homogeneity Model for Water Exchange in the Brain: I. Theoretical Derivation *J Cereb Blood Flow Metab*. 1998;18:1365-1377.

8. Lee T-Y, Purdie TG, Stewart E. CT Imaging of Angiogenesis. *Q J Nucl Med*. 2003;47:171-187.

9. Yuh BI, Cohan RH. Different Phases of Renal Enhancement: Role in Detecting and Characterizing Renal Masses During Helical CT. *Am J Roentgenol*. 1999;173:747-755.

10. Bae KT. Intravenous Contrast Medium Administration and Scan Timing at CT: Considerations and Approaches. *Radiology*. 2010;256:32-61.

11. International commission on radiological protection, Adult reference computational phantoms, ICRP Publication 110. *Ann ICRP 39*. 2009;2:48-51.

12. van Olden RW, van Acker BA, Koomen GC, et al. Time course of inulin and creatinine clearance in the interval between two haemodialysis treatments. *Nephrol Dial Transplant*. 1995;10:2274-2280.

13. Marants R, Qirjazi E, Grant CJ, et al. Renal Perfusion during Hemodialysis: Intradialytic Blood Flow Decline and Effects of Dialysate Cooling. *J Am Soc Nephrol*. 2019;30:1086-1095.

14. Szeto C, Kwan BC, Chow K, et al. Predictors of residual renal function decline in patients undergoing continuous ambulatory peritoneal dialysis. *Periton Dialysis Int*. 2015;35:180-188.

15. McKane W, Chandna SM, Tattersall JE, et al. Identical decline of residual renal function in high-flux biocompatible hemodialysis and CAPD. *Kidney Int*. 2002;61:256-265.

16. Ferguson TW, Garg AX, Sood MM, et al. Association Between the Publication of the Initiating Dialysis Early and Late Trial and the Timing of Dialysis Initiation in Canada. *JAMA Intern Med*. 2019;179:934-941.

17. Dawson P, Peters M. Dynamic Contrast Bolus Computed Tomography for the Assessment of Renal Function. *Invest Radiol*. 1993;28:1039-1042.

18. Scott RP, Quaggin SE. The cell biology of renal filtration. *J Cell Bio*. 2015;209:199-210.

19. Bokacheva L, Rusinek H, Zhang JL, et al. Estimates of Glomerular Filtration Rate From MR Renography and Tracer Kinetic Models. *J Magn Reson Imaging*. 2009;29:371-382.

20. López-Novoa JM, Rodríguez-Peña AB, Ortiz A, et al. Etiopathology of chronic tubular, glomerular and renovascular nephropathies: Clinical implications. *J Transl Med*. 2011;9:1-26.

21. Marotti M, Hricak H, Terrier F, et al. MR in Renal Disease: Importance of Cortical-Medullary Distinction. *Magn Reson Med*. 1987;5:160-172.

22. Deray G. Dialysis and iodinated contrast media. *Kidney Int*. 2006;69:S25-S29.

23. Donnelly PK, Burwell N, McBurney A, et al. Hemodialysis and Iopamidol Clearance after Subclavian Venography. *Invest Radiol*. 1993;28:629-632.

24. Davenport MS, Perazella MA, Yee J, et al. Use of Intravenous Iodinated Contrast Media in Patients with Kidney Disease: Consensus Statements from the American College of Radiology and the National Kidney Foundation. *Radiology*. 2020;0:1-9.

25. Ferrero A, Takahashi N, Vrtiska TJ, et al. Understanding, justifying, and optimizing radiation exposure for CT imaging in nephrourology. *Nat Rev Urol*. 2019;16:231-244.

26. Tsur N, Menashe I, Haviv YS. Risk Factors Before Dialysis Predominate as Mortality Predictors in Diabetic Maintenance Dialysis patients. *Sci Rep*. 2019;9:1-8.

CHAPTER 5

5 Summary and Future Directions

For the better part of a century, hemodialysis (HD) has been used to treat individuals with impaired renal function.[1] As the medical field progressed and technology advanced, HD-based renal replacement therapy has been become more effective, efficient, and safe. However, despite the evolution of this important treatment modality, end-stage renal disease (ESRD) patients on HD continue to suffer from various comorbidities, substandard quality of life, and low rates of survival.[2] By exploring how HD impacts different organs and vascular beds, along with the downstream clinical consequences of these effects, the mechanisms behind the development of HD complications can be understood and potential therapeutic solutions can be developed.

This philosophy was applied to the research projects of this thesis, where computed tomography perfusion (CTP) imaging was used to non-invasively assess multi-organ hemodynamics during HD. CT perfusion is a dynamic contrast-enhanced imaging technique that can provide absolute measurements of various hemodynamic parameters. All three projects were based on data collected from a single clinical trial, where HD patients were randomized to receive either standard or cooled HD first in a two-visit, crossover study design. During each visit, CTP imaging was performed before, during and after HD without any interruption to the patient's treatment.

The novel findings of our research studies provide important groundwork regarding the effects of HD on the kidneys and liver, and the therapeutic potential of dialysate cooling (DC) for the hemodynamic and functional protection of these organs. In this final chapter of the thesis, the project objectives will be revisited, important research findings

will be summarized, clinical impact will be considered, and potential future research directions will be discussed.

5.1 Summary of Projects: Motivations, Objectives and Findings

5.1.1 Project 1: kidney blood flow and residual renal function loss

The maintenance of even minimal levels of residual renal function (RRF) in ESRD patients correlates with improved clinical outcomes and survival.[3] However, RRF characteristically declines rapidly upon the initiation of HD,[4] with recurrent renal ischemic insults hypothesized to be responsible.[5] This hypothesis was tested in the first project of this thesis, which had the following objectives:

1. Examine how HD affects renal perfusion
2. Explore the relationship between changes in renal perfusion and myocardial dysfunction (a hallmark of HD-induced circulatory stress) during HD
3. Investigate whether cooling can protect the kidneys from HD-induced circulatory stress

Renal perfusion and myocardial injury (i.e., myocardial stunning) were evaluated using CTP imaging and speckle-tracking echocardiography, respectively. The most important findings of this project are as follows:

1. Renal perfusion deceased to 81.6% of baseline ($P<0.005$) during HD and recovered to 95.1% of baseline after HD
2. There was a correlation between the severity of renal ischemia and the number of stunned myocardial segments during HD ($r=-0.33$; $P<0.05$)

3. With DC, renal perfusion deceased to 89.2% of baseline during HD and recovered to 94.3% of baseline after HD

We demonstrated that renal perfusion significantly deceases during HD and that DC trends towards mitigating this decrease. In addition, renal ischemia correlated with myocardial injury during HD. Recurring renal ischemic insults over many HD sessions represents the preliminary pathophysiological characterization of HD-mediated residual renal function loss in this patient population.

5.1.2 Project 2: liver blood flow and function, and endotoxemia

Endotoxemia correlates with the presence of cardiovascular complications and a higher mortality risk, and is commonly found in HD patients, who have increased endotoxin levels compared to healthy people and earlier stage chronic kidney disease (CKD) patients.[6] The liver is normally responsible for clearing endotoxin,[7] suggesting that HD may disrupt liver hemodynamics and function. This idea was explored in the second project of this thesis, which had the following objectives:

1. Examine how HD affects hepatic perfusion and function
2. Explore the relationship between changes in hepatic perfusion and endotoxin levels during HD
3. Investigate if cooling can maintain liver hemodynamics and limit systemic exposure to endotoxin

Hepatic perfusion, hepatic function (i.e., clearance rate of indocyanine green, ICG) and endotoxin levels were assessed using CTP imaging, pulse-dye densitometry and the

limulus amoebocyte lysate assay, respectively. The most important findings of this project are as follows:

1. During HD, portal vein perfusion increased to 111.1% of baseline (P=0.14) and the ICG clearance rate deceased to 85.5% of baseline (P=0.016)
2. Endotoxin levels increased to 119.6% of baseline during HD (P=0.15) and to 128.4% of baseline after HD (P=0.037)
3. With DC, all of these changes were mitigated: portal vein perfusion changed to 100.8% of baseline during HD, ICG clearance rate changed to 95.2% of baseline during HD, and endotoxin levels changed to 107.8% and 105.3% of baseline during and after HD, respectively

We showed that there is concurrent redistribution of hepatic perfusion and decrease in liver function during HD, and that DC trends towards ameliorating these changes. Together, these changes help explain the high prevalence of endotoxemia observed in HD patients.

5.1.3 Project 3: measuring GFR in HD patients using CTP

The current clinical protocol for assessing glomerular filtration rate (GFR) in ESRD patients on HD is cumbersome, time-consuming and inaccurate,[8] causing the adjustment of a patient's HD prescription in order to optimize renal replacement therapy to be difficult to perform and often ignored in the clinical setting.[9] However, CTP-based measurement of GFR has the potential to overcome the limitations of conventional measurement techniques[10] and was the focus of the third project of this thesis, which had the following objectives:

1. Develop methodology for CTP-based GFR assessment
2. Explore the feasibility of using CTP imaging to quantify GFR in HD patients
3. Assess how GFR changes over the course of HD

The filtration rate constant and cortical mass of the kidneys were measured by applying distributed parameter-based tracer kinetic modelling analysis and boosting corticomedullary differentiation, respectively, to CTP images. The most important findings of this project are as follows:

1. Baseline measured GFR values were 2.6 and 2.6 mL/min/1.73m^2 (left kidney) and 1.7 and 1.5 mL/min/1.73m^2 (right kidney) for the first and second visits, respectively
2. Total baseline measured GFR values were 4.3 and 4.0 mL/min/1.73m^2 (not significantly different) for the first and second visits, respectively
3. GFR appeared to fluctuate over the course of HD during both study visits (first visit: before to during to after HD → 4.3 to 2.2 to 2.4 mL/min/1.73m^2, second visit: before to during to after HD → 4.0 to 2.3 to 3.3 mL/min/1.73m^2)

Our novel methodology yielded physiologically realistic GFR values in actual HD patients. These results, together with the speed, utility and accessibility of CTP imaging, showcases the clinical feasibility of this approach.

5.2 Clinical impact

The novel methodology and important findings outlined in the research projects of this thesis have the potential to impact the clinical management of HD patients in a positive and meaningful way. The hemodynamic and functional measurements we performed help to identify some of the previously unexplored effects of HD-induced

circulatory stress on the kidneys and liver, which introduces new avenues for clinical research and therapeutic intervention.

5.2.1 Heterogeneity of hemodynamic response to HD

One of the most prominent features of our renal and hepatic perfusion data was the observed heterogeneity in hemodynamic response to HD-induced circulatory stress. In particular, we found that renal perfusion decreased during HD in approximately two thirds of patients, with the remaining third having no change, or even an increase, in kidney blood flow. Similarly, changes in hepatic perfusion (total, hepatic arterial, portal venous) during HD varied among patients, with about half of patients having increased blood flow and the other half having decreased blood flow. By studying this heterogeneity in response (which is characteristic of HD patients[11-13]) in more patients, we might be able to predict an individual's hemodynamic response to HD and develop strategies to mitigate the potential negative effects.

The primary factors involved in determining how a vascular bed will hemodynamically react to HD-induced circulatory stress include: (1) the cardiac output response, (2) the baroreflex sensitivity, and (3) additional organ-specific autoregulatory mechanisms.[11] These factors have been explored and described to varying degrees in CKD and ESRD, but have not yet been integrated together with perfusion measurements to fully describe the heterogeneous response of patients to HD. In particular, (1) cardiac output has been shown to decrease during HD,[14,15] (2) patients with compromised baroreflex sensitivity have been found to be more vulnerable to ultrafiltration,[11] and (3) the kidney's hemodynamic regulation mechanisms (e.g., myogenic reflex,

tubuloglomerular feedback, renin-angiotensin system) become impaired in kidney disease.[16-18] The relationship between kidney disease and/or HD, and the liver's hemodynamic regulation (e.g., hepatic arterial buffer response, hepatorenal reflex[19,20]), is unknown.

We conducted a preliminary analysis of the relationship between changes in cardiac output, blood pressure, and renal/hepatic perfusion in our patients. Based on the Stewart-Hamilton equation, cardiac output was determined from CTP[21-23] as follows:

$$Cardiac\ Output = \frac{amount\ of\ contrast\ administered}{area\ under\ contrast\ concentration-vs-time\ curve}$$

There were a few key findings of this analysis:

- During HD, there were significant drops in cardiac output (P=0.01) and blood pressure (P=0.001), coinciding with the results of previous studies[14,24]
- During HD, changes in cardiac output correlated with changes in renal perfusion (r=0.38, P=0.004) and hepatic perfusion (r=0.66, P=0.007)
- Approximately half of patients demonstrated a drop in both cardiac output and blood pressure during HD, but these patients did not necessarily have a corresponding decrease in organ perfusion, suggestive of organ-specific autoregulatory activity
    - Project 1: 14/29 patients (48%) demonstrated a drop in both cardiac output and blood pressure during HD → of these, 11/14 (79%) patients demonstrated a drop in renal perfusion
    - Project 2: 8/15 patients (53%) demonstrated a drop in both cardiac output and blood pressure during HD → of these, 4/8 (50%) patients demonstrated a drop in hepatic perfusion

These interesting results help to emphasize the importance of studying the hemodynamic response to HD-induced circulatory stress, as well as the role of CTP in measuring multi-organ perfusion and cardiac output (i.e., possible to assess renal perfusion, hepatic perfusion and cardiac output from a single CTP scan).

5.2.2 CTP for hemodynamic and functional measurements in HD patients

Patients with ESRD typically receive their HD treatments in a clinical setting (rather than at home). Therefore, the ideal modality for acquiring intradialytic hemodynamic measurements is one that is minimally invasive, does not disrupt HD treatment, and can be performed rapidly. These criteria are satisfied by CTP, an imaging modality that is readily available, relatively inexpensive, and that can perform multi-organ physiologic measurements in approximately two minutes without disrupting HD. While magnetic resonance imaging and positron emission tomography can be used to perform intradialytic perfusion measurements,[14,25-27] these modalities are hindered by contraindications (metal, pacemaker, etc.), availability, and scan time concerns, limiting their use for this application. The research projects of this thesis were the first to ever use CTP for acquiring hemodynamic measurements during HD. Despite its advantages, CTP imaging has a couple of drawbacks: it requires the administration of exogenous contrast media, and it exposes the patient to ionizing radiation. However, the severity of these drawbacks has been ameliorated with time, thanks to innovations in technology, improvements in methodology, changes in clinical practice, and conducting of higher-quality clinical trials.

The main sources of evidence for contrast-induced nephropathy (CIN) are based on studies with some combination of the following aspects:[28]

- Use of “unsafe” contrast media (i.e., ionic, high-osmolarity, etc.)
- Contrast was administered intraarterially for invasive angiocardiographic procedures
- No control groups where contrast material was not administered
- Not designed to directly assess the relationship between intravenous contrast media administration and CIN

To date, no large-scale randomized control trials have been conducted to more definitively conclude whether modern contrast-enhanced imaging protocols (e.g., CTP) cause CIN, particularly in patients with GFR <30 mL/min/1.73m^2.[29] However, over the past decade or so, a number of reviews, observational studies controlling for known confounders, meta-analyses, and retrospective studies utilizing propensity-matched analysis have consistently found that the incidence of diminished renal function does not significantly differ between patients receiving contrast-enhanced versus non-contrast imaging scans.[28,29] While more work is required to accurately and confidently characterize the relationship between contrast administration and changes in renal function, the clinical utility of CTP (and other modern contrast-enhanced imaging techniques), together with the current level of scientific evidence, supports the use of this modality for performing the important intradialytic hemodynamic and functional measurements presented in the research projects of this thesis.

Patients involved in our studies received a radiation dose of approximately 8 mSv during every CTP scan. This dose is equivalent to about ten abdominal radiographs and

is approximately three times greater than the local natural annual background dose (~3 mSv).[30] While this dose is nontrivial, it is important to note that, as previously mentioned in chapter 4, it typically takes decades for radiation-induced cancer to manifest.[31] Patients with ESRD receiving maintenance HD have an average age of >60 years and a life expectancy of under five years.[32] Considering these time frames, the lifespan of HD patients exposed to radiation from medical imaging is likely not be affected in any significant way. In addition, CT dose-reduction techniques and technologies have been the focus of many research initiatives, with various approaches finding their way into the clinical workflow. For example, automatic exposure control (modulation of tube current based on regional x-ray attenuation) and iterative reconstruction, together with gradual improvements in filter and detector designs and technologies, are all current advancements in CT dose-reduction that are currently being implemented.[33,34] Novel approaches that are being researched, such as compressed sensing (reconstruction of reduced-projection image data) and machine learning techniques (e.g., deep learning for reconstruction and/or denoising of low-dose image data), represent exciting prospects in dose-reduction technology.[35,36]

5.2.3 Effectiveness of DC

In all the research projects of this thesis, DC was applied as a therapeutic intervention to ameliorate HD-induced circulatory stress. We implemented a fixed-temperature cooling approach, whereby the dialysate was cooled to 35°C for all patients, regardless of baseline body temperature or body temperature fluctuations during HD. It was consistently found that with DC, changes in perfusion and function did not differ

significantly from changes seen during standard HD. Although this prevented us from concluding that DC was an effective intradialytic intervention in these studies, we did observe that cooling did not cause harm in terms of worsening the severity of changes in perfusion and function during HD, and even trended towards positively affecting these metrics.

Two plausible reasons for the ineffectiveness of DC in our studies are (a) that we used a fixed-temperature cooling approach, and (b) that there was only a single session of cooled HD.

Several forms of DC have been explored in research studies, with the most prevalent types being fixed-temperature cooling (as in our studies), baseline-temperature cooling (based on pre-HD body temperature), and feedback-temperature cooling (based on continual monitoring of body temperature during HD to adjust DC level).[37-39] While being the easiest to implement, fixed-temperature cooling ignores the relatively wide range of baseline body temperatures among individuals.[40] As a result, DC could range from <0.5°C to >2°C depending on the individual, helping to explain why its effectiveness and tolerability was not universal in our studies. On the other hand, trials implementing baseline-temperature cooling or feedback-temperature cooling have observed a greater effectiveness of DC, demonstrating the importance of an individualized approach to DC.[41-43] While it is possible to implement baseline-temperature cooling universally, feedback-temperature cooling requires additional resources (e.g., biofeedback temperature monitoring device) that limits its clinical uptake.[37,38]

Most research studies exploring DC were similar to ours in terms of design, where patients were randomized to receive a single or a few sessions of standard or cooled HD

first before being crossed over to the other arm of the study.[37,38] While this sort of design is appropriate for evaluating acute HD-induced hemodynamic and functional changes (e.g., IDH, renal and hepatic perfusion, myocardial stunning, etc.), it does not enable the study of long-term consequences of DC on downstream clinical outcomes. For instance, although we observed only trends toward improvements in renal and hepatic perfusion and function with DC during a single HD session, it may be that if this intervention was implemented consistently over the course of several months/years that significant clinical outcomes (e.g., smaller decline in RRF, lower levels of endotoxemia, etc.) could be seen.

Because of the different types of cooling approaches, various metrics for determining cooling efficacy, and limited longitudinal study of cooling effectiveness, the clinical potential of DC has been questioned and its clinical uptake has been slow. However, there is currently a large-scale, multi-center randomized control trial being conducted (MyTEMP trial[44]) that aims to definitively demonstrate the effectiveness of baseline-temperature DC by reporting major cardiovascular outcomes over the course of several years.

5.3 Next Steps

Moving forward, there are several important and exciting next steps related to the research work of this thesis. Our work has demonstrated that CTP is a favorable imaging modality for use during HD: scan time is very short, axial coverage is generous (i.e., can image multiple structures in a single scan), and there is no interruption to HD treatment. Therefore, CTP can be used for assessing the effects of HD-induced circulatory stress on other organs and vascular beds, as well as evaluating the efficacy of other therapeutic

interventions. As alluded to in previous sections, it may be worthwhile to explore other types of DC, other intradialytic therapeutic interventions entirely, or even combining multiple interventions, for ameliorating HD-induced circulatory stress and maintaining renal and hepatic perfusion and function during HD.

The first and second projects of this thesis were performed with a relatively small number of participants and assessed intradialytic changes in renal and hepatic perfusion and function over the course of just a single standard HD session. It would be interesting to perform longitudinal studies with more participants where metrics of interest (e.g., intradialytic change in renal and hepatic perfusion) are correlated with the corresponding clinical outcomes of relevance over a longer time period (e.g., changes in RRF and endotoxemia levels after one year). These kinds of analyses would give greater context to, and increase the clinical value of, the perfusion and function measurements performed in this thesis.

Next, while no true gold standard GFR measurement approach exists for ESRD patients on HD, some sort of validation study is necessary to strengthen the findings of the third project. As the best metrics to evaluate the clinical utility of a technique are clinical outcomes and survival, it may be worthwhile to perform a study where these metrics (in addition to, for instance, residual urine output volume) are correlated to HD patient GFR values measured using both our CTP-based technique, as well as measured using inulin clearance with timed urine collection. If our CTP-based approach yields the better results, then it has the potential to become the new gold standard GFR measurement technique in HD patients.

Finally, we have begun working on a collaborative, multidisciplinary project that is focused on designing and running virtual HD sessions. Using CTP data from HD patients, we are able to generate 3D reconstructions of multi-organ perfusion (Figure 5.1) for fractal dimension texture analysis and heterogeneity quantification. Then, by combining the reconstruction data together with various biophysical inputs (e.g., mathematically optimized spatial blood flow distribution, organ shape, blood vessel morphometry, autoregulation mechanisms, etc.), a mathematical model of the patient-specific response to HD-induced circulatory stress can be generated. From here, it would be possible to simulate and run in silico sessions of HD while having full control over the various adjustable technical and clinical parameters. This will allow us to predict the patient-specific response to HD, as well as to optimize treatment parameters accordingly, prior to exposing ESRD patients to the circulatory stress of HD.

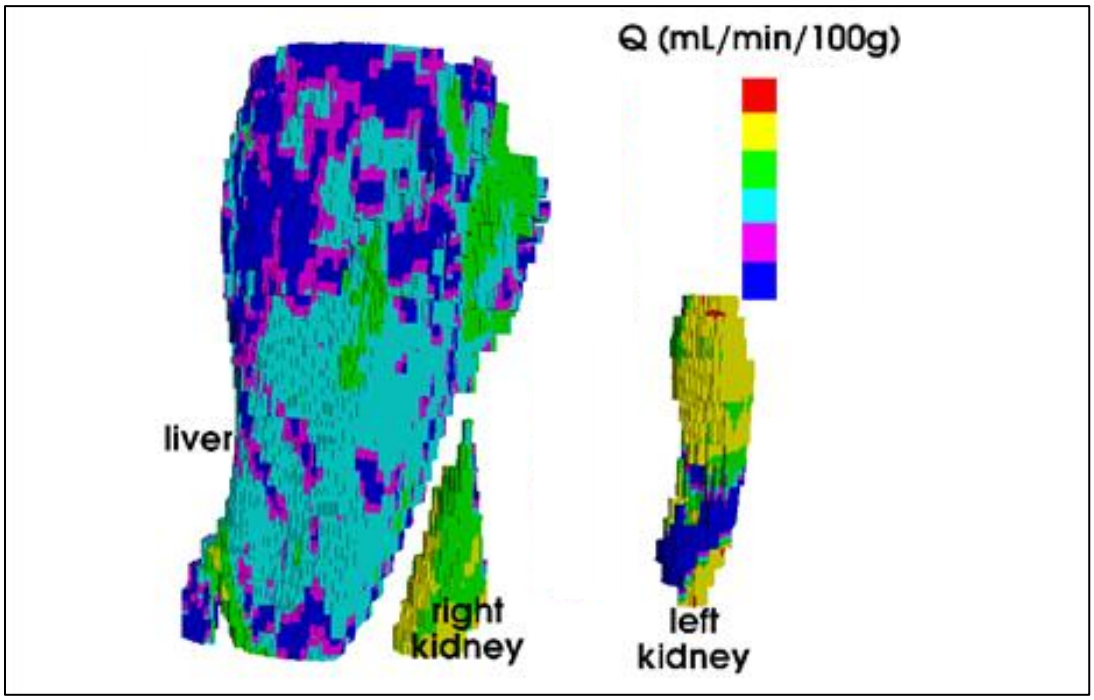

Figure 5.1 CTP-based 3D reconstructions of multi-organ perfusion. Reconstructions of the liver and kidneys are shown. Image courtesy of Dr. Sanjay Kharche.

5.4 References

1. Yeun JY, Depner TA, *Principles of Hemodialysis*, in *Chronic Kidney Disease, Dialysis, and Transplantation - A Companion to Brenner and Rector's The Kidney*, J. Himmelfarb and M.H. Sayegh, Editors. 2010, Saunders Elsevier: Philadelphia, PA, USA. p. 277-302.

2. McIntyre CW. Recurrent Circulatory Stress: The Dark Side of Dialysis. *Semin Dialysis*. 2010;23:449-451.

3. Mathew AT, Fishbane S, Obi Y, et al. Preservation of residual kidney function in hemodialysis patients: reviving an old concept. *Kidney Int*. 2016;90:262-271.

4. Jansen MAM, Hart AAM, Korevaar JC, et al. Predictors of the rate of decline of residual renal function in incident dialysis patients. *Kidney Int*. 2002;62:1046-1053.

5. Shafi T, Jaar BG, Plantinga LC, et al. Association of Residual Urine Output with Mortality, Quality of Life, and Inflammation in Incident Hemodialysis Patients: The CHOICE (Choices for Healthy Outcomes in Caring for End-Stage Renal Disease) Study. *Am J Kidney Dis*. 2010;56:348-358.

6. McIntyre CW, Harrison LE, Eldehni MT, et al. Circulating endotoxemia: a novel factor in systemic inflammation and cardiovascular disease in chronic kidney disease. *Clin J Am Soc Nephrol*. 2011;6:133-141.

7. Caridis DT, Reinhold RB, Woodruff PWH. Endotoxemia in man. *Lancet*. 1972;299:1381-1386.

8. Shafi T, Levey AS. Measurement and Estimation of Residual Kidney Function in Dialysis Patients. *Adv Chronic Kidney Dis*. 2018;25:93-104.

9. Davenport A. Measuring residual renal function in dialysis patients: can we dispense with 24-hour urine collection? *Kidney Int*. 2016;89:978-980.

10. Grenier N, Quaia E, Prasad PV, et al. Radiology Imaging of Renal Structure and Function by Computed Tomography, Magnetic Resonance Imaging, and Ultrasound. *Semin Nucl Med*. 2011;41:45-60.

11. Chesterton LJ, Selby NM, Fialova J, et al. Categorization of the hemodynamic response to hemodialysis: The importance of baroreflex sensitivity. *Hemodial Int*. 2010;14:18-28.

12. Marinovich R, Li Z, Tamasi T, et al. Hemodynamic response to non-pneumatic anti-shock compression garments in patients with renal dysfunction. *BMC Nephrol*. 2020;21:1-7.

13. Barbieri C, Cattinelli I, Neri L, et al. Development of an Artificial Intelligence Model to Guide the Management of Blood Pressure, Fluid Volume, and Dialysis Dose in End-Stage Kidney Disease Patients: Proof of Concept and First Clinical Assessment. *KIdney Dis*. 2019;5:28-33.

14. Buchanan C, Mohammed A, Cox E, et al. Intradialytic Cardiac Magnetic Resonance Imaging to Assess Cardiovascular Responses in a Short-Term Trial of Hemodiafiltration and Hemodialysis. *J Am Soc Nephrol*. 2017;28:1269-1277.

15. Chaignon M, Chen WT, Tarazi RC, et al. Effect of Hemodialysis on Blood Volume Distribution and Cardiac Output. *Hypertension*. 1981;3:327-332.

16. Slomowitz L. Tubuloglomerular Feedback in Chronic Renal Failure. *Nephron*. 1987;45:264-271.

17. Kredieit RT. Preservation of Residual Kidney Function and Urine Volume in Patients on Dialysis. *Clin J Am Soc Nephrol*. 2017;12:377-379.

18. Burke M, Pabbidi MR, Farley J, et al. Molecular Mechanisms of Renal Blood Flow Autoregulation. *Curr Vasc Pharmacol*. 2014;12:845-858.

19. Eipel C, Abshagen K, Vollmar B. Regulation of hepatic blood flow: The hepatic arterial buffer response revisited. *World J Gastroenterol*. 2010;16:6046-6057.

20. Lang F, Tschernko E, Schulze E, et al. Hepatorenal reflex regulating kidney function. *Hepatol*. 1991;14:590-594.

21. Pienn M, Kovacs G, Tscherner M, et al. Determination of cardiac output with dynamic contrast-enhanced computed tomography. *Int J Cardiovasc Imaging*. 2013;29:1871-1878.

22. Raman SV, Tran T, Simonetti OP, et al. Dynamic computed tomography to determine cardiac output in patients with left ventricular assist devices. *J Thorac Cardiovasc Surg*. 2009;137:1213-1217.

23. Mahnken AH, Klotz E, Hennemuth A, et al. Measurement of cardiac output from a test-bolus injection in multislice computed tomography. *Eur Radiol*. 2003;13:2498-2504.

24. Shoji T, Tsubakihara Y, Fujii M, et al. Hemodialysis-associated hypotension as an independent risk factor for two-year mortality in hemodialysis patients. *Kidney Int*. 2004;66:1212-1220.

25. McIntyre CW, Burton JO, Selby NM, et al. Hemodialysis-Induced Cardiac Dysfunction Is Associated with an Acute Reduction in Global and Segmental Myocardial Blood Flow. *Clin J Am Soc Nephrol*. 2008;3:19-26.

26. Dasselaar JJ, Slart RHJA, Knip M, et al. Haemodialysis is associated with a pronounced fall in myocardial perfusion. *Nephrol Dial Transplant*. 2009;24:604-610.

27. Polinder-Bos HA, Garcia DV, Kuipers J, et al. Hemodialysis Induces an Acute Decline in Cerebral Blood Flow in Elderly Patients. *J Am Soc Nephrol*. 2018;29:1317-1325.

28. McDonald RJ, McDonald JS, Bida JP, et al. Intravenous Contrast Material-induced Nephropathy: Causal or Coincident Phenomenon? *Radiology*. 2013;267:106-119.

29. Davenport MS, Perazella MA, Yee J, et al. Use of Intravenous Iodinated Contrast Media in Patients with Kidney Disease: Consensus Statements from the American College of Radiology and the National Kidney Foundation. *Radiology*. 2020;0:1-9.

30. Mettler FA, Huda W, Yoshizumi TT, et al. Effective Doses in Radiology and Diagnostic Nuclear Medicine: A Catalog. *Radiology*. 2008;248:254-263.

31. Ferrero A, Takahashi N, Vrtiska TJ, et al. Understanding, justifying, and optimizing radiation exposure for CT imaging in nephrourology. *Nat Rev Urol*. 2019;16:231-244.

32. Canadian Institute for Health Information. Annual Statistics on Organ Replacement in Canada: Dialysis, Transplantation and Donation, 2009 to 2018. 2019;

33. Kalra MK, Sodickson AD, Mayo-Smith WW. CT Radiation: Key Concepts for Gentle and Wise Use. *Radiographics*. 2015;35:1706-1721.

34. Lee T, Chhem RK. Impact of new technologies on dose reduction in CT. *Eur Radiol*. 2010;76:28-35.

35. Enjilela E, Lee T, Hsieh J, et al. Ultra-Low-Dose Sparse-View Quantitative CT Liver Perfusion Imaging. *Tomography*. 2017;3:175-179.

36. Greffier J, Hamard A, Pereira F, et al. Image quality and dose reduction opportunity of deep learning image reconstruction algorithm for CT: a phantom study. *Eur Radiol*. 2020;10.1007/s00330-020-06724-w. doi:10.1007/s00330-020-06724-w:

37. Mustafa RA, Bdair F, Akl EA, et al. Effect of Lowering the Dialysate Temperature in Chronic Hemodialysis: A Systematic Review and Meta-Analysis. *Clin J Am Soc Nephrol*. 2016;11:442-457.

38. Larkin JW, Reviriego-Mendoza MM, Usvyat LA, et al. To cool, or too cool: Is reducing dialysate temperature the optimal approach to preventing intradialytic hypotension? *Semin Dialysis*. 2017;30:501-508.

39. Gullapudi VRL, Kazmi I, Selby NM. Techniques to improve intradialytic haemodynamic stability. *Curr Opin Nephrol Hypertens*. 2018;27:413-419.

40. Obermeyer Z, Samra JK, Mullainathan S. Individual differences in normal body temperature: longitudinal big data analysis of patient records. *BMJ*. 2017;359:1-8.

41. Odudu A, Eldehni MT, McGann GP, et al. Randomized Controlled Trial of Individualized Dialysate Cooling for Cardiac Protection in Hemodialysis Patients. *Clin J Am Soc Nephrol*. 2015;10:1408-1417.

42. Eldehni MT, Odudu A, McIntyre CW. Randomized Clinical Trial of Dialysate Cooling and Effects on Brain White Matter. *J Am Soc Nephrol*. 2015;26:957-965.

43. Maggiore Q, Pizzarelli F, Santoro A, et al. The Effects of Control of Thermal Balance on Vascular Stability in Hemodialysis Patients: Results of the European Randomized Clinical Trial. *Am J Kidney Dis*. 2002;40:280-290.

44. Al-Jaishi AA, McIntyre CW, Sontrop JM, et al. Major Outcomes With Personalized Dialysate TEMPerature (MyTEMP): Rationale and Design of a Pragmatic, Registry-Based, Cluster Randomized Controlled Trial. *Can J Kidney Health Dis*. 2020;7:1-18.

Appendices

Appendix A: Supplementary Results for Chapter 3

In addition to liver excretory function, hepatic injury due to HD-induced circulatory stress was also assessed by measuring liver enzyme levels before and after standard and cooled HD. A summary of the relative changes in enzyme levels from baseline is presented in Table A1.

Table A1: Changes in liver enzyme levels with respect to baseline following standard and cooled HD. The measured enzymes included aspartate transaminase, alanine transaminase, alkaline phosphatase, and gamma glutamyl transpeptidase, and were used as measures of liver injury resulting from HD-induced circulatory stress.

Liver Enzyme	% Change Relative to Baseline	
	After Standard HD	*After Cooled HD*
Aspartate Transaminase	+19.7	+16.1
Alanine Transaminase	+10.0	+11.3
Alkaline Phosphatase	+11.8	+7.5
Gamma Glutamyl Transpeptidase	+16.7	+11.8

Appendix B: Supplementary Results for Chapter 4

The GFR was measured in 6 patients whose kidneys were completely captured with CT perfusion scanning. Summaries of computed GFR values, renal cortical perfusion values, and renal cortical extraction efficiency values for these patients are given in Tables B1, B2, and B3, respectively.

Table B1: Calculated GFR based on CT perfusion imaging measurements. Results are organized according to visit (visit 1 or visit 2, top half of table) and HD type (standard HD or cooled HD, bottom half of table), where imaging was performed before, during and after HD. GFR was computed for left (L) and right (R) kidneys separately, then summed together for total (T) GFR. Shading represents HD sessions where dialysate cooling was applied.

	GFR (mL/min/1.73m^2) – Organized by Visit																	
Pt #	Visit 1									Visit 2								
	Before HD			During HD			After HD			Before HD			During HD			After HD		
	L	R	T	L	R	T	L	R	T	L	R	T	L	R	T	L	R	T
1	6.6	1.6	8.2	4.0	0.6	4.6	3.2	0.4	3.6	7.7	1.1	8.8	3.5	0.9	4.4	3.7	1.3	5.0
2	1.0	0.6	1.6	0.5	0.3	0.7	1.0	0.6	1.7	1.1	0.5	1.6	0.2	0.2	0.5	0.9	0.7	1.6
3	1.0	1.7	2.7	0.7	1.3	2.1	0.7	1.2	1.9	0.8	1.8	2.6	1.0	2.1	3.0	1.7	2.6	4.3
4	0.7	0.4	1.0	0.0	0.3	0.4	0.3	0.3	0.6	0.2	0.1	0.3	0.4	0.2	0.6	0.5	0.4	0.9
5	3.2	3.4	6.5	2.0	1.9	3.9	2.2	2.0	4.2	3.5	3.0	6.5	1.8	1.9	3.7	2.7	2.6	5.3
6	3.0	2.5	5.5	0.7	0.8	1.5	1.3	1.3	2.6	2.1	2.3	4.4	0.8	0.8	1.6	1.4	1.0	2.4
	GFR (mL/min/1.73m^2) – Organized by HD Type																	
Pt #	Standard HD									Cooled HD								
	Before HD			During HD			After HD			Before HD			During HD			After HD		
	L	R	T	L	R	T	L	R	T	L	R	T	L	R	T	L	R	T
1	6.6	1.6	8.2	4.0	0.6	4.6	3.2	0.4	3.6	7.7	1.1	8.8	3.5	0.9	4.4	3.7	1.3	5.0
2	1.0	0.6	1.6	0.5	0.3	0.7	1.0	0.6	1.7	1.1	0.5	1.6	0.2	0.2	0.5	0.9	0.7	1.6
3	1.0	1.7	2.7	0.7	1.3	2.1	0.7	1.2	1.9	0.8	1.8	2.6	1.0	2.1	3.0	1.7	2.6	4.3
4	0.7	0.4	1.0	0.0	0.3	0.4	0.3	0.3	0.6	0.2	0.1	0.3	0.4	0.2	0.6	0.5	0.4	0.9
5	3.5	3.0	6.5	1.8	1.9	3.7	2.7	2.6	5.3	3.2	3.4	6.5	2.0	1.9	3.9	2.2	2.0	4.2
6	3.0	2.5	5.5	0.7	0.8	1.5	1.3	1.3	2.6	2.1	2.3	4.4	0.8	0.8	1.6	1.4	1.0	2.4

Table B2: Measured renal cortical perfusion based on CT perfusion imaging. Values are organized according to visit (visit 1 or visit 2, top half of table) and HD type (standard HD or cooled HD, bottom half of table), where imaging was performed before, during and after HD. Cortical perfusion was measured for left (L) and right (R) kidneys separately. Shading represents HD sessions where dialysate cooling was applied.

	Renal Cortical Perfusion (mL/min/100g) – Organized by Visit											
Pt #	Visit 1						Visit 2					
	Before HD		During HD		After HD		Before HD		During HD		After HD	
	L	R	L	R	L	R	L	R	L	R	L	R
1	121.6	36.9	79.6	24.1	59.6	15.9	154.1	28.2	98.9	30.0	97.6	41.7
2	22.6	22.4	21.0	17.6	34.1	20.7	24.5	22.9	9.2	9.2	27.9	25.6
3	22.1	31.7	18.4	26.4	32.0	29.6	34.9	38.8	27.0	45.4	57.3	102.5
4	25.2	11.6	27.0	11.0	14.8	12.0	8.8	7.6	19.0	6.8	14.9	10.7
5	24.2	26.3	24.8	24.9	24.7	32.3	32.4	30.3	27.9	31.7	36.4	32.1
6	15.3	12.7	7.9	5.6	13.5	11.2	17.3	16.3	12.6	7.6	11.6	9.8
	Renal Cortical Perfusion (mL/min/100g) – Organized by HD Type											
Pt #	Standard HD						Cooled HD					
	Before HD		During HD		After HD		Before HD		During HD		After HD	
	L	R	L	R	L	R	L	R	L	R	L	R
1	121.6	36.9	79.6	24.1	59.6	15.9	154.1	28.2	98.9	30.0	97.6	41.7
2	22.6	22.4	21.0	17.6	34.1	20.7	24.5	22.9	9.2	9.2	27.9	25.6
3	22.1	31.7	18.4	26.4	32.0	29.6	34.9	38.8	27.0	45.4	57.3	102.5
4	25.2	11.6	27.0	11.0	14.8	12.0	8.8	7.6	19.0	6.8	14.9	10.7
5	32.4	30.3	27.9	31.7	36.4	32.1	24.2	26.3	24.8	24.9	24.7	32.3
6	15.3	12.7	7.9	5.6	13.5	11.2	17.3	16.3	12.6	7.6	11.6	9.8

Table B3: Measured renal cortical extraction efficiency based on CT perfusion imaging. Values are organized according to visit (visit 1 or visit 2, top half of table) and HD type (standard HD or cooled HD, bottom half of table), where imaging was performed before, during and after HD. Cortical extraction efficiency was measured for left (L) and right (R) kidneys separately. Shading represents HD sessions where dialysate cooling was applied.

	Renal Cortical Extraction Efficiency – Organized by Visit											
Pt #	Visit 1						Visit 2					
	Before HD		During HD		After HD		Before HD		During HD		After HD	
	L	R	L	R	L	R	L	R	L	R	L	R
1	0.4591	0.6155	0.5589	0.4875	0.6711	0.5371	0.4030	0.6439	0.5187	0.7694	0.5151	0.6214
2	0.7055	0.7204	0.5762	0.5022	0.6261	0.9079	0.7617	0.6716	0.6736	0.7177	0.7414	0.7407
3	0.5148	0.5338	0.6191	0.6722	0.4160	0.6027	0.4364	0.4854	0.7017	0.6231	0.4900	0.3379
4	0.4115	0.6803	0.3755	0.8949	0.5919	0.6781	0.4380	0.5513	0.3354	0.6582	0.6135	0.6835
5	0.7356	0.7374	0.5642	0.6478	0.7121	0.5100	0.6539	0.6803	0.5337	0.5597	0.5620	0.6487
6	0.7259	0.6809	0.5754	0.7001	0.6689	0.5985	0.7230	0.7001	0.4165	0.5635	0.6624	0.6001
	Renal Cortical Extraction Efficiency – Organized by HD Type											
Pt #	Standard HD						Cooled HD					
	Before HD		During HD		After HD		Before HD		During HD		After HD	
	L	R	L	R	L	R	L	R	L	R	L	R
1	0.4591	0.6155	0.5589	0.4875	0.6711	0.5371	0.4030	0.6439	0.5187	0.7694	0.5151	0.6214
2	0.7055	0.7204	0.5762	0.5022	0.6261	0.9079	0.7617	0.6716	0.6736	0.7177	0.7414	0.7407
3	0.5148	0.5338	0.6191	0.6722	0.4160	0.6027	0.4364	0.4854	0.7017	0.6231	0.4900	0.3379
4	0.4115	0.6803	0.3755	0.8949	0.5919	0.6781	0.4380	0.5513	0.3354	0.6582	0.6135	0.6835
5	0.6539	0.6803	0.5337	0.5597	0.5620	0.6487	0.7356	0.7374	0.5642	0.6478	0.7121	0.5100
6	0.7259	0.6809	0.5754	0.7001	0.6689	0.5985	0.7230	0.7001	0.4165	0.5635	0.6624	0.6001

Appendix C: Copyright Release Form for Figure 1.2

SPRINGER NATURE LICENSE
TERMS AND CONDITIONS

Jun 02, 2020

This Agreement between Western University -- Raanan Marants ("You") and Springer Nature ("Springer Nature") consists of your license details and the terms and conditions provided by Springer Nature and Copyright Clearance Center.

License Number	4840931474741
License date	Jun 02, 2020
Licensed Content Publisher	Springer Nature
Licensed Content Publication	Springer eBook
Licensed Content Title	Dialysis Equipment
Licensed Content Author	N. K. Man, J. Zingraff, P. Jungers
Licensed Content Date	Jan 1, 1995
Type of Use	Thesis/Dissertation
Requestor type	academic/university or research institute
Format	print and electronic

Portion	figures/tables/illustrations
Number of figures/tables/illustrations	1
Will you be translating?	no
Circulation/distribution	1 - 29
Author of this Springer Nature content	no
Title	Exploring the Effects of Hemodialysis on Renal and Hepatic Blood Flow and Function using CT Perfusion Imaging
Institution name	Western University
Expected presentation date	Jul 2020
Portions	Figure 4-2 (chapter 4, page 34)

Total	0.00 CAD

Terms and Conditions

Springer Nature Customer Service Centre GmbH
Terms and Conditions

This agreement sets out the terms and conditions of the licence (the **Licence**) between you and **Springer Nature Customer Service Centre GmbH** (the **Licensor**). By clicking 'accept' and completing the transaction for the material (**Licensed Material**), you also confirm your acceptance of these terms and conditions.

1. Grant of License

1. 1. The Licensor grants you a personal, non-exclusive, non-transferable, world-wide licence to reproduce the Licensed Material for the purpose specified in your order only. Licences are granted for the specific use requested in the order and for no other use, subject to the conditions below.

1. 2. The Licensor warrants that it has, to the best of its knowledge, the rights to license reuse of the Licensed Material. However, you should ensure that the material you are requesting is original to the Licensor and does not carry the copyright of another entity (as credited in the published version).

1. 3. If the credit line on any part of the material you have requested indicates that it was reprinted or adapted with permission from another source, then you should also seek permission from that source to reuse the material.

2. Scope of Licence

2. 1. You may only use the Licensed Content in the manner and to the extent permitted by these Ts&Cs and any applicable laws.

2. 2. A separate licence may be required for any additional use of the Licensed Material, e.g. where a licence has been purchased for print only use, separate permission must be obtained for electronic re-use. Similarly, a licence is only valid in the language selected and does not apply for editions in other languages unless additional translation rights have been granted separately in the licence. Any content owned by third parties are expressly excluded from the licence.

2. 3. Similarly, rights for additional components such as custom editions and derivatives require additional permission and may be subject to an additional fee. Please apply to Journalpermissions@springernature.com/bookpermissions@springernature.com for these rights.

2. 4. Where permission has been granted **free of charge** for material in print, permission may also be granted for any electronic version of that work, provided that the material is incidental to your work as a whole and that the electronic version is essentially equivalent to, or substitutes for, the print version.

2. 5. An alternative scope of licence may apply to signatories of the STM Permissions Guidelines, as amended from time to time.

3. Duration of Licence

3. 1. A licence for is valid from the date of purchase ('Licence Date') at the end of the relevant period in the below table:

Scope of Licence	Duration of Licence
Post on a website	12 months
Presentations	12 months
Books and journals	Lifetime of the edition in the language purchased

4. Acknowledgement

4. 1. The Licensor's permission must be acknowledged next to the Licenced Material in print. In electronic form, this acknowledgement must be visible at the same time as the figures/tables/illustrations or abstract, and must be hyperlinked to the journal/book's homepage. Our required acknowledgement format is in the Appendix below.

5. Restrictions on use

5. 1. Use of the Licensed Material may be permitted for incidental promotional use and minor editing privileges e.g. minor adaptations of single figures, changes of format, colour and/or style where the adaptation is credited as set out in Appendix 1 below. Any other changes including but not limited to, cropping, adapting, omitting material that affect the meaning, intention or moral rights of the author are strictly prohibited.

5. 2. You must not use any Licensed Material as part of any design or trademark.

5. 3. Licensed Material may be used in Open Access Publications (OAP) before publication by Springer Nature, but any Licensed Material must be removed from OAP sites prior to final publication.

6. Ownership of Rights

6. 1. Licensed Material remains the property of either Licensor or the relevant third party and any rights not explicitly granted herein are expressly reserved.

7. Warranty

IN NO EVENT SHALL LICENSOR BE LIABLE TO YOU OR ANY OTHER PARTY OR ANY OTHER PERSON OR FOR ANY SPECIAL, CONSEQUENTIAL, INCIDENTAL OR INDIRECT DAMAGES, HOWEVER CAUSED, ARISING OUT OF OR IN CONNECTION WITH THE DOWNLOADING, VIEWING OR USE OF THE MATERIALS REGARDLESS OF THE FORM OF ACTION, WHETHER FOR BREACH OF CONTRACT, BREACH OF WARRANTY, TORT, NEGLIGENCE, INFRINGEMENT OR OTHERWISE (INCLUDING, WITHOUT LIMITATION, DAMAGES BASED ON LOSS OF PROFITS, DATA, FILES, USE, BUSINESS OPPORTUNITY OR CLAIMS OF THIRD PARTIES), AND
WHETHER OR NOT THE PARTY HAS BEEN ADVISED OF THE POSSIBILITY OF SUCH DAMAGES. THIS LIMITATION SHALL APPLY NOTWITHSTANDING ANY FAILURE OF ESSENTIAL PURPOSE OF ANY LIMITED REMEDY PROVIDED HEREIN.

8. Limitations

8. 1. ***BOOKS ONLY:*** Where **'reuse in a dissertation/thesis'** has been selected the following terms apply: Print rights of the final author's accepted manuscript (for clarity, NOT the published version) for up to 100 copies, electronic rights for use only on a personal website or institutional repository as defined by the Sherpa guideline

9. Termination and Cancellation

9. 1. Licences will expire after the period shown in Clause 3 (above).

9. 2. Licensee reserves the right to terminate the Licence in the event that payment is not received in full or if there has been a breach of this agreement by you.

Appendix 1 — Acknowledgements:

For Journal Content:
Reprinted by permission from **[the Licensor]**: **[Journal Publisher** (e.g. Nature/Springer/Palgrave)] **[JOURNAL NAME] [REFERENCE CITATION** (Article name, Author(s) Name), **[COPYRIGHT]** (year of publication)

For **Advance Online Publication papers:**
Reprinted by permission from **[the Licensor]**: **[Journal Publisher** (e.g. Nature/Springer/Palgrave)] **[JOURNAL NAME] [REFERENCE CITATION** (Article name, Author(s) Name), **[COPYRIGHT]** (year of publication), advance online publication, day month year (doi: 10.1038/sj.[JOURNAL ACRONYM].)

For Adaptations/Translations:
Adapted/Translated by permission from **[the Licensor]**: **[Journal Publisher** (e.g. Nature/Springer/Palgrave)] **[JOURNAL NAME] [REFERENCE CITATION** (Article name, Author(s) Name), **[COPYRIGHT]** (year of publication)

Note: For any republication from the British Journal of Cancer, the following credit line style applies:

Reprinted/adapted/translated by permission from **[the Licensor]**: on behalf of Cancer Research UK: : **[Journal Publisher** (e.g. Nature/Springer/Palgrave)] **[JOURNAL NAME] [REFERENCE CITATION** (Article name, Author(s) Name), **[COPYRIGHT]** (year of publication)

For **Advance Online Publication** papers:
Reprinted by permission from The **[the Licensor]**: on behalf of Cancer Research UK: **[Journal Publisher** (e.g. Nature/Springer/Palgrave)] **[JOURNAL NAME] [REFERENCE CITATION** (Article name, Author(s) Name), **[COPYRIGHT]** (year of publication), advance online publication, day month year (doi: 10.1038/sj.[JOURNAL ACRONYM])

For Book content:
Reprinted/adapted by permission from **[the Licensor]**: **[Book Publisher** (e.g. Palgrave Macmillan, Springer etc) **[Book Title]** by **[Book author**(s)] **[COPYRIGHT]** (year of publication)

Other Conditions:

Version 1.2

Appendix D: Copyright Release Form for Figures 1.4 and 1.5

EDIZIONI MINERVA MEDICA S.p.A

Journals Department

To: Dr. Raanan Marants

Torino – June 5, 2020

Dear Dr. Raanan Marants,

Thank you for your request to reprint material from **Q J Nucl Med**. The content you are currently requesting is figure 1 from:

Figure 2 and Figure 3.

Source: From Lee TY, Purdie TG, Stewart E. CT imaging of angiogenesis. Q J Nucl Med. 2003;47(3):171-187.

PhD thesis

Permission is granted provided that the material to be used has appeared in our publication without credit or acknowledgement to another source; proper credit is given to our publication(s). You must acknowledge Edizioni Minerva Medica in the following manner:

Reprinted by permission of Edizioni Minerva Medica from: ***Q J Nucl Med 2003;47(3):171-187.***

Please be advised that:

1. **Permission to use Figure 2 and Figure 3 from Q J Nucl Med. 2003;47(3):171-187 is applicable to this Project only. For subsequent uses, including additional printings, duplications or new editions, you must reapply for permission and pay an additional permission fee.**

2. **You may not use Figure 2 and Figure 3 from Q J Nucl Med. 2003;47(3):171-187 in products created for, on behalf of, or sponsored by any pharmaceutical manufacturer, seller, distributor or marketer without additional permission from us.**

3. **You may not modify, change the style of, manipulate or alter in any other manner Figure 2 and Figure 3 from Q J Nucl Med. 2003;47(3):171-187 432 except to remove or suppress labels.**

Permission is granted free of charge.

Appendix E: Copyright Release Form for Manuscript

Copyright Clearance Center | Marketplace™

American Society of Nephrology - License Terms and Conditions

This is a License Agreement between Raanan Marants ("You") and American Society of Nephrology ("Publisher") provided by Copyright Clearance Center ("CCC"). The license consists of your order details, the terms and conditions provided by American Society of Nephrology, and the CCC terms and conditions.

All payments must be made in full to CCC.

Order Date	28-May-2020	**Type of Use**	Republish in a thesis/dissertation
Order license ID	1038080-1	**Publisher**	AMERICAN SOCIETY OF NEPHROLOGY
ISSN	1046-6673	**Portion**	Chapter/article

LICENSED CONTENT

Publication Title	Journal of the American Society of Nephrology : JASN	**Rightsholder**	American Society of Nephrology
Article Title	Renal Perfusion during Hemodialysis: Intradialytic Blood Flow Decline and Effects of Dialysate Cooling.	**Publication Type**	Journal
		Start Page	1086
		End Page	1095
Author/Editor	AMERICAN SOCIETY OF NEPHROLOGY.	**Issue**	6
Date	01/01/1990	**Volume**	30
Language	English		
Country	United States of America		

REQUEST DETAILS

Portion Type	Chapter/article	**Rights Requested**	Main product
Page range(s)	1086-1095	**Distribution**	Worldwide
Total number of pages	10	**Translation**	Original language of publication
Format (select all that apply)	Print, Electronic	**Copies for the disabled?**	No
Who will republish the content?	Academic institution	**Minor editing privileges?**	Yes
Duration of Use	Life of current and all future editions	**Incidental promotional use?**	No
Lifetime Unit Quantity	Up to 499	**Currency**	CAD

NEW WORK DETAILS

Title	Exploring the Effects of Hemodialysis on Renal and Hepatic Blood Flow and Function using CT Perfusion Imaging	**Institution name**	Western University
		Expected presentation date	2020-07-09
Instructor name	Ting-Yim Lee, Christopher McIntyre		

ADDITIONAL DETAILS

Order reference number	N/A	**The requesting person / organization to appear on the license**	Raanan Marants

REUSE CONTENT DETAILS

Title, description or numeric reference of the portion(s)	Renal Perfusion during Hemodialysis: Intradialytic Blood Flow Decline and Effects of Dialysate Cooling	**Title of the article/chapter the portion is from**	Renal Perfusion during Hemodialysis: Intradialytic Blood Flow Decline and Effects of Dialysate Cooling.
Editor of portion(s)	McIntyre, Christopher W.; Lee, Ting-Yim; Grant, Claire J.; Qirjazi, Elena; Marants, Raanan	**Author of portion(s)**	McIntyre, Christopher W.; Lee, Ting-Yim; Grant, Claire J.; Qirjazi, Elena; Marants, Raanan
Volume of serial or monograph	30	**Issue, if republishing an article from a serial**	6
Page or page range of portion	1086-1095	**Publication date of portion**	2019-05-03

CCC Republication Terms and Conditions

1. Description of Service; Defined Terms. This Republication License enables the User to obtain licenses for republication of one or more copyrighted works as described in detail on the relevant Order Confirmation (the "Work(s)"). Copyright Clearance Center, Inc. ("CCC") grants licenses through the Service on behalf of the rightsholder identified on the Order Confirmation (the "Rightsholder"). "Republication", as used herein, generally means the inclusion of a Work, in whole or in part, in a new work or works, also as described on the Order Confirmation. "User", as used herein, means the person or entity making such republication.

2. The terms set forth in the relevant Order Confirmation, and any terms set by the Rightsholder with respect to a particular Work, govern the terms of use of Works in connection with the Service. By using the Service, the person transacting for a republication license on behalf of the User represents and warrants that he/she/it (a) has been duly authorized by the User to accept, and hereby does accept, all such terms and conditions on behalf of User, and (b) shall inform User of all such terms and conditions. In the event such person is a "freelancer" or other third party independent of User and CCC, such party shall be deemed jointly a "User" for purposes of these terms and conditions. In any event, User shall be deemed to have accepted and agreed to all such terms and conditions if User republishes the Work in any fashion.

3. Scope of License; Limitations and Obligations.

3.1. All Works and all rights therein, including copyright rights, remain the sole and exclusive property of the Rightsholder. The license created by the exchange of an Order Confirmation (and/or any invoice) and payment by User of the full amount set forth on that document includes only those rights expressly set forth in the Order Confirmation and in these terms and conditions, and conveys no other rights in the Work(s) to User. All rights not expressly granted are hereby reserved.

3.2. General Payment Terms: You may pay by credit card or through an account with us payable at the end of the month. If you and we agree that you may establish a standing account with CCC, then the following terms apply: Remit Payment to: Copyright Clearance Center, 29118 Network Place, Chicago, IL 60673-1291. Payments Due: Invoices are payable upon their delivery to you (or upon our notice to you that they are available to you for downloading). After 30 days, outstanding amounts will be subject to a service charge of 1-1/2% per month or, if less, the maximum rate allowed by applicable law. Unless otherwise specifically set forth in the Order Confirmation or in a separate written agreement signed by CCC, invoices are due and payable on "net 30" terms. While User may exercise the rights licensed immediately upon issuance of the Order Confirmation, the license is automatically revoked and is null and void, as if it had never been issued, if complete payment for the license is not received on a timely basis either from User directly or through a payment agent, such as a credit card company.

3.3. Unless otherwise provided in the Order Confirmation, any grant of rights to User (i) is "one-time" (including the editions and product family specified in the license), (ii) is non-exclusive and non-transferable and (iii) is subject to any and all limitations and restrictions (such as, but not limited to, limitations on duration of use or circulation) included in the Order Confirmation or invoice and/or in these terms and conditions. Upon completion of the licensed use, User shall either secure a new permission for further use of the Work(s) or immediately cease any new use of the Work(s) and shall render inaccessible (such as by deleting or by removing or severing links or other locators) any further copies of the Work (except for copies printed on paper in accordance with this license and still in User's stock at the end of such period).

3.4. In the event that the material for which a republication license is sought includes third party materials (such as photographs, illustrations, graphs, inserts and similar materials) which are identified in such material as having been used by permission, User is responsible for identifying, and seeking separate licenses (under this Service or otherwise) for, any of such third party materials; without a separate license, such third party materials may not be used.

3.5. Use of proper copyright notice for a Work is required as a condition of any license granted under the Service. Unless otherwise provided in the Order Confirmation, a proper copyright notice will read substantially as follows: "Republished with permission of [Rightsholder's name], from [Work's title, author, volume, edition number and year of copyright]; permission conveyed through Copyright Clearance Center, Inc. " Such notice must be provided in a reasonably legible font size and must be placed either immediately adjacent to the Work as used (for example, as part of a by-line or footnote but not as a separate electronic link) or in the place where substantially all other credits or notices for the new work containing the republished Work are located. Failure to include the required notice results in loss to the Rightsholder and CCC, and the User shall be liable to pay liquidated damages for each such failure equal to twice the use fee specified in the Order Confirmation, in addition to the use fee itself and any other fees and charges specified.

3.6. User may only make alterations to the Work if and as expressly set forth in the Order Confirmation. No Work may be used in any way that is defamatory, violates the rights of third parties (including such third parties' rights of copyright, privacy, publicity, or other tangible or intangible property), or is otherwise illegal, sexually explicit or obscene. In addition, User may not conjoin a Work with any other material that may result in damage to the reputation of the Rightsholder. User agrees to inform CCC if it becomes aware of any infringement of any rights in a Work and to cooperate with any reasonable request of CCC or the Rightsholder in connection therewith.

4. Indemnity. User hereby indemnifies and agrees to defend the Rightsholder and CCC, and their respective employees and directors, against all claims, liability, damages, costs and expenses, including legal fees and expenses, arising out of any use of a Work beyond the scope of the rights granted herein, or any use of a Work which has been altered in any unauthorized way by User, including claims of defamation or infringement of rights of copyright, publicity, privacy or other tangible or intangible property.

5. Limitation of Liability. UNDER NO CIRCUMSTANCES WILL CCC OR THE RIGHTSHOLDER BE LIABLE FOR ANY DIRECT, INDIRECT, CONSEQUENTIAL OR INCIDENTAL DAMAGES (INCLUDING WITHOUT LIMITATION DAMAGES FOR LOSS OF BUSINESS PROFITS OR INFORMATION, OR FOR BUSINESS INTERRUPTION) ARISING OUT OF THE USE OR INABILITY TO USE A WORK, EVEN IF ONE OF THEM HAS BEEN ADVISED OF THE POSSIBILITY OF SUCH DAMAGES. In any event, the total liability of the Rightsholder and CCC (including their respective employees and directors) shall not exceed the total amount actually paid by User for this license. User assumes full liability for the actions and omissions of its principals, employees, agents, affiliates, successors and assigns.

6. Limited Warranties. THE WORK(S) AND RIGHT(S) ARE PROVIDED "AS IS". CCC HAS THE RIGHT TO GRANT TO USER THE RIGHTS GRANTED IN THE ORDER CONFIRMATION DOCUMENT. CCC AND THE RIGHTSHOLDER DISCLAIM ALL OTHER WARRANTIES RELATING TO THE WORK(S) AND RIGHT(S), EITHER EXPRESS OR IMPLIED, INCLUDING WITHOUT LIMITATION IMPLIED WARRANTIES OF MERCHANTABILITY OR FITNESS FOR A PARTICULAR PURPOSE. ADDITIONAL RIGHTS MAY BE REQUIRED TO USE ILLUSTRATIONS, GRAPHS, PHOTOGRAPHS, ABSTRACTS, INSERTS OR OTHER PORTIONS OF THE WORK (AS OPPOSED TO THE ENTIRE WORK) IN A MANNER CONTEMPLATED BY USER; USER UNDERSTANDS AND AGREES THAT NEITHER CCC NOR THE RIGHTSHOLDER MAY HAVE SUCH ADDITIONAL RIGHTS TO GRANT.

7. Effect of Breach. Any failure by User to pay any amount when due, or any use by User of a Work beyond the scope of the license set forth in the Order Confirmation and/or these terms and conditions, shall be a material breach of the license created by the Order Confirmation and these terms and conditions. Any breach not cured within 30 days of written notice thereof shall result in immediate termination of such license without further notice. Any unauthorized (but licensable) use of a Work that is terminated immediately upon notice thereof may be liquidated by payment of the Rightsholder's ordinary license price therefor; any unauthorized (and unlicensable) use that is not terminated immediately for any reason (including, for example, because materials containing the Work cannot reasonably be recalled) will be subject to all remedies available at law or in equity, but in no event to a payment of less than three times the Rightsholder's ordinary license price for the most closely analogous licensable use plus Rightsholder's and/or CCC's costs and expenses incurred in collecting such payment.

8. Miscellaneous.

8.1. User acknowledges that CCC may, from time to time, make changes or additions to the Service or to these terms and conditions, and CCC reserves the right to send notice to the User by electronic mail or otherwise for the purposes of notifying User of such changes or additions; provided that any such changes or additions shall not apply to permissions already secured and paid for.

8.2. Use of User-related information collected through the Service is governed by CCC's privacy policy, available online here:https://marketplace.copyright.com/rs-ui-web/mp/privacy-policy

8.3. The licensing transaction described in the Order Confirmation is personal to User. Therefore, User may not assign or transfer to any other person (whether a natural person or an organization of any kind) the license created by the Order Confirmation and these terms and conditions or any rights granted hereunder; provided, however, that User may assign such license in its entirety on written notice to CCC in the event of a transfer of all or substantially all of User's rights in the new material which includes the Work(s) licensed under this Service.

8.4. No amendment or waiver of any terms is binding unless set forth in writing and signed by the parties. The Rightsholder and CCC hereby object to any terms contained in any writing prepared by the User or its principals, employees, agents or affiliates and purporting to govern or otherwise relate to the licensing transaction described in the Order Confirmation, which terms are in any way inconsistent with any terms set forth in the Order Confirmation and/or in these terms and conditions or CCC's standard operating procedures, whether such writing is prepared prior to, simultaneously with or subsequent to the Order Confirmation, and whether such writing appears on a copy of the Order Confirmation or in a separate instrument.

8.5. The licensing transaction described in the Order Confirmation document shall be governed by and construed under the law of the State of New York, USA, without regard to the principles thereof of conflicts of law. Any case, controversy, suit, action, or proceeding arising out of, in connection with, or related to such licensing transaction shall be brought, at CCC's sole discretion, in any federal or state court located in the County of New York, State of New York, USA, or in any federal or state court whose geographical jurisdiction covers the location of the Rightsholder set forth in the Order Confirmation. The parties expressly submit to the personal jurisdiction and venue of each such federal or state court.If you have any comments or questions about the Service or Copyright Clearance Center, please contact us at 978-750-8400 or send an e-mail to support@copyright.com.

v 1.1

Appendix F: Curriculum Vitae

RAANAN MARANTS, MSc

EDUCATION

Western University, London, Canada — Sep 2015 – Jul 2020
PhD candidate (expected: 2019), Medical Biophysics
Master of Clinical Medical Biophysics, June 2018

Carleton University, Ottawa, Canada — Sep 2013 – Aug 2015
MSc, Medical Physics

York University, Toronto, Canada — Sep 2009 – Apr 2013
BSc with Honors, Biophysics (First Class distinction)

RELEVANT SKILLS & EXPERIENCE

- Skilled in programming and coding with MATLAB, Python, C++, Mathematica, LabVIEW, Java
- Experienced with machining, working with phantoms, electronics and circuits
- Proficient in image processing and analysis, including segmentation (manual and machine learning-based), registration, reconstruction, and texture/heterogeneity quantification
- Experienced in multi-modality functional imaging, including CT and perfusion imaging, optical imaging and pulsed oximetry, ultrasound and echocardiography, confocal microscopy
- Strong understanding of dual energy and cone-beam CT, PET and SPECT, various MRI techniques
- Experienced with small beam dosimetry and various dosimeters (MOSFET, radiochromic film, TLD)
- Proficient with using electromagnetic, x-ray and optical techniques for target position/motion tracking
- Experience with beam delivery adaptation based on real-time in-room imaging during radiotherapy
- Skilled in linac quality assurance, specializing in Varian (iX and TrueBeam) and CyberKnife machines
- Proficient in designing, reviewing, and optimizing radiotherapy treatment plans on different platforms, including the Pinnacle system and CyberKnife's MultiPlan system

RESEARCH EXPERIENCE

PhD Thesis, Robarts Research Institute, London, Canada — Sep 2015 – Jul 2020
Assessing multi-organ hemodynamic changes during hemodialysis using CT perfusion imaging

- Used perfusion imaging and tracer kinetic modeling to quantify and describe how hemodialysis affects organ-specific blood flow and function in end-stage renal disease
- Demonstrated significant reduction in renal perfusion during hemodialysis, which is a potential key pathophysiological factor leading to residual renal function decline in end-stage renal disease patients
- Developed a semi-automated algorithm to import, adjust, segment and perform quantitative analysis on CT images and multi-parametric functional maps

MSc Thesis, The Ottawa Hospital Cancer Center, Ottawa, Canada — Sep 2013 – Aug 2015
Evaluating the 4D RADPOS dosimetry system for dose and position QA of CyberKnife radiotherapy

- Performed end-to-end Monte Carlo-based treatment planning for CyberKnife and gained proficiency in small beam dosimetry and SBRT plan optimization
- Conducted dosimetric and positional evaluations of CyberKnife using custom phantom types and configurations under various beam delivery regimes, demonstrating with RADPOS that CyberKnife's motion tracking system struggles to compensate for irregular patient motion patterns
- Developed a semi-automated algorithm to import CyberKnife and RADPOS position data, transform the data into a common coordinate system, and perform numerical and graphical analysis

Research Assistant, Kidney Clinical Research Unit, London, Canada Sep 2017 – Jul 2020
Exploring patient-specific response to dialysis using mathematical models of organ perfusion

- Assisted with performing 3D reconstructions of multi-organ blood flow using CT perfusion images for fractal dimension texture analysis and heterogeneity quantification
- Helped generate patient-specific models of perfusion based on mathematically optimized spatial blood flow distribution, organ shape, blood vessel morphometry, and autoregulation mechanisms

Research Assistant, York University, Toronto, Canada May 2013 – Aug 2013
Assessing novel detector designs for high-energy particle physics applications with in silico models

- Performed computer simulations of particle beams incident on a detector as an application for CERN CVD diamond anti-proton beam detectors
- Developed a parallel computing-based program in Mathematica and LabVIEW to determine particle beam parameters and coordinates based on intensity values from simulated detector

NSERC-USRA Research Assistant, York University, Toronto, Canada May 2011 – Sep 2011
Construction and characterization of interference filter-stabilized diode lasers

- Assisted with construction of home-made, interference filter-stabilized diode lasers for use in industry-standard commercial gravimeters and cold atom experiments
- Designed custom circuits and mechanical parts for laser system augmentation, and performed laser system characterization in terms of line width and mode structure

RAY (Research At York) Research Assistant, York University, Toronto, Canada Jan 2011 – Apr 2011
Fluorescence measurements of mitochondrial and chloroplast activity in Eremosphaera viridis

- Examined the use of Rhodamine 123 and chlorophyll autofluorescence to monitor the physiological action of mitochondrial respiration and chloroplast photosynthetic activity in algae cells
- Performed 3D reconstructions of mitochondrial and chloroplast spatial locations using confocal microscopy and quantified fluorescence intensity to characterize mitochondrial-chloroplast interactions

PUBLICATIONS, PRESENTATIONS & ABSTRACTS

Peer-Reviewed Publications and Abstracts

- Marants R, Qirjazi E, Grant CJ, Lee TY, McIntyre CW. Renal Perfusion during Hemodialysis: Intradialytic Blood Flow Decline and Effects of Dialysate Cooling. *J Am Soc Nephrol*. 2019;30:1086-1095 (publication)
- Marants R, Vandervoort E, Cygler JE. Evaluation of the 4D RADPOS Dosimetry System for Dose and Position Quality Assurance of CyberKnife. *Med Phys*. 2018;45:4030-4044 (publication)
- Filler G, Ramsaroop A, Stein R, Grant CJ, Marants R, So A, McIntyre CW. Is Testosterone Detrimental to Renal Function? *Kidney Int Rep*. 2016;1:306-310 (publication)
- Marants R, Vandervoort E, Cygler JE. Quality Assurance Using the RADPOS System for 4D Radiotherapy with CyberKnife. *Med Phys*. 2015;42:3485-3485 (poster presentation, AAPM 2015)
- Marants R, Vandervoort E, Cygler JE. Dose and Position Quality Assurance Using the RADPOS System for 4D Radiotherapy with CyberKnife. *IFMBE Proceedings*. 2015;51:599-602 (oral presentation, IUPESM World Congress 2015)
- Marants R, Vandervoort E, Cygler JE. Dose and Position Quality Assurance Using the 4D RADPOS System for CyberKnife Radiotherapy. *Med Phys*. 2014;41:11-11 (poster presentation, COMP 2014)

Publications in Preparation

- Marants R, Qirjazi E, Lee TY, McIntyre CW. Exploring the Link Between Hepatic Perfusion and Systemic Endotoxemia in Hemodialysis Patients
- Marants R, McIntyre CW, Lee TY. Feasibility of Measuring Glomerular Filtration Rate in End-Stage Renal Disease Patients using CT Perfusion Imaging

National and International Conferences

- Marants R, Qirjazi E, Grant CJ, Lee TY, McIntyre CW. Using CT Perfusion Imaging to Measure Kidney Blood Flow during Hemodialysis in End-Stage Kidney Disease Patients (oral presentation, AAPM 2019)
- Marants R, Qirjazi E, Grant CJ, Lee TY, McIntyre CW. Residual Renal Function Loss in Hemodialysis Patients: Is Kidney Stunning the Culprit & Can Dialysate Cooling Help? (poster presentation, ASN 2018)
- Qirjazi E, Marants R, Mio MA, Urquhart B, Lee TY, McIntyre CW. Hepatic Response to Cooler Hemodialysis (poster presentation, ASN 2018)
- Kharche SR, Marants R, Qirjazi E, Kassay AD, Joseph J, McDougall KD, Lee TY, McIntyre CW. Understanding the Effects of Hemodialysis on Blood Flow: An Imaging-Mathematical Modeling Study (poster presentation, ASN 2018)
- Marants R, Grant CJ, Qirjazi E, McIntyre CW, Lee TY. Renal CT Perfusion Imaging during Hemodialysis: Relating Kidney Blood Flow to Residual Renal Function Loss (oral presentation, CARO-COMP-CAMRT 2018)
- Marants R, Qirjazi E, McIntyre CW, Lee TY. Dialysate Cooling during Hemodialysis: Assessment of Liver Hemodynamics using CT Perfusion Imaging (oral presentation and science highlight, AAPM 2018)
- Marants R, Grant CJ, McIntyre CW, Lee TY. CT Perfusion Imaging of the Liver during Hemodialysis: Assessment of Hepatic Blood Flow Distribution (oral presentation, COMP 2017)
- Marants R, Grant CJ, Lee TY, McIntyre CW. Renal Perfusion Falls during Hemodialysis: An Explanation for the Loss of Residual Renal Function in Dialysis Patients (poster presentation, ASN 2016)
- Grant CJ, Marants R, Tonial N, Velenosi T, Urquhart B, Lee TY, McIntyre CW. Hepatic Response to Hemodialysis: Consequences for Uremic Toxin Exposures and Multi-Organ Injury (poster presentation, ASN 2016)
- Mok C, Winter S, Beica H, Barrett B, Berthiaume R, Vorozcovs A, Yachoua F, Afkhami-Jeddi N, Marants R, Aggarwal M, Kumarakrishnan A. Atom Trapping Laboratory for Upper Level Undergraduate Students (poster presentation, APS DAMOP 2012)
- Afkhami-Jeddi N, Marants R, Berthiaume R, Kumarakrishnan A. Analysis of Stability of Homebuilt Diode Lasers for Precise Measurements of Gravitational Acceleration (oral presentation, CUPC 2011)

Local and Regional Conferences

- Marants R, Qirjazi E, McIntyre CW, Lee TY. Exploring the Effects of Standard and Cooled Hemodialysis on Liver Hemodynamics and Systemic Endotoxemia using CT Perfusion Imaging (oral presentation, London Imaging Discovery 2019)
- Marants R, Qirjazi E, McIntyre CW, Lee TY. Exploring the Link Between Liver Blood Flow and Systemic Endotoxemia during Hemodialysis: A CT Perfusion Study (poster presentation, Robarts Retreat 2019)
- Marants R, Qirjazi E, Grant CJ, McIntyre CW, Lee TY. Exploring the Effects of Standard and Cooled Hemodialysis on Renal Blood Flow using CT Perfusion (oral presentation, ImNO and LHRD 2019)
- Marants R, Qirjazi E, McIntyre CW, Lee TY. Evaluating the Effects of Dialysate Cooling on Liver Hemodynamics during Hemodialysis: A CT Perfusion Study (poster presentation, Robarts Retreat 2018)
- Marants R, Qirjazi E, McIntyre CW, Lee TY. How does Dialysate Cooling during Hemodialysis affect Kidney Blood Flow and Residual Renal Function? A CT Perfusion Study (electronic poster presentation, London Imaging Discovery 2018)
- Marants R, Qirjazi E, McIntyre CW, Lee TY. Exploring the Effects of Dialysate Cooling on Liver Hemodynamics during Hemodialysis with CT Perfusion (poster presentations, ImNO and LHRD 2018)

- Marants R, Grant CJ, McIntyre CW, Lee TY. CT Perfusion Imaging of the Liver during Hemodialysis: Assessment of Changes in Liver Perfusion Distribution and Hepatic Function (poster presentation, Robarts Retreat 2017)
- Marants R, Grant CJ, Jiang N, Huang IL, Wang Q, Lee TY, McIntyre CW. Renal Perfusion Falls during Hemodialysis: An Explanation for the Loss of Residual Renal Function in Dialysis Patients (poster presentations, ImNO and LHRD 2017)
- Marants R, Grant CJ, Stewart EE, Hadway J, McIntyre CW, Lee TY. CT Perfusion Imaging for Evaluating the Effects of Dialysis on Liver Perfusion (oral presentation, London Imaging Discovery 2016)
- Marants R, Grant CJ, Stewart EE, Hadway J, McIntyre CW, Lee TY. Evaluating the Effects of Dialysis on Liver Perfusion using CT Perfusion Imaging (poster presentations, ImNO and LHRD 2016)

Other Publications (not peer-reviewed)

- Winter S, Beica H, Mok C, Barrett B, Berthiaume R, Vorozcovs A, Yachoua F, Afkhami-Jeddi N, Marants R, Aggarwal M, Kumarakrishnan A. Resource Letter for Advanced Laboratory Courses on Laser Spectroscopy and Atom Trapping. 2013.
- Marants R, Lew RR. Viridae Flourescence: Fluorescence intensity measurements of mitochondrial and chloroplast activity in Eremosphaera viridis. 2011.

AWARDS & SCHOLARSHIPS

Certificate of merit poster award
London Imaging Discovery Day
London, Canada, Jun 2018

Honorable mention poster award
Imaging Network Ontario Symposium
Toronto, Canada, Mar 2018

Cum Laude abstract award
Imaging Network Ontario Symposium
Toronto, Canada, Mar 2016

CAMPEP QA-Ship
Western University, London, Canada
2017 – 2019, $3000/year

Schulich Graduate Scholarship & Western Graduate Research Scholarship
Western University, London, Canada
2015 – 2020, $8800/year

COMP Student Council Travel Award & Graduate Student Travel/Research Award
Carleton University, Ottawa, Canada
2014, $1000

Carleton University Department Scholarship
Carleton University, Ottawa, Canada
2013 – 2014, $3000/year

NSERC Undergraduate Student Research Award
York University, Toronto, Canada
2011, $6000

YorkU Renewable Entrance Scholarship & Science and Engineering Entrance Scholarship
York University, Toronto, Canada
2009 – 2010, $3000/year

WORK & TEACHING EXPERIENCE

Radiotherapy Quality Assurance London Regional Cancer Program, London, Canada 2017 – 2019

- Independently performed weekly, biweekly and monthly quality assurance tests (mechanical and machine output) for two Varian radiotherapy linear accelerators (iX and TrueBeam)
- Provided detailed quality assurance reports to medical physicists and radiation therapists

Teaching Assistant Carleton University, Ottawa, Canada 2013 – 2015

- Lead students through tutorials and laboratory experiments, offering support and promoting critical thinking and application of classroom and textbook concepts
- Performed grading of laboratory reports and tutorial tests, as well as proctoring during tests and exams

VOLUNTEER EXPERIENCE

Discovery Days in Health Sciences St. Joseph's Health Care, London, Canada 2017 and 2018

- Presented and promoted medical science research to visiting high school students
- Discussed post-secondary education options and pathways with students

Let's Talk Science York University & Carleton University, Toronto and Ottawa, Canada 2012 and 2015

- Promoted the study of science to elementary school students by introducing them to basic scientific principles and leading them through engaging hands-on demonstrations and experiments
- Demonstrated and explained various experimental aspects of an undergraduate biophysics laboratory to visiting high school students

Emergency Ward Mackenzie Richmond Hill Hospital, Richmond Hill, Canada 2012 – 2013

- Assisted with medical procedures such as suturing and casting
- Prepared clean patient beds and sorted medical charts

Undergraduate Biophysics Laboratory York University, Toronto, Canada 2010

- Performed and evaluated various biophysics laboratory experimental setups and procedures
- Installation, configuration and repair of experiment-specific equipment

LANGUAGES

- Native proficiency in English
- Professional working proficiency in Russian
- Limited working proficiency in French and Hebrew

EXTRACURRICULAR ACTIVITIES

Intramural Sports Western University, London, Canada 2017 – 2019

- Helped put together teams and organize practices for a variety of co-ed team sports

Medical Biophysics CAMPEP Club Chair Western University, London, Canada 2017 – 2018

- Organized club meetings for CAMPEP students to discuss medical physics news and conferences, work on CCPM problem sets, and listen to presentations by guest speakers
- Communicated with and arranged for guest speakers (including medical physics residents, clinical medical physicists, Western alumni) to present at club meetings

Biophysics Club Member York University, Toronto, Canada 2010 – 2013

- Promoted biophysics program to prospective students and biophysics courses to current students
- Assisted with organizing club meetings and events, such as guest lectures and demonstrations

Ballroom Dance Club Instructor York University, Toronto, Canada 2010

- Planned classes and taught basic ballroom dancing choreography and techniques
- Helped organize special events and social outings for club members

Competitive Ballroom Dancing Dance Mania & Dance Life Studios, Toronto, Canada 1999 – 2013

- Performed at city-wide recitals and shows, and competed in local, national and international competitions
- 2012 Ontario Pre-Champ Ballroom and Latin champion and Champ Ballroom and Latin top 8 finalist